LEVERAGING GOOGLE EARTH ENGINE TO ANALYSE VERY HIGH SPATIAL RESOLUTION UNMANNED AERIAL VEHICLE DATA TO GUIDE AND INFORM PRECISION AGRICULTURE IN SMALLHOLDER FARMS

Report to the

WATER RESEARCH COMMISSION

by

Shaeden Gokool[1,6], Ameera Yacoob[1], Maqsooda Mahomed[1], Richard Kunz[1], Alistair Clulow[1,2], Mbulisi Sibanda[3], Vivek Naiken[1], Kershani Chetty[1] and Tafadzwanashe Mabhaudhi[1,4,5]

[1]Centre for Water Resources Research, School of Agriculture and Science, University of KwaZulu-Natal

[2]Discipline of Agrometeorology, School of Agriculture and Science, University of KwaZulu-Natal

[3]Department of Geography, Environmental Studies and Tourism, University of the Western Cape,

[4]Centre for Transformative Agricultural and Food Systems, School of Agriculture and Sciences, University of KwaZulu-Natal

[5]Centre of Climate Change and Planetary Health, London School of Hygiene and Tropical Medicine

[6]South African Environmental Observation Network (SAEON), Grasslands-Forests-Wetlands Node,

WRC Report No.3239/1/25

ISBN 978-0-6392-0756-8

March 2026

Obtainable from:

Water Research Commission
Private Bag X03
Gezina, 0031
South Africa

hendrickm@wrc.org.za or download from www.wrc.org.za

This is the final report of WRC project no. C2019/2020-00088.

EXECUTIVE SUMMARY

Smallholder farms are major contributors to the improvement of food security and socio-economic development. However, their potential to address food insecurity challenges is limited by the availability of critical resources that they have at their disposal. Subsequently, they require an innovative and cost-effective approach to improve their operations, so that they can optimise their productivity, whilst sustainably utilising the available resources. The adoption of Precision Agricultural (PA) practices is well-suited to deliver on the aforementioned targets. The emergence of Unmanned Aerial Vehicles (UAVs) and their use in agricultural activities have become more prevalent and they have been touted as an ideal tool for facilitating PA practices on smallholder farms. However, there is a need to better understand how these technologies are being applied in such settings and then to identify and evaluate the potential UAV-based methods, to facilitate the application of PA practices by smallholder farmers.

To this end, we first undertook a comprehensive scoping review and bibliometric analysis of the available literature on the actual application of PA that is facilitated by UAVs in a smallholder farm setting. The rationale for this was to identify the research themes, the potential strengths and limitations, as well as the opportunities for the future. The results of these investigations revealed that UAVs have largely been used for monitoring crop growth and development, for guiding fertiliser management, as well as for crop mapping, but they also have the potential to facilitate other PA practices. Several factors may moderate the potential of these technologies. However, due to continuous technological advancements and the reduction in ownership and operational costs, there remains much cause for optimism regarding the future application of UAVs and the associated technologies, with respect to them informing policy, planning and operational decision-making.

Following the scoping review, several potential techniques were identified that can be implemented to improve the operational efficiency and productivity of these farms. However, given the limited application of these approaches within the smallholder farm setting, there is a need to evaluate these methods, by taking into consideration the unique socioeconomic circumstances that these farms experience. For this purpose, we identified three major thematic areas, to test and evaluate the potential of UAV-based approaches to facilitate PA practices.

These include: i) mapping cultivated areas, ii) quantifying crop water use, and iii) assessing crop health, with the focus on quantifying the crop water stress. With advances in geospatial cloud computing having created new and exciting possibilities in the remote sensing arena, we explored and demonstrated the utility of the advanced image processing capabilities of the Google Earth Engine (GEE) geospatial cloud computing platform to process and analyse a very high spatial resolution multispectral UAV image for mapping Land Use Land Cover (LULC) within smallholder farms. The results showed that LULC could be mapped at a 0.50 m spatial resolution with an overall accuracy of 91%. Overall, we found GEE to be an extremely useful platform for conducting an advanced image analysis on UAV imagery and for the rapid communication of the results.

Since our current understanding of the use of UAV technologies for evaluating the crop water status and facilitating precision water management applications is inadequate, we aimed to address this knowledge gap by conducting a comprehensive assessment of suitable UAV-based evapotranspiration (ET) estimation techniques that can be implemented within a resource-constrained smallholder farm setting. A vegetation index-based ET modelling technique was identified and applied within a small-scale sugarcane field to quantify the water use, and the accuracy of these estimates was ascertained by making comparisons against measured data. Various Vegetation Indices (VIs) derived from UAV-acquired multispectral imagery were used as a surrogate for the crop coefficient to estimate ET, and these estimates were then validated against ground-based Eddy Covariance (EC) measurements. The results of these investigations demonstrated that the best-performing model yielded a coefficient of determination (R^2) of 0.63, a Root Mean Square Error (RMSE) of 0.67 and a Mean Absolute Error (MAE) of 0.52, when compared to the measured ET. Furthermore, the characteristics of this model make it well-suited for smallholder farm applications, due to its relative simplicity and reduced data requirements.

Considering that widespread water scarcity, erratic weather patterns and arid conditions increasingly compromise agricultural productivity in South Africa, many smallholder farmers across the region, who predominantly practise dryland agriculture, suffer substantial yield losses, due to water-related challenges caused by unreliable rainfall. Therefore, there is an urgent need for appropriate water stress detection techniques, in order to understand the impacts of water deficits on crop growth and development.

While UAV-based sensors are well-suited for smallholder farm applications, most multi-spectral sensors that are used in PA applications lack the spectral resolution to detect water stress by using commonly-applied remote sensing-based techniques. In the light of this challenge, we developed a novel machine learning-based framework that integrated UAV-acquired multispectral data with Sentinel-2 satellite imagery for predicting water stress, and we evaluated the veracity of these estimates against the key phenological growth indicators that were measured throughout the duration of the study period. The UAV-based water stress indicator derived from the application of Machine Learning (ML) techniques showed good performance when compared against the satellite-based water stress indicator, achieving an R^2 of 0.95, with an RMSE and MAE of 0.03 and 0.02, respectively, which effectively captured the spatiotemporal water stress during key growth phases. Strong correlations between the predicted water stress and parameters, such as the Normalised Difference Vegetation Index (NDVI), the green NDVI (GNDVI), and the Optimised Soil Adjusted Vegetation Index (OSAVI), enhance the robustness of the models. In addition, the modelled water stress showed a good correlation with the measured ET ($R^2 = 0.60$) and the water deficit index ($R^2 = 0.62$) derived from in-situ measurements, which further highlighted the ability of the model to account for water stress.

The findings presented in this study have demonstrated the considerable potential that UAV technology has for quantifying the spatiotemporal crop growth dynamics within smallholder farms, whilst they also highlighted their broader application in other aspects of PA. Although the adoption of PA practices, facilitated by the use of UAV technology, has the potential to radically transform the African agricultural sector, particularly in the case of the smallholder farmer, it is important to note that affordability, digital literacy, technical expertise and stringent regulatory frameworks are barriers that may prevent the widespread adoption of these technologies for smallholder farm applications. Therefore, before these technologies are readily adopted to guide and inform agricultural management and decision-making within smallholder farming systems, further research is still required, in order to develop confidence in the application of these UAV-based methods, as well as to refine these methods, so that they are well-suited for application within the resource-constrained smallholder farmer context. Future research opportunities may include: i) conducting a more comprehensive knowledge review, rather than just a traditional literature review, ii) investigating the potential of similar, but lower cost, UAV technologies, and iii) exploring and evaluating the potential of future technological advancements, to enhance the potential of UAV-based PA practices.

In addition to demonstrating the potential of UAVs to facilitate PA practices within a resource-constrained smallholder farm setting, this project has laid the foundation for enhancing the capacity of South Africans to use Smart technologies to guide their policy and inform decision-making, whilst also facilitating South Africa to become a major role player in the digital water space. Through this project, human capacity development took place in the form of i) strengthening and enhancing institutional capacity, (ii) capacity development of early-career and established researchers, as well as postgraduates, and iii) community engagement and knowledge transfer, to improve agricultural output of smallholders and food security. During the course of this project, one MSc student was directly supported by the project, whereas one MSc and one Honours student received indirect support.

All three students have successfully graduated. Early career researchers and first-time project leaders, Drs Shaeden Gokool and Maqsooda Mahomed, have received invaluable mentorship and guidance from their senior project team members, which has contributed immensely to the progress that has been made and has equipped them to be successful project leaders in the future. Furthermore, regular community engagement has been a strong feature of this project, as project team members and the local community of Swayimane, particularly the farmers, have worked closely together to share their knowledge and to ensure that the objectives of the project directly cater to their present and future needs.

ACKNOWLEDGEMENTS

The research reported here formed part of a non-solicited project that was initiated, funded and managed by the Water Research Commission (WRC) in Key Strategic Area 4 (Water Utilisation in Agriculture). The Project Team is sincerely grateful to the WRC for funding and managing this project. The Project Team also acknowledges the following members of the Reference Group for their valuable contributions and guidance:

Dr L Nhamo	Water Research Commission (Chairperson)
Prof NS Mpandeli	Water Research Commission
Dr SN Hlophe-Ginindza	Water Research Commission
Mr T Newby	Private (Associate-GeoTerra Image)
Prof A van Niekerk	Stellenbosch University
Ms N Mjadu	Department of Agriculture
Prof M van der Laan	Agricultural Research Council
Ms N Masemola	Department of Agriculture

In addition to the financial and technical support received from the WRC, the authors would like to extend their gratitude to the following people, institutions and organisations:

- The University of KwaZulu-Natal (UKZN), the University of the Western Cape and the London School of Hygiene and Tropical Medicine, for the provision of the necessary facilities and resources to successfully complete this project.
- Fellow-UKZN colleagues, Gary Denton, Evania Chetty, Knowledge Muchonyerwa, Thando Mthembu, Brice Gijsbertsen, Trylee Matongera and Celuxolo Dlamini, for their invaluable assistance throughout the duration of the project.
- AET security for the provision of additional resources throughout the duration of the project, with special mention to Thulani Ncwane for accompanying the Project Team to the site and assisting with the field measurements.
- A very big thank you to the smallholder farming community of Swayimane, for affording us the opportunity to conduct this research; it has enabled us to grow and develop by learning from each other.

- A special mention is reserved for Luyanda Gwala and his family, who provided us with access to their property and crops and who regularly assisted us throughout the duration of this project. You have been vital to the success of this project.

TABLE OF CONTENTS

LIST OF FIGURES

LIST OF TABLES

LIST OF ABBREVIATIONS

AGB	Aboveground Biomass
AfOX	Africa Oxford Initiative
AWS	Automatic Weather Station
CART	Classification and Regression Tree
CRF	Conditional Random Fields
CRP	Calibrated Reflectance Panel
CSV	Comma Separated Value
CWRR	Centre for Water Resources Research
CWSI	Crop Water Stress Index
DAFF	Department of Agriculture Forestry and Fisheries
EBC	Energy Balance Closure
EC	Eddy Covariance
EVI	Enhanced Vegetation Index
FAO	Food and Agricultural Organisation
FCDO	Foreign, Commonwealth & Development Office (UK)
GCP	Ground Control Point
GCS	Global Citation Score
GEE	Google Earth Engine
GLM	Generalised Linear Model
$_{G}$NDVI	Green Normalised Difference Vegetation Index
GNSS	Global Navigation Satellite System
GTB	Gradient Tree Boost
H	Sensible Heat Flux
HFP	Heat Flux Plate
INR	Institute of Natural Resources
IRR	Infrared Radiometer
Kc	Crop Coefficient
kNN	K-nearest Neighbour

LAI	Leaf Area Index
LE	Latent Heat Flux
LST	Land Surface Temperature
LULC	Land Use Land Cover
MAE	Mean Absolute Error
ML	Machine Learning
MLA	Machine Learning Algorithm
NDVI	Normalised Difference Vegetation Index
NDWI	Normalised Difference Water Index
NIR	Near-Infrared
OA	Overall Accuracy
OBIA	Object-based Image Analysis
OSAVI	Optimised Soil Adjusted Vegetation Index
PA	Precision Agriculture or Producer Accuracy
PPK	Post Processing Kinematic
PRISMA-ScR	The preferred reporting items for systematic reviews and meta-analyses extension for scoping reviews
R^2	Coefficient of Determination
NDVIre	Red-edge Normalised Difference Vegetation Index
RF	Random Forest
RGB	Red, Green and Blue
RMSE	Root Mean Square Error
ROI	Region of Interest
RS	Remote Sensing
TIR	Thermal Infrared
TRK	Real Time Kinematic
SADC	Southern African Development Community
SAVI	Soil Adjusted Vegetation Index
SCN	Stochastic Configuration Network
SPAD	Soil Plant Analysis Development

SSA	Sub-Saharan Africa
SVM	Support Vector Machine
SWIR	Shortwave Infrared
TCs	Total Citations
TCARI	Transformed Chlorophyll Absorption in Reflectance Index
UAV	Unmanned Aerial Vehicle
UKZN	University of KwaZulu-Natal
USA	United States of America
VI	Vegetation Index
VIs	Vegetation Indices
VTOL	Vertical Take-off and Landing
VWC	Volumetric Water Content
WRC	Water Research Commission
WDI	Water Deficit Index
WoS	Web of Science

LIST OF SYMBOLS

Δ	Slope of the saturated vapour pressure curve (kPa $°C^{-1}$)
γ	Psychrometric constant (kPa $°C^{-1}$)
Chl	Total chlorophyll concentration per unit leaf area (µmol m^{-2})
ET	Evapotranspiration (mm day^{-1})
ETo	Reference evapotranspiration (mm day^{-1})
ETa	Actual evapotranspiration (mm day^{-1})
ETp	Potential evapotranspiration (mm day^{-1})
G	Germination or Soil Heat Flux (depending on context) (-/ W m^{-2}/ MJ m^{-2} day^{-1})
H	Sensible heat flux (W m^{-2} or MJ m^{-2} day^{-1})
Kc	Crop coefficient (Dimensionless)
Ks	Soil water stress coefficient (Dimensionless)
LE	Latent heat flux (W m^{-2} or MJ m^{-2} day^{-1})
M	Maturation or SPAD value (depending on context) (Dimensionless)
RH	Relative Humidity (%)
Rn	Net radiation (W m^{-2} or MJ m^{-2} day^{-1})
T	Air temperature or Tillering (depending on context) (°C/ -)
Ta	Air Temperature (°C)
Tc	Canopy Temperature (°C)
TSWP	Total soil water profile (mm^{-1})
u_2	Wind speed (m s^{-1})
w	Wind speed (used for LE covariance) (m s^{-1})
q	Specific humidity (kg kg^{-1})
e_s	Saturated vapour pressure (kPa)
e_a	Actual vapour pressure (kPa)

REPOSITORY OF DATA

For details related to the project's data, please contact:

Shaeden Gokool (Project Leader)
Centre for Water Resources Research
School of Agriculture and Science
University of KwaZulu-Natal
Private Bag X01, Scottsville 3209
Pietermaritzburg, South Africa
Email: gokools@ukzn.ac.za

1 INTRODUCTION

1.1 Background and rationale

The rapid expansion of the human population, coupled with the impacts of climate and Land Use Land Cover (LULC) changes, are significant factors that presently contribute to food insecurity issues worldwide (Hall et al., 2017). Since this situation is projected to progressively worsen in the future, improving food security, with a focus on the provision of nutritious food that is produced in an environmentally-sustainable manner, is high on the political agenda of governments throughout the world (Paloma et al., 2020). According to Fan and Rue (2020), over the next few decades, agricultural practices will need to undergo a major overhaul in order to meet the aforementioned targets.

Smallholder farms, which are typically less than two hectares in size, contribute an inordinate amount to food production, relative to the area that they occupy, and they therefore can play a pivotal role in tackling food security challenges (Wolfenson, 2013; Lowder et al., 2014; Kamara et al., 2019; Kpienbaareh et al., 2021). In many developing countries around the world, smallholder farms are not only major contributors to agricultural production and food security, but they are also one of the main drivers of socio-economic growth (Kamara et al., 2019). Despite their relative importance, smallholder farms generally lack the resources of their larger-scale commercial counterparts. Subsequently, their agricultural productivity potential is often not realised, which results in these farms not effectively contributing to addressing the food security and socio-economic challenges (DAFF, 2012; Kamara et al., 2019; Nhamo et al., 2020). In order to remedy this situation, smallholder farmers in developing countries require innovative, evidence-based and low-cost solutions that can assist them in optimising their productivity (Agidew & Singh, 2017; Nhamo et al., 2020).

Several studies have demonstrated the potential of using remote sensing technologies for agricultural applications; however, these applications have typically involved the use of satellite-earth observation or manned aerial vehicles (Manfreda et al., 2018). Satellite-earth observation datasets and associated products are able to provide information at various spatial, spectral and temporal resolutions. However, their application in smallholder farm settings is limited, as the spatial resolution of open-access datasets or products is too coarse to capture the heterogeneity that is generally found within smallholder farms.

Whereas more advanced satellite-earth observation systems and manned-aerial vehicles, which can capture data at finer spatial resolutions (metre to sub-metre spatial resolution), are often too costly for widespread smallholder agricultural applications (Cucho-Padin et al., 2019). Furthermore, satellite revisits and repeat cycles, coupled with the influence of cloud cover, reduce the frequency at which the data can be captured and processed (Manfreda et al., 2018; Nhamo et al., 2020). Recently, precision agricultural practices, facilitated by the use of Unmanned Aerial Vehicles (UAVs), have been gaining traction in the agricultural sector (Radoglou-Grammatikis et al., 2020; Cucho-Padin et al., 2020; Delavarpour et al., 2021). UAVs have been shown to hold vast potential for agricultural applications, as relatively low-flying UAVs can potentially capture very high spatial resolution data at various spectral resolutions (depending on the optical properties of the on-board camera). Moreover, data can be captured autonomously at user-determined intervals, with this data being less severely impacted by the effects of cloud cover, thus allowing for data to be captured more frequently than the satellite-based approaches (Torres-Sánchez et al., 2014; Manfreda et al., 2018; Bennet et al., 2020; Cucho-Padin et al., 2020).

The aforementioned features, as well as their relatively lower costs, have seen UAVs emerge as a promising tool for smallholder agricultural applications (Salami et al., 2014; Cucho-Padin et al., 2020). While a great deal of potential exists for the use of UAVs in smallholder agricultural applications, processing the UAV data is more complex than capturing the imagery. UAV data processing can be computationally intensive and may require expensive specialised software and user expertise that are not always readily available (Bennet et al., 2020). Advances in geospatial cloud computing platforms, such as the Google Earth Engine (GEE), have provided a means to address these limitations, by providing users with, inter alia, high level computational power and sophisticated image analysis techniques (Gorelick et al., 2020). According to Bennet et al. (2020), with the increased use of UAVs for various applications and the growing popularity of utilising cloud-based computing platforms for image analysis, it is important to develop reproducible and adaptable techniques that can be easily shared, in order to facilitate a more efficient analysis of UAV imagery for future applications. To this end, the focus of this project will be to explore and demonstrate the use of GEE and multispectral UAV imagery to enhance the productivity of smallholder farms by mapping the cultivated areas, quantifying the crop water use and assessing the health of these crops.

1.2 Project aims and objectives

The overall aim of this project is to explore and demonstrate the utility of using multispectral UAV imagery and geospatial cloud computing to enhance the productivity of smallholder farms, by mapping the cultivated areas, quantifying the crop water use and assessing the crop health. The following specific objectives have been identified to fulfil the main aim of the project:

- To provide a literature review on the use of UAVs as a tool, in order to facilitate precision agriculture relating to spatiotemporal crop growth dynamics.
- To develop and set up advanced image analysis techniques in GEE, in order to develop reproducible and adaptable data processing and analysis procedures.
- To provide seasonal maps of LULC to monitor spatiotemporal changes.
- To validate (against in-situ observations) remote sensing-based methods that can be employed to estimate evapotranspiration (ET), by using multispectral UAV imagery.
- To assess the spatiotemporal crop health dynamics by using vegetation indices that can provide information, such as vegetation density, leaf chlorophyll content and water stress.
- To facilitate knowledge transfer, through the development of web-based interactive and spatially-explicit maps of crops, which can be readily shared online and are relatively easy to interpret.

1.3 Project scope

This project built upon and extended the research that is currently underway in WRC Project No. WRC K5/2791//4 entitled the "Use of drones in monitoring crop health, water stress, crop water requirements and improve on crop water productivity to enhance precision agriculture and irrigation scheduling". This was achieved by including a more intensive field-based component to allow for the longer-term evaluation of the accuracy of the derived outputs, by using the UAV imagery, and to also demonstrate how the use of UAV imagery fares in comparison to the use of freely-available satellite-earth observation data, which has been commonly used for PA applications.

Central to these efforts, were: (i) the collection of ground truth data to validate the accuracy of the LULC maps that were produced, (ii) the measurement/estimation of ET, using traditional field-based approaches, and (iii) the measurement of vegetation indices that can be used as a proxy for vegetation health.

1.4 Structure of the report

Overall, the report is organised into seven chapters. However, the specific focus of a particular Chapter or Chapters is structured and organised according to the objectives that are identified for each project Deliverable. These are described below and they are summarised in Figures 1.1 and 1.2:

- Chapters one and two, respectively, provide a brief overview of the study and a comprehensive review of the literature relating to the use of UAVs to facilitate precision agricultural applications on smallholder farms (Objective one).
- Chapter three provides a description of the study site, whilst Chapter four provides a comprehensive analysis which focuses on evaluating the potential of utilising UAV-acquired data and geospatial cloud computing, in order to map croplands within the smallholder farm setting (Objectives two and three).
- The focus of Chapter five is to identify and evaluate the potential of UAV-based methods to facilitate precision water management, with particular focus on ET estimation (Objective four). The emphasis is placed upon trying to identify or develop methods that are best-suited to the socio-economic circumstances of smallholder farmers within the region and to establish the veracity of these approaches, by means of comparisons against in-situ measurements.
- Many smallholder farmers, who predominantly practice dryland agriculture, suffer substantial yield losses, due to water-related challenges that are caused by unreliable rainfall. Since most UAV-based multi-spectral sensors that are used in PA applications lack the spectral resolution to detect water stress, when using commonly-applied remote sensing-based techniques, the focus of Chapter six is to develop and evaluate a novel ML-based framework that integrates UAV-acquired multispectral data with Sentinel-2 satellite imagery for predicting water stress.

- Chapter seven provides a synthesis of the key findings. This involves: (i) revisiting the objectives of the study and a summary of the key findings, (ii) the contributions of research to new knowledge, (iii) the challenges experienced during the duration of this study, (iv) the future research opportunities, and v) the concluding remarks.

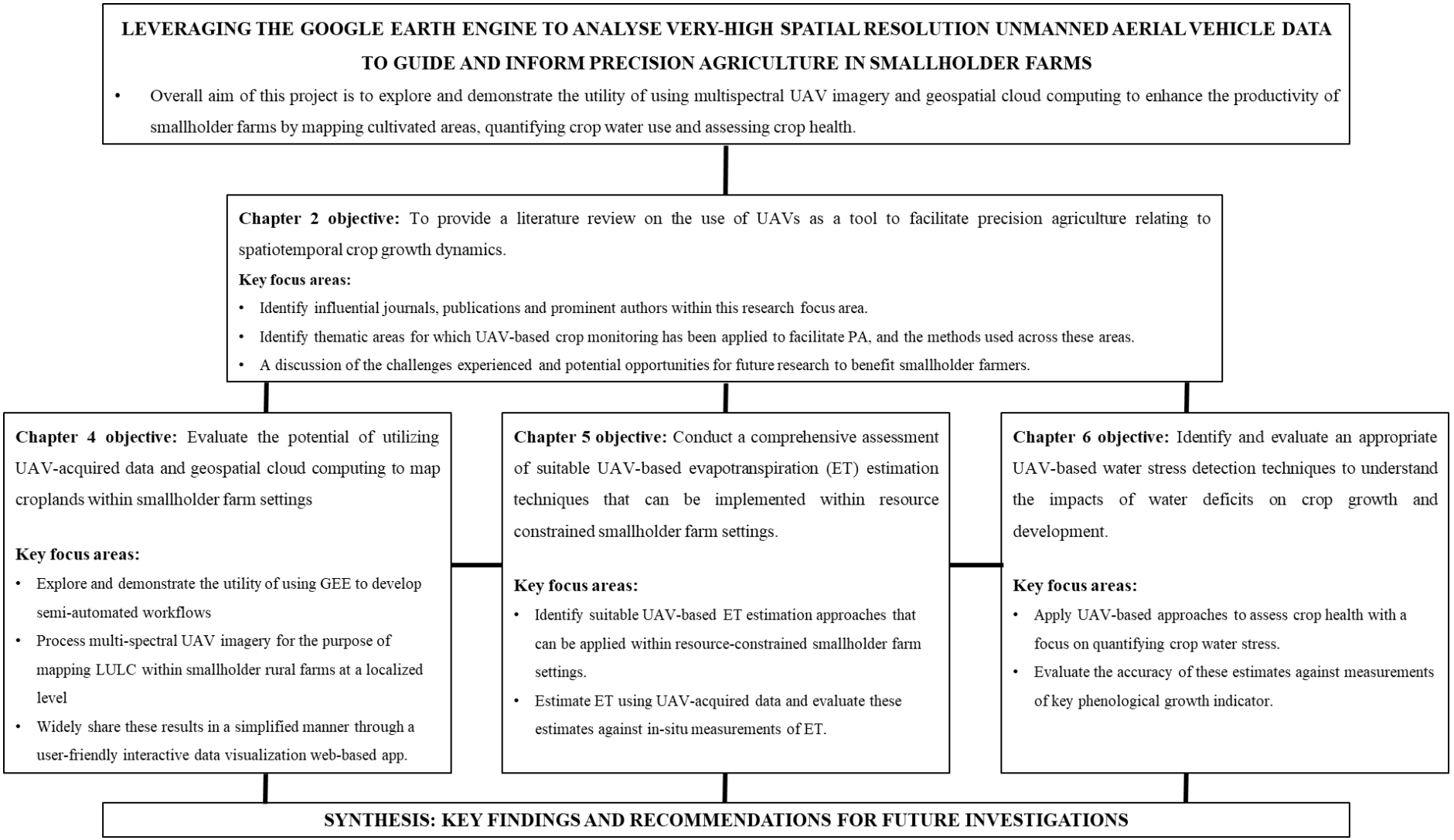

Figure 1.1 Conceptual framework of the study

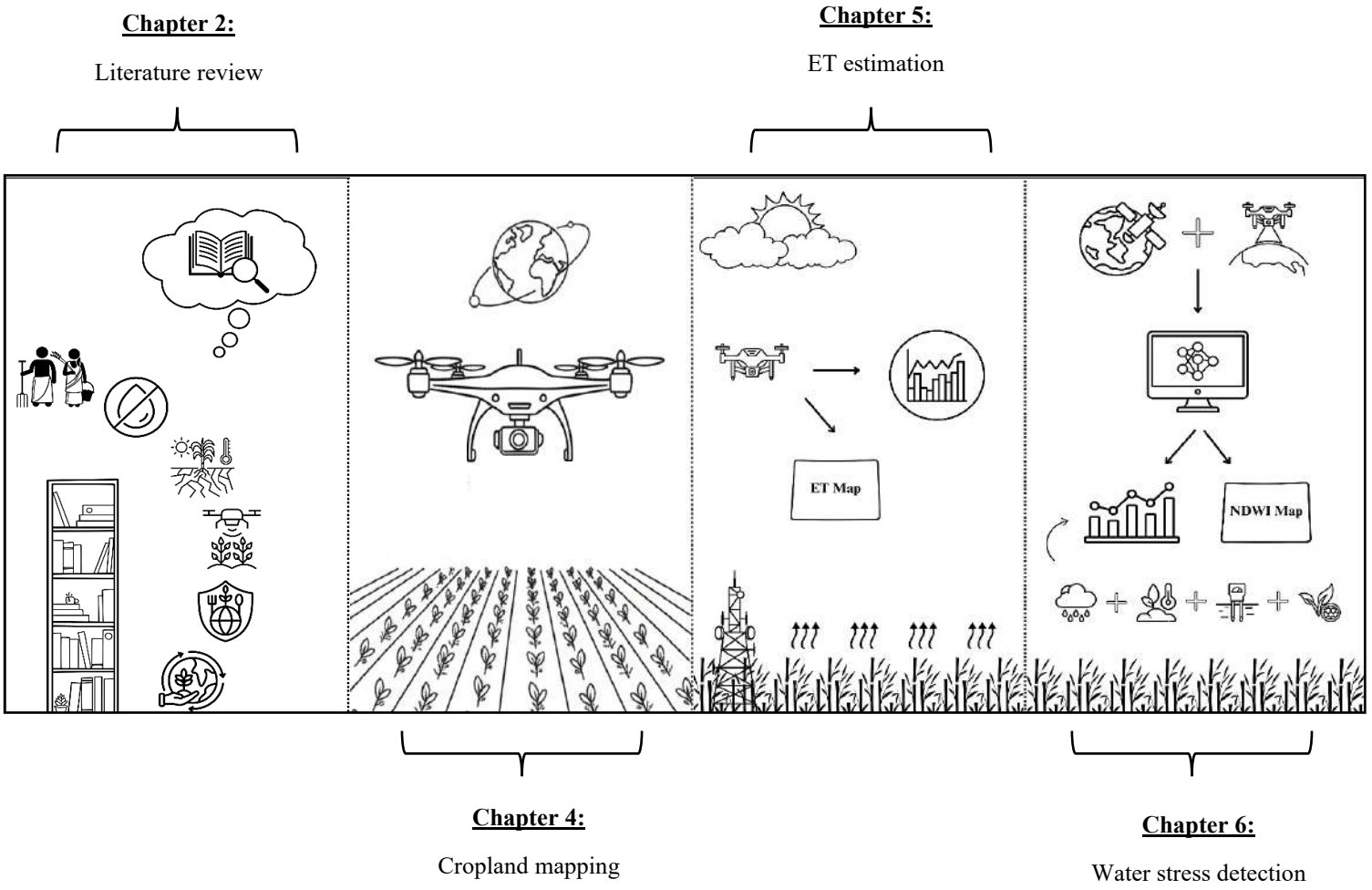

Figure 1.2 Key focus areas within each chapter

1.5 References

AGIDEW AA and SINGH KN (2017) The implications of land use and land cover changes for rural household food insecurity in the North-eastern highlands of Ethiopia: the case of the Teleyayen sub-watershed. *Agriculture & Food Security* **6**.

BENNET MK, YOUNES N and JOYCE K (2020) Automating Drone Image Processing to Map Coral Reef Substrates using Google Earth Engine. *Drones* **4** (3).

CUCHO-PADIN G, LOAYZA H, PALACIOUS S, BALCAZAR M, CARBAJAL M and QUIROZ R (2020) Development of low-cost remote-sensing tools and methods for supporting smallholder agriculture. *Applied Geomatics* **12** 247–263.

DELAVARPOUR N, KOPARAN C, NOWATZKI J, BAJWA S and SUN X (2021) A Technical Study on UAV Characteristics for Precision Agriculture Applications and Associated Practical Challenges. *Remote Sensing* **13**.

DEPARTMENT OF AGRICULTURE, FORESTRY AND FISHERIES (DAFF) (2012) A framework for the development of smallholder farmers through cooperatives development. Directorate Co-operative and Enterprise Development, Department of Agriculture, Forestry and Fisheries, South Africa.

FAN S and RUE C (2020) The Role of Smallholder Farms in a Changing World. The Role of Smallholder Farms in Food and Nutrition Security.

GORELICK N, HANCHER M, DIXON M, ILYUSCHENKO S, THAU D and MOORE R (2017) Google Earth Engine: Planetary-scale geospatial analysis for everyone. *Remote Sensing of Environment* **202** 18–27.

HALL C, DAWSON TP, MACDIARMID JI, MATTHEW RB and SMITH P (2017) The impact of population growth and climate change on food security in Africa: looking ahead to 2050. *International Journal of Agricultural Sustainability* **15**(2) 124–135.

KAMARA A, CONTEH A, RHODES ER and COOKE RA (2019) The Relevance of Smallholder Farming to African Agricultural Growth and Development. *African Journal of Food, Agriculture, Nutrition and Development* **19**(1) 14043–14065.

KPIENBAAREH D, SUN X, WANG J, LUGINAAH I, KERR RB, LUPAFYA E and DAKISHONI L (2021) Crop Type and Land Cover Mapping in Northern Malawi using the Integration of Sentinel-1, Sentinel-2, and PlanetScope Satellite Data. *Remote Sensing* **13**.

LOWDER S, SKOET J and SINGH S (2014) What do we really know about the number and distribution of farms and family farms in the world? Background paper for the state of food and agriculture 2014, ESA working paper 14–02 (Rome: Food and Agriculture Organization of the United Nations (FAO), Agricultural Development Economics Division, 2014).

MANFREDA S, MCCABE M, MILLER P, LUCAS R, PAJUELO MV, MALLINIS G, BEN DOR E, HELMAN D, ESTES L, CIRAOLO G, MÜLLEROVÁ J, TAURO F, DE LIMA MI, DE LIMA JLMP, MALTESE A, FRANCES F, CAYLOR K, KOHV M, PERKS M, RUIZ-PÉREZ G, SU Z, VICO G and TOTH B (2018) On the use of unmanned aerial systems for environmental monitoring. *Remote Sensing* **10** 641.

NHAMO L, MAGIDI J, NYAMUGAMA A, CLULOW AD, SIBANDA M, CHIMONYO VGP and MABHAUDHI T (2020) Prospects of Improving Agricultural and Water Productivity through Unmanned Aerial Vehicles. *Agriculture* **10** 256.

PALOMA SGY, RIESGO L and LOUHICHI K (2020) The Role of Smallholder Farms in Food and Nutrition Security. Impact Analysis of Agri-Food Policies on Food and Nutrition Security in SSA.

RADOGLOU-GRAMMATIKIS P, SARIGIANNIDIS P, LAGKAS T and MOSCHOLIOS I (2020) A compilation of UAV applications for precision agriculture. *Computer Networks* **172**.

SALAMÍ E, BARRADO C and PASTOR E (2014) UAV flight experiments applied to the remote sensing of vegetated areas. *Remote Sensing* **6** 11051–11081.

TORRES-SÁNCHEZ J, PEÑA JM, DE CASTRO AI and LÓPEZ-GRANADOS F (2014) Multi-temporal mapping of the vegetation fraction in early-season wheat fields using images from UAV. *Computers and Electronics in Agriculture* **103** 104–113.

WOLFENSON K (2013) Coping with the food and agriculture challenge: smallholders' agenda. Food and Agriculture Organization of the United Nations, Rome, Italy.

2 LITERATURE REVIEW

2.1 Introduction

Food insecurity has been gradually increasing and remains a major concern for the global population (Hall et al., 2017; Paloma et al., 2020; Panday et al., 2020; Segarra et al., 2020; FAO, 2021; Rejeb et al., 2022). While agricultural production has substantially increased over the past few decades, the demand for food to sustain the expanding population continues to increase (Nhamo et al., 2020). The limited availability of arable land and water resources, the impacts of climate change, and the need to promote environmentally-sustainable agricultural practices (Elahi et al., 2022a; Elahi & Khalid, 2022; Zhang et al., 2022) are likely to accentuate the pressures that are exerted upon the existing agricultural food production systems (Abbas et al., 2022a, b; Elahi et al., 2022b).

Therefore, eradicating hunger and malnutrition by 2030 appears to be an elusive goal, which has been further compounded by the impacts of the COVID-19 pandemic (Panday et al., 2020). Considering that many of the abovementioned challenges are likely to play a more prominent role in the future, the longevity and productivity of these agricultural food production systems are under significant threat (Segarra et al., 2020). With many of these systems unable to keep pace with the existing food demands, there is a need to improve their sustainability and productivity (Matton et al., 2015). This is particularly relevant for smallholder farms which, despite their relatively small size (< two hectares), are major contributors to agricultural food production, food security and socio-economic development (Kamara et al., 2019).

However, many of these smallholder farmers lack the critical resources and financial support. Subsequently, their actual productivity severely lags their potential, which ultimately limits their ability to improve the food security (Kamara et al., 2019; Nhamo et al., 2020). To remedy this situation, these smallholder farmers require cost-effective and context-specific information to guide their operations, in order to maximise their productivity, whilst optimally utilising their available resources (Agidew et al., 2017; Nhamo et al., 2020). Over the past decade, the precision agriculture (PA) paradigm has been gaining traction within the agricultural sector, and it is potentially well-suited to deliver on these targets.

PA practices involve the application of several bespoke management interventions and strategies that are guided and informed by the state-of-the-art data collection, analysis and communication technologies to enhance crop productivity, to reduce the unnecessary losses of critical resources, such as water and nutrients, as well as to mitigate the potentially harmful impacts on the environment (Boursianis et al., 2020; Sishodia et al., 2020). According to Boursianis et al. (2020), the agricultural sector has appeared to be embracing the fourth industrial revolution in recent times, with remote sensing technologies featuring quite prominently in PA applications.

Although remote sensing has been used for various agricultural applications since the late 1970s, recent advancements in satellite-earth observation technologies, UAVs and geospatial cloud computing have created new and exciting possibilities, in order to utilise these technologies more effectively as decision-support tools and to optimise agricultural operations, by supporting crop management interventions, such as monitoring, mapping, irrigation and plant diagnosis, to name a few (Sishodia et al., 2020; Bukowiecki et al., 2021; Rejeb et al., 2022). However, the use of these technologies, specifically for crop monitoring, to guide PA applications, such as fertiliser application and management, crop water use, crop vigour and yield assessment, have featured most prominently across smallholder multi-cropping farming systems (Yonah et al., 2018; El-Hendawy et al., 2019; Adewopo et al., 2020; Argento et al., 2021; Brewer et al., 2022a).

Despite their potential for PA applications, the characteristics of remote sensing sensors, i.e. their spatial, spectral and temporal resolution, largely dictate how these technologies can be utilised effectively. Generally, a trade-off exists between the spatiotemporal resolution of freely-available and publicly-accessible satellite-earth observation datasets. For example, Landsat (at 30 m) and Moderate Resolution Imaging Spectroradiometer (at 250 m) imagery are characterised by spatial resolutions that are generally too coarse for small fields with mixed crops. Furthermore, the temporal resolution of satellite sensors, which can be further compounded by cloud cover, may limit their feasibility for the routine monitoring of crops throughout the growing season (Schut et al., 2018; Wahab et al., 2018; Yonah et al., 2018; Bollas et al., 2021; Defourny et al., 2019).

While more advanced satellite-earth observation systems and manned-aerial vehicles can overcome these spatiotemporal limitations, the costs associated with data acquisition through these platforms often limit their use for widespread PA applications (Cucho-Padin et al., 2020).

The unique characteristics of UAVs, also known as drones, such as their ability to provide a cost-efficient means of accessing high-quality, spatially-explicit data at user-defined intervals, have seen them emerge as one of the most promising tools to facilitate PA practices (Cucho-Padin et al., 2020; Panday et al., 2020; Sibanda et al., 2021). Despite their immense potential, these technologies possess limitations, which may limit their feasibility for PA applications (Panday et al., 2020; Sibanda et al., 2021; Rejeb et al., 2022). With the application of UAVs in agriculture becoming more prevalent, and their potential to facilitate PA practices in smallholder farms being increasingly recognised, it is important to develop a deeper understanding regarding the state of play on the use of UAVs for crop monitoring, in order to facilitate PA practices in the context of smallholder farms.

While the evaluation of UAVs for PA has been well-documented (Panday et al., 2020), there are limited reviews that focus specifically on smallholder farm applications. Nhamo et al. (2020) examined the potential PA applications of UAVs in smallholder farms to improve their water use efficiency and to enhance agricultural productivity. Sibanda et al. (2021) evaluated the potential of using UAVs to assess the water quality and quantity. They highlighted existing challenges and prospective opportunities to utilise these technologies, in order to improve crop water productivity in smallholder farms. Although these reviews were comprehensive and yielded new and invaluable insights, they focus largely on the potential of UAVs, specifically in mapping the quality and quantity of irrigation water and evaluating their potential in mapping irrigated farms. As a result, our knowledge and understanding of how these technologies are being utilised to monitor crops and facilitate PA practices in smallholder farms is limited.

In order to address this knowledge gap, we have provided an up-to-date and concise bibliometric and systematic evaluation of the literature pertaining to the actual application of UAVs for crop monitoring on smallholder farms, in order to facilitate PA. This study also complements the aforementioned reviews and expands upon the existing body of knowledge on this emerging topical research focus area. Furthermore, this review serves as a potentially-useful resource for acquiring a greater insight into the use of UAVs, to facilitate PA practices on smallholder farms. To this end, this study performed a scoping review to explore and evaluate the use of UAVs to monitor crops in smallholder farms, in order to facilitate PA. Within the context of this study, the term ‘crops’ includes grains, fruits or vegetables.

The techniques involved in bibliometric and scientometric research, such as mapping, clustering, co-citation and co-occurrence analyses, are commonly utilised to gain a greater perspective on a particular research topic (Waltman et al., 2010; Rejeb et al., 2022). The use of tools to facilitate this process, such as Biblioshiny and VOSviewer, has become a common practice among researchers (Bhagat et al., 2022; Mühl et al., 2022; da Costa et al., 2023), as they allow for trends to be more easily identified and visualised by: (i) highlighting the research that has shaped our understanding of a particular research focus area, (ii) identifying key themes within the literature, (iii) illuminating the links between these themes, and iv) exploring their evolution over time (Linnenluecke et al., 2020; Brika et al., 2021; Sibanda et al., 2021; Rejeb et al., 2022).

This scoping review addressed the following specific objectives:

- The identification of influential journals, publications and prominent authors within this research focus area;
- The identification of thematic areas whereby UAV-based crop monitoring has been applied, to facilitate PA, and the methods that are used across these areas; and
- A discussion of the challenges that are experienced and the potential opportunities for future research, in order to benefit smallholder farmers.

This review is organised as follows: following this introduction in Section 2.1, the methods used to select and evaluate the literature are presented in Section 2.2, while the key findings of the bibliometric analysis are described in Section 2.3. In Section 2.4, we present an overview of the general trends, challenges and future opportunities that are related to using UAVs to monitor crops on smallholder farms, to facilitate PA. Finally, the conclusions and limitations of the study are presented in Section 2.5.

2.2 Materials and methods

The bibliometric database was compiled on the 06th of December 2022 by searching the Scopus and Web of Science (WoS) abstracts and citation databases for keywords and variants, using the following query string: “("smallholder farm*" OR "smallholder farming" OR "smallholder agriculture" OR "small scale farm*" OR "small scale agriculture") AND ("UAV" OR "Drone")”.

The selection and structure of keywords that were used during the search was an iterative process, which was guided by the authors' experience in this particular research focus area, as well as the previous literature that was identified through preliminary searches in Google Scholar. The search was conducted without applying any constraints on the timespan; however, articles that were not published in accredited peer-reviewed journals and not written in English were excluded. The search results returned 36 and 31 references for Scopus and WoS, respectively. The retrieved references (n = 67) were then saved and imported into the R environment (using the bibliometrix-R package). They were combined into a single database, before being screened for their eligibility. The preferred reporting items for systematic reviews and meta-analyses extension for scoping reviews (PRISMA-ScR) framework (Tricco et al., 2018) was used to avoid biased reporting, by guiding decisions relating to the selection of articles to be included or excluded from the review (Figure 2.1). The eligibility criteria for the review were defined as follows; (i) the focus of the study was exclusively on the actual application of UAV technologies for monitoring crops in a smallholder farm setting, to facilitate PA, and (ii) the full-length article was available and accessible.

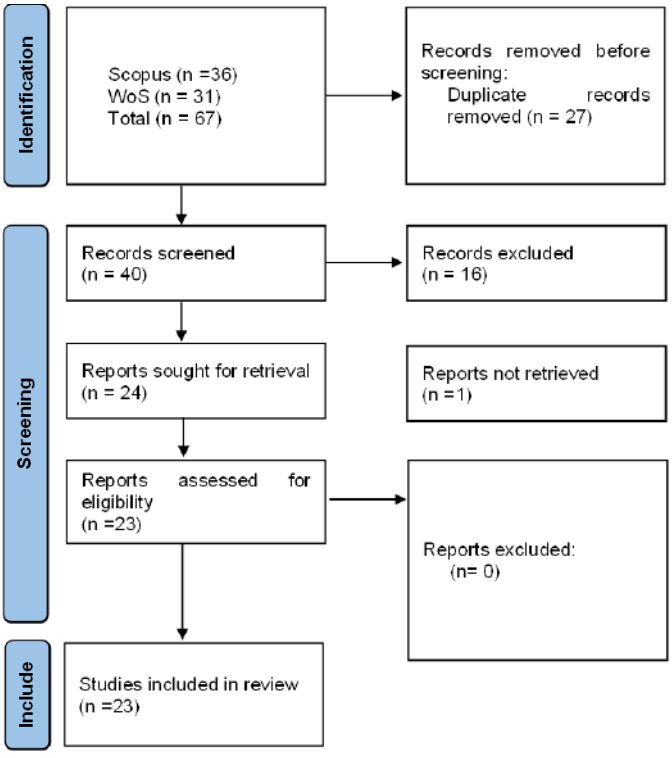

Figure 2.1 PRISMA-ScR flow diagram for article selection

Duplicate records that were identified within the initial search were removed, and two researchers examined the remaining articles to ensure that they conformed to the eligibility criteria. After screening the titles and abstracts of these articles, 24 full-length articles were identified as being eligible and were sought for downloading. However, one of these articles was inaccessible. No additional articles were sought following this process. Once the final database (n = 23) had been compiled, key bibliometric data were then extracted, analysed and mapped, by using the Biblioshiny App and VOSviewer software (van Eck et al., 2010; Aria et al., 2017) to address the objectives of the study.

2.3 Results

2.3.1 Historical evolution

A summary of the key statistics regarding the final literature dataset is provided in Table 2.1. Research on using UAVs to monitor the crops on smallholder farms, in order to facilitate PA, first emerged in 2016 and it has been gradually increasing with a compound annual growth rate of ~ 31%. The highest productivity was achieved in 2020, with eight articles being published this year, which represent ~ 36% of the total publications (Figure 2.2).
The period 2017-2018 had the highest average Total Citations (TCs) per publication, peaking at 30.80. In comparison, the highest average TCs per year occurred in 2021 at 16.5.

Table 2.1 A summary of the key bibliographic information about the final literature dataset

Description	Results	Description	Results
Timespan	2016-2022	Keywords Plus (ID)	187
Number of journals	15	Author's Keywords (DE)	81
Number of publications	23	Authors	131
Annual Growth Rate %	30.77	Authors of single-authored docs	0
Document Average Age	2.26	Single-authored docs	0
Average citations per doc	17.13	Co-Authors per doc	6.57
References	1071	International co-authorships %	8.70

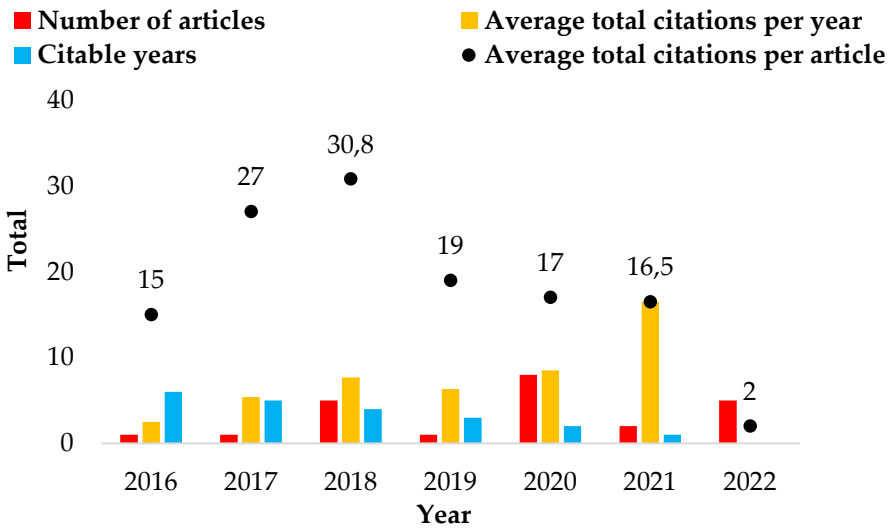

Figure 2.2 Annual distribution of average yearly citations and publications pertaining to the use of UAVs to facilitate PA on smallholder farms

2.3.2 Most influential journals

The final literature database consisted of 15 journals with 23 publications on using UAVs to monitor crops on smallholder farms, to facilitate PA. The journals, *Drones* and *Remote Sensing*, have the highest number of articles, accounting for ~ 35 % of the total number of publications. *Drones* also retain its position at the top of the rankings for TCs, with 109. Therefore, this is the dominant journal in this particular research focus area. Figure 2.3 provides a graphical illustration of the core journals that are classed according to Bradford's Law, which is used to establish the relationship between published articles and the journals they have been published in.

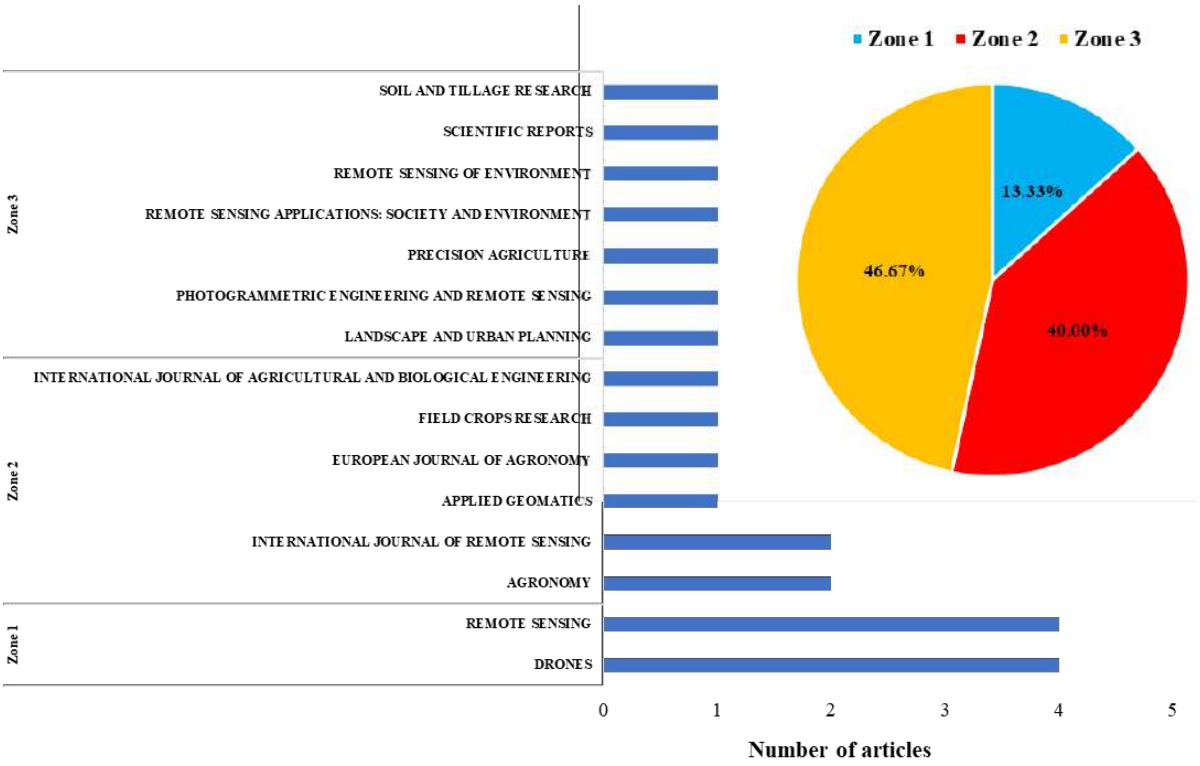

Figure 2.3 Classification of journals, according to Bradford's Law, which contribute to the publication of research pertaining to the use of UAVs to facilitate PA on smallholder farms

According to Bradford's Law, there are broadly three zones that can be used to categorise the frequency of citations emanating from journals for a particular research focus area. Zone 1 represents the most influential journals, as they are cited most frequently in that subject area and are likely attract the greatest interest from researchers. Zones 2 and 3 represent the journals with the average and least citations, respectively (Ranjbari et al., 2022).

Based on Bradford's Law, eight articles were published in two journals that were categorised as Zone 1; eight were published in six journals that were categorised as Zone 2, and seven were published in seven journals that were categorised as Zone 3. As shown in Table 2.2, *Drones* and *Remote Sensing* also appear at the top of the most influential journals, when ranked according to their productivity, TCs and citation impact (H-index).

Table 2.2 Productivity of the publication sources ranked in the table, according to the number of articles published

Journal	Number of publications	TCs	h-index	Publication year start
DRONES	4	109	3	2018
REMOTE SENSING	4	26	3	2016
AGRONOMY	2	22	2	2019
INTERNATIONAL JOURNAL OF REMOTE SENSING	2	30	2	2018
APPLIED GEOMATICS	1	12	1	2020
EUROPEAN JOURNAL OF AGRONOMY	1	1	1	2022
FIELD CROPS RESEARCH	1	46	1	2018
INTERNATIONAL JOURNAL OF AGRICULTURAL AND BIOLOGICAL ENGINEERING	1	27	1	2017
PHOTOGRAMMETRIC ENGINEERING AND REMOTE SENSING	1	7	1	2020
PRECISION AGRICULTURE	1	29	1	2021
REMOTE SENSING APPLICATIONS: SOCIETY AND ENVIRONMENT	1	13	1	2020
REMOTE SENSING OF ENVIRONMENT	1	34	1	2020
SCIENTIFIC REPORTS	1	4	1	2020
SOIL AND TILLAGE RESEARCH	1	34	1	2020
LANDSCAPE AND URBAN PLANNING	1	0	0	2022

2.3.3 Analysis of publications by country

Regarding the geographic distribution of published research on the use of UAVs to monitor crops on smallholder farms, to facilitate PA, 14 countries have been involved in this particular research field. China, South Africa, Nigeria, Switzerland and the USA are the only countries to have produced more than one publication on the use of UAVs to facilitate PA on smallholder farms and account for ~ 61% of the total number of publications. While these countries rank within the top five for the number of publications produced, when considering TCs and the average citations per publication, only China features consistently within the top five. Collaborations between authors have been mostly restricted to the countries in which they reside; however, there are a few examples of international collaboration (Figure 2.4). In total, four unique collaboration links are identified, with the strength of these links remaining the same for each collaboration, i.e. only a single published co-authored publication has emanated from each of these links.

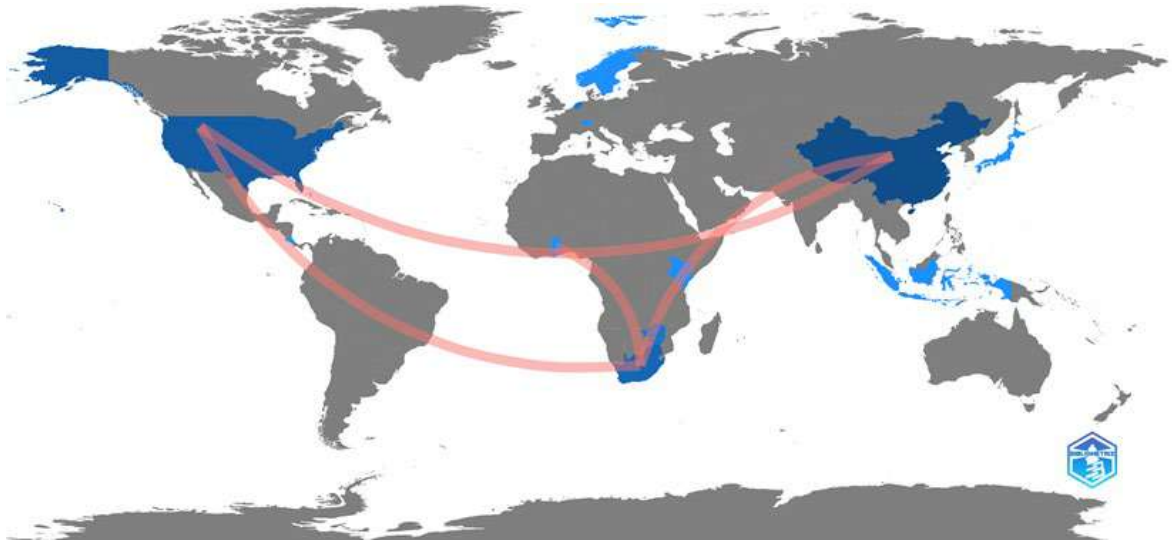

Figure 2.4 Global publications and collaborations, whereby the darker the shade of blue represents the larger the number of publications, with the lines indicating international collaboration

2.3.4 Most influential authors and citation analysis

A total of 131 authors contributed to the 23 publications on using UAVs to facilitate PA on smallholder farms; however, none were single-authored. One-hundred-and-fifteen authors published only a single article, whereas 16 published two or more.

The key author-level performance metrics of the 16 authors with more than one publication are shown in Figure 2.5. Vimbayi Chimonyo, Alistair Clulow, Tafadzwanashe Mabhaudhi and Mbulisi Sibanda have been the most active authors in this particular research focus area. Ola Hall and Magnus Jirström have received the highest number of citations. The publications were analysed according to their Global Citation Score (GCS), their average TCs per year and their normalised citation score (Table 2.3). The GCS is representative of the TCs, a publication that is received in the abstract and citation databases (Scopus and Web of Science) that were used and that includes citations received from publications in other disciplines (Ranjbari et al., 2022).

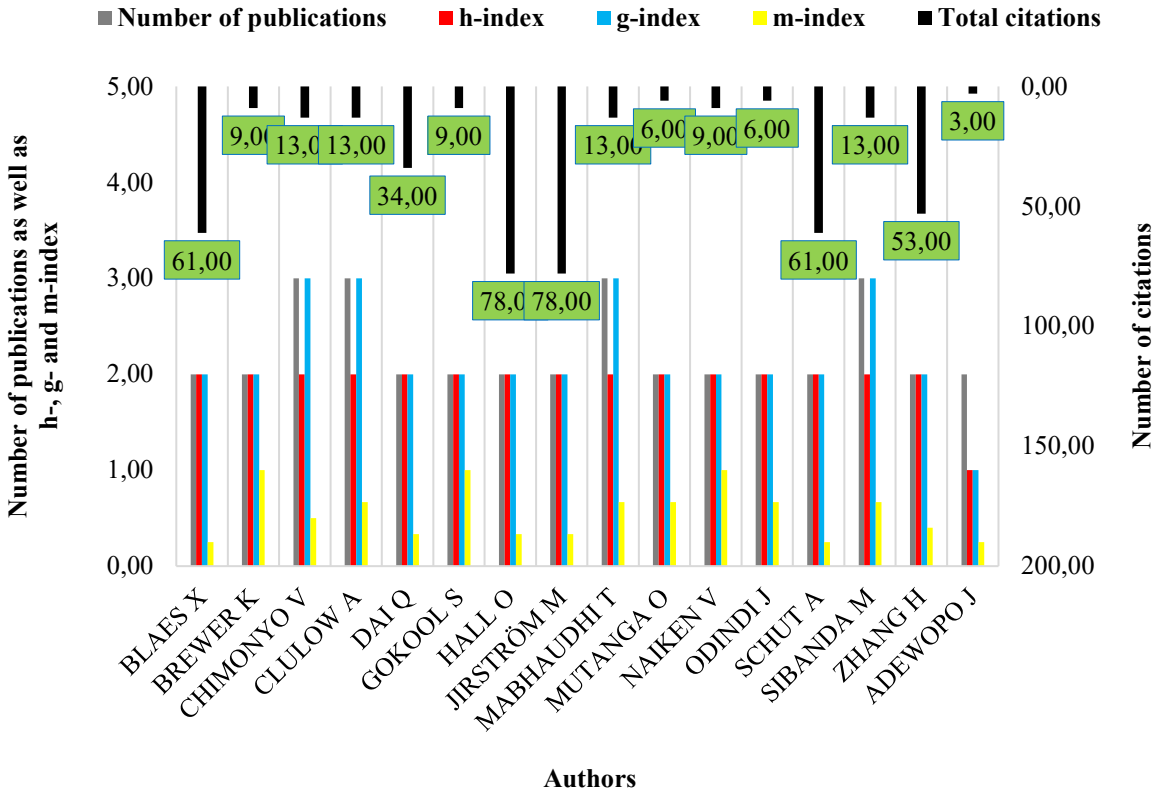

Figure 2.5 Analysis of key author-level citation metrics for authors with more than one publication

The publication by Wahab et al. (2018), which evaluated the use of a UAV-derived vegetation index to assess the vigour and yield of maize during its various growth stages, received the highest number of TCs, and it is among four publications to have received more than ten citations per year. Their investigations demonstrated that using a UAV-derived vegetation index could adequately quantify the growth and vigour of maize, despite the complex heterogeneous nature of the smallholder farming systems from which it was derived.

The highest-ranking publication with regards to average TCs per year is by Argento et al. (2021), which is also among the top five for most TCs. Argento et al. (2021) explored using UAV-derived data to guide variable rate fertiliser application in small-medium-scale farming systems. Their study revealed that the use of UAV-derived data was able to guide management decisions and contributed to the improved efficiency of fertiliser application by ~ 10%, which was achieved by redistributing and reducing the amount of fertiliser that was applied.

Table 2.3 Global citation score of publications (in chronological order) relating to the use of UAVs to facilitate PA on smallholder farms

Author	Journal	TCs	TC per year	Normalised TC
Blaes et al. (2016)	Remote Sensing	15	2.14	1
Du et al. (2017)	International Journal of Biological and Agricultural Engineering	27	4.5	1
Wahab et al. (2018)	Drones	51	10.2	1.66
Schut et al. (2018)	Field Crops Research	46	9.2	1.49
Hall et al. (2018)	Drones	27	5.4	0.88
Wang et al. (2018)	International Journal of Remote Sensing	17	3.4	0.55
Yonah et al. (2018)	International Journal of Remote Sensing	13	2.6	0.42
Chen et al. (2019)	Agronomy	19	4.75	1
Zhao et al. (2020)	Remote Sensing of Environment	34	11.33	2
Guo et al. (2020)	Soil and Tillage Research	34	11.33	2
Chew et al. (2020)	Drones	29	9.67	1.71
Breunig et al. (2020)	Remote Sensing Applications: Society and Environment	13	4.33	0.76
Cucho-Pardin et al. (2020)	Applied Geomatics	12	4	0.71
Peter et al. (2020)	American Society for Photogrammetry and Remote Sensing	7	2.33	0.41
Gracia-Romero et al. (2020)	Scientific Reports	4	1.33	0.24
Adewopo et al. (2020)	Agronomy	3	1	0.18
Argento et al. (2021)	Precision Agriculture	29	14.5	1.76
Ndlovu et al. (2021)	Remote Sensing	4	2	0.24
Brewer et al. (2022a)	Remote Sensing	7	7	3.5
Brewer et al. (2022b)	Drones	2	2	1
Jiang et al. (2022)	European Journal of Agronomy	1	1	0.5
Kleinschroth et al. (2022)	Landscape and Urban Planning	0	0	0
Alabi et al. (2022)	Remote Sensing	0	0	0

The most highly-cited paper, based on the normalised citation performance metric, was Brewer et al. (2022a). In this study, the authors utilised UAV-acquired multispectral imagery, in concert with machine learning, to predict the chlorophyll content of smallholder maize during the various phenological growth stages. The results of the study demonstrated that the spatiotemporal variability in chlorophyll could be accurately estimated, based on the aforementioned approach, and that it could therefore serve as an important tool for supporting management applications within smallholder farms. In addition to the aforementioned studies, others that are worth noting are studies by Guo et al. (2020) and Zhao et al. (2020). While these studies did not feature at the top of any of the citation performance metrics, they were the only studies to feature in the top-five across the various citation metrics used. Guo et al. (2020) demonstrated how time-series multispectral imagery, captured by a UAV and machine learning, could be used to develop soil models, in order to predict the field-scale soil organic carbon. Zhao et al. (2020) developed a unique approach based on conditional random fields (CRF) to map crops within heterogeneous smallholder farms by using UAV-acquired red, green and blue (RGB) and hyperspectral imagery. The results of the study demonstrated that improved classification performance could be attained by using the CRF method, when utilising high spatial and spectral resolution datasets.

2.3.5 Analysis of keyword frequency, growth and co-occurrence

The author keywords and the keywords-plus metric offered in the Bibiloshiny package were used to evaluate the most relevant words or phrases within the final literature dataset. Keywords-plus identifies the words or phrases that routinely appear in the titles of the publication's references, but not within the publication's title or author's keywords (Abafe et al., 2022). The most frequently-used author keywords that have appeared more than once are presented in Figure 2.6. The presence of 'Drones' among the top-5 author keywords demonstrates that there is variability in the use of terms by authors to describe UAV technologies, but 'UAV' is the more popular option.

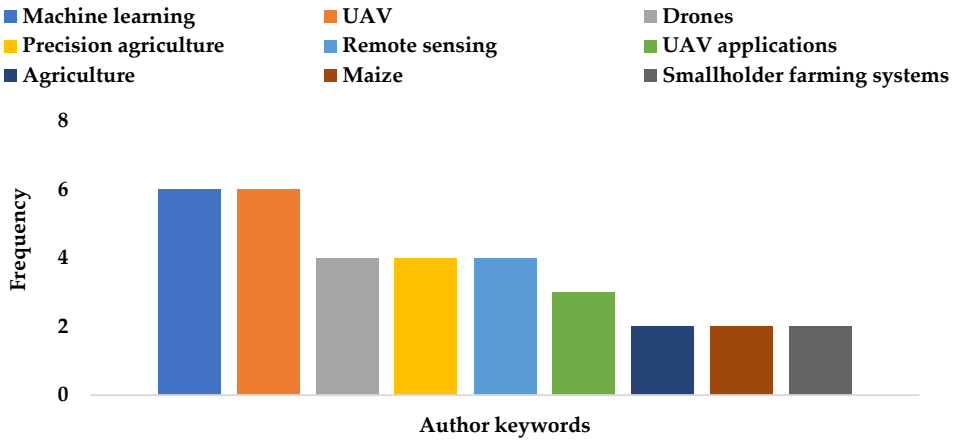

Figure 2.6 Frequency of author's keywords

The words 'remote sensing', 'unmanned aerial vehicles (UAV)', and 'crops' are among the top-five keywords plus (Figure 2.7). The presence of words such as 'food security', 'nitrogen', 'chlorophyll' and 'fertilisers' provide an indication of some of the key focus areas of UAV applications within smallholder farms. Whereas the presence of 'machine learning' in both the author keywords and keywords plus indicates the preference to utilise these approaches when working with UAV-acquired data. VOSviewer software version 1.6.18 was used to develop a keyword co-occurrence network. The co-occurrence analysis (Figure 2.8) was performed on a total of 13 keywords with a frequency of ≥ 4 selected from the 245 keywords within the final literature database. Three clusters of related terms, depicted in different colours, were identified. The keywords are represented by nodes, where the size of the nodes represents their frequency of occurrence, with the distance between the nodes representing the strength of their relationship.

The three clusters may serve as broad indicators of the general trends in using UAVs to facilitate PA on smallholder farms. The blue cluster (five keywords) contains 'UAV', 'machine learning', and 'precision agriculture' among its keywords, which could imply the use of machine learning-based approaches to develop predictive models, by using UAV-acquired data to guide PA practices. Keywords in the green cluster indicate that UAV-derived Vegetation Indices (VIs) are often used to monitor the spatiotemporal crop growth dynamics, with maize being among the most frequently-studied crops. This is potentially due to it being a staple crop that is often grown within many smallholder farming systems. While not providing any detailed insights, the keywords in the red cluster reaffirm the notion of the utility of UAV-based remote sensing techniques for crop monitoring and management on smallholder farms.

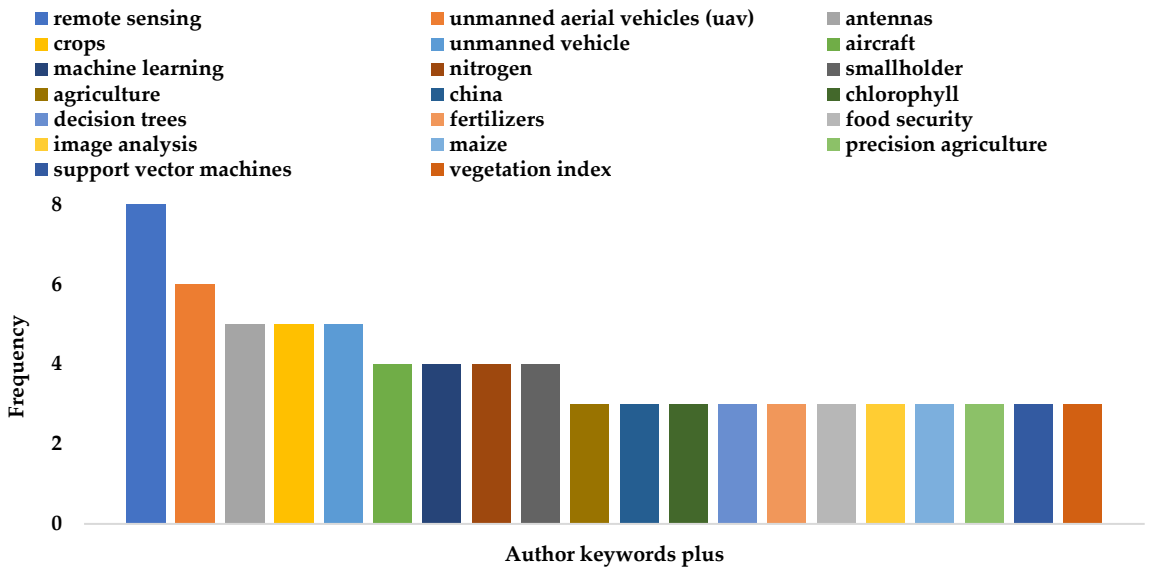

Figure 2.7 Frequency of top-20 keywords plus

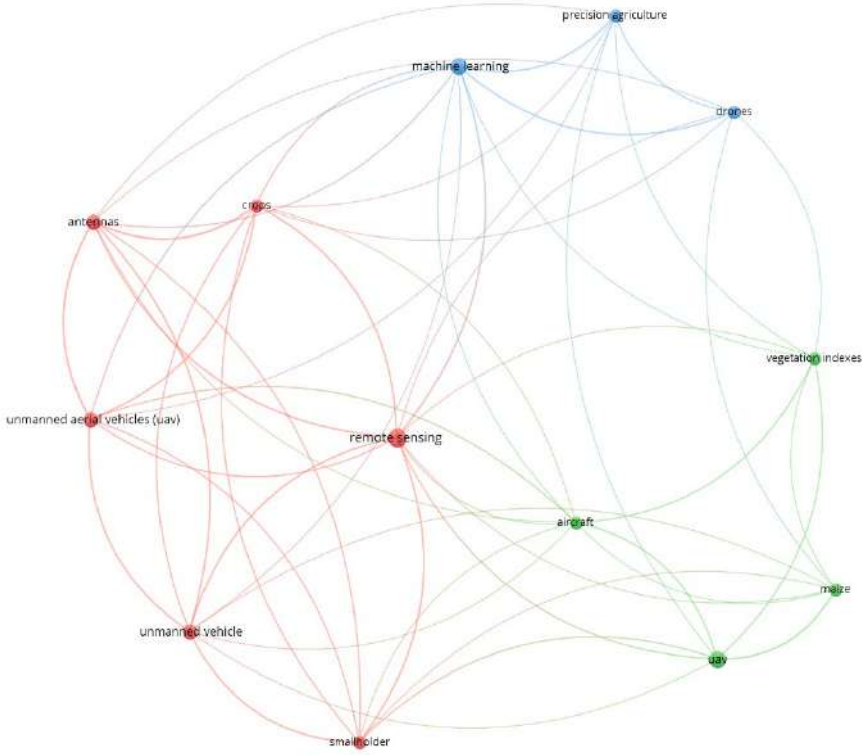

Figure 2.8 Co-occurrence network of the keyword that appeared at least four times within the final literature database

2.4 Discussion

2.4.1 Overview of research themes and methods

Clustering techniques were employed in this study, to aid in identifying the broad themes relating to the case study applications on the use of UAVs to monitor crops in smallholder farms, in order to facilitate PA. In addition, the literature was also examined to establish whether other relevant themes were not identified during the clustering analysis. Following the clustering analysis and examination of the literature, three broad themes were identified, namely, (i) the monitoring of crop development and the estimation of yields, (ii) fertiliser management, and (iii) image classification, with the focus on crop mapping. Although these themes can be presented and discussed in isolation, most of the analysed studies addressed multiple themes, even though their focus may have been centred around only one. It should also be noted that while these studies differed concerning how the UAV-derived data will be utilised to facilitate PA practices, there are many similarities regarding how the data is captured, processed and analysed, in order to develop the outputs that are used to guide management decisions. Subsequently, the discussion presented below provides a general overview of how the UAV-derived data were used to address the aforementioned themes.

Monitoring the development of crops throughout the growing season and estimating the yields at key growth stages can indicate whether they are experiencing water stress, have become diseased or are lacking nutrients (Wahab et al., 2018; Nhamo et al., 2020; Radoglou-Grammatikis et al., 2020). Hence, it is amongst the most common PA applications that are facilitated by UAVs within smallholder farms. The health of a crop influences its biophysical properties which, in turn, impacts the reflectance spectrum of these crops (Gracia-Romero et al., 2020). The ability of UAVs to explicitly capture these spatial variations in reflectance on demand, and to relate it to the crop's health, provides farmers with a powerful tool for facilitating early interventions that can prevent significant crop yield losses. For example, with nitrogen being one of the most yield-limiting nutrients during crop production, using UAV-derived data to detect the leaf chlorophyll content, which is closely related to leaf nitrogen, can aid in assessing the plant’s health and vigour (Wahab et al., 2018). Such information can then guide fertiliser management decisions (Gracia-Romero et al., 2020; Argento et al., 2021).

Water stress is another example of a major limiting factor in crop production. UAV-derived data can be used to estimate water stress indicators, which are then used to guide irrigation decisions (Ndlovu et al., 2021; Brewer et al., 2022b). UAV-derived VIs are often used to monitor the physiological status of crops, due to their simplicity and their ability to monitor vegetation cover, growth and vigour (Nhamo et al., 2020; Yeom et al., 2018). The selection of the spectral bands or VIs that are used will often depend on their respective strengths or weaknesses for a particular application, the user-personal preference and the spectral resolution of the imaging sensor. From a vegetation mapping and monitoring perspective, multispectral cameras were among the most widely used. This can be attributed to their ability to acquire sufficient data across several portions of the electromagnetic spectrum, in order to extensively monitor the vegetation characteristics at a relatively low cost (Sibanda et al., 2021).

The Normalised Difference Vegetation Index (NDVI) was the most commonly-utilised vegetation index. However, several other popular and useful vegetation indices were used in the reviewed studies to monitor crop development, such as the Green Normalised Difference Vegetation Index (GNDVI), the Enhanced Vegetation Index (EVI), the red-edge Normalised Difference Vegetation Index (NDVIre) and the Soil Adjusted Vegetation Index (SAVI).

In addition to the VIs that are derived from data acquired across the visible and near-infrared portions of the electromagnetic spectrum, the acquisition and use of thermal data was also shown to be beneficial in monitoring crop water stress and relating it to vegetation health (Brewer et al., 2022b). Adewopo et al. (2020) also noted that UAV-derived data can also allow for crop structural parameters to be estimated, such as the plant height, which may potentially improve the monitoring of crop development or the estimation of yields.

In general, the methods that were applied in the reviewed studies to monitor crop development, to estimate the yield or to guide fertiliser management decisions, typically involved the combined use of one or more UAV-derived vegetation indices and/or the plant structural data that have been captured simultaneously with the in-situ measurements of plant physiological variables, such as its chlorophyll content, yield, Aboveground Biomass (AGB), plant height or nitrogen content. The most popular approach was the development of regression-based models to capture the relationship between the in-situ measurements and UAV-derived data, so that it can be used to estimate a particular variable of interest.

Various estimation models were developed and applied in the reviewed studies; they range from simplistic parametric linear models (Blaes et al., 2016; Schut et al., 2018; Wahab et al., 2018; Adewopo et al., 2020; Breunig et al., 2020; Peter et al., 2020; Argento et al., 2021) to more complex non-parametric machine learning-based models (Ndlovu et al., 2021; Brewer et al., 2022a, b). While each of these models possesses its inherent strengths and weaknesses, the choice of model will generally be influenced by user experience or personal preference, the quality and quantity of training, the validation data and the computational resources.

For researchers, policymakers and managers to develop strategies that are aimed at enhancing the productivity of smallholder farms, whilst simultaneously ensuring the sustainable and optimal use of critical resources, it is essential for them to possess accurate information on the location and distribution of crops and to then determine how this changes, in response to management interventions or environmental influences (Nhamo et al., 2020). To this end, LULC mapping, with a focus on crop mapping, is often a central part of most PA applications.

While various techniques were employed in the reviewed studies to map crops, with varying degrees of success, the general approach to crop mapping was fairly similar. Training data which consist of the known locations of various LULC classes, were usually collected first, either from ground surveys or a visual inspection of the high spatial resolution imagery. Once the training data were collected, they were split into training and validation subsets. Spectral and/or textural data were then collected for each subset. The choice of spectral bands, VIs or textural features that were used during the classification process was likely to be subjective and dependent on factors such as the spectral resolution of the sensor, the spectral or textural similarities between the LULC classes and the user experience or personal preference. Thereafter, this data were used as inputs to machine learning- (Hall et al., 2018; Cucho-Padin et al., 2020; Zhao et al., 2020) or deep learning-based (Zhao et al., 2020; Jiang et al., 2022) approaches to classify the images, with the random forest, support vector machine and deep neural networks being among the preferred methods of choice.

While the three broad themes that were identified during the analyses of the final literature dataset represented some of the most common PA applications facilitated by UAVs, two potentially noteworthy exclusions were the use of UAVs for weed management and water use estimation. Poor weed management is one of the most significant contributors to poor crop productivity and the quality of the products.

Due to the various issues associated with conventional weed management approaches, integrated or site-specific weed management, facilitated by UAV-derived data, has become a popular management strategy. Since integrated weed management promotes efficiency and sustainability, this approach is well-suited for smallholder farm applications. It should be explored further, as it can improve the quantity and quality of crop yields, whilst reducing the economic expenses, the labour requirements and the inefficient use of limited resources (Esposito et al., 2021; Kawamura et al., 2021).

The accurate estimation of water use or evapotranspiration (ET) can play an important role in PA on smallholder farms and it serves various purposes, such as assessing the crop water stress, guiding irrigation decisions, drought monitoring and improving the management of the available water resources (Nhamo et al., 2021; Niu et al., 2022). This is particularly important from a smallholder farmer's perspective, as they are among the most vulnerable groups to the impacts of climate change and water scarcity.

While UAV-derived data may be suited for smallholder farm applications, various UAV-based ET estimation methods can potentially be utilised (Nhamo et al., 2021; Niu et al., 2022), even though knowledge of their strengths and limitations within the smallholder farm setting is fairly limited. Therefore, an opportunity exists for future research to further explore how these technologies can be used best, to facilitate improved water resources management decisions on smallholder farms.

2.4.2 Challenges and opportunities

The discussions thus far have highlighted the immense potential that UAVs have for monitoring crops on smallholder farms to facilitate PA. However, their actual application in these settings lags behind their potential. Considering the findings of the studies which comprised the final literature dataset, as well as the sentiments described in Nhamo et al. (2020), Sibanda et al. (2021) and Rejeb et al. (2022), there are several factors that contribute to this situation. These are summarised as follows:

- The lack of sufficient in-situ data for model development and testing: Many of the methods described in the literature depend on using sufficient good quality in-situ estimates to develop and validate the models that are used to estimate the key variables. However, such data are not always readily available or easily attainable. Furthermore, the data that are collected may only be representative of specific conditions.

This may limit the applicability of the developed models under a range of circumstances, i.e. models may be site- or crop-specific.

- UAV and sensor specifications: The size and type of UAV, batteries, payload capacity, flight range and endurance influence the geographical extent that can be covered during a single flight. Subsequently, UAVs may not be suited to large-scale agricultural applications. Furthermore, due to the limited payload capacity, the sensors that are typically used are lightweight, with a relatively low spectral resolution, which limits their feasibility for particular applications.
- Weather conditions: While the ability of UAVs to capture data is less severely impacted by cloud-cover, adverse weather conditions, such as strong winds or rainy conditions, can pose significant challenges to data collection.
- Affordability: Many smallholder farmers are financially constrained; therefore, while UAVs may provide them with invaluable information to improve their productivity, they may not necessarily be able to profit from this, due to their inability to respond, as and when required. Furthermore, the cost of ownership of UAVs is relatively high, and it may rise further, if higher spectral resolution sensors or data processing software are required. While these costs may be compensated for over time, through the acquisition of data on-demand and the benefits that are achieved through their improved agricultural operations, the initial financial outlay may put these technologies out of reach for many potential users.
- Inadequate farming resources and infrastructure: In many regions, increasing electricity costs and unreliable electricity supply can prove to be problematic for UAV operations, as batteries and controls require frequent charging.
- Technical capacity: The operation and maintenance of UAVs and data processing to derive meaningful outputs require skilled expertise, which may not be readily available.
- Civil aviation regulations: Due to the potential risks that may arise from UAV operations, many regions have stringent regulatory frameworks that govern civil aviation activities. Subsequently, the operation of UAVs may be restricted to certain applications, or users may be required to acquire a pilot license.

- Computational resources: The collection, processing, storage, dissemination and visualisation of UAV data can be quite computationally intensive. This may require potential users to purchase additional resources or to learn new skills on how to handle the large volumes of data that accompany the use of UAVs.

Notwithstanding the above limitations, there is much cause for optimism regarding the increased use of UAVs to monitor crops on smallholder farms, in order to facilitate PA. With the cost of these technologies steadily decreasing over time and the continuous advancements in UAVs, sensors and data processing platforms, many potential benefits and opportunities exist that warrant further investigation, some of which are described below:

- While integrated weed management and water-use estimation were identified and recommended as two major themes that should be explored further, assessing the irrigation water quality and quantity, monitoring and mapping the soil attributes, or developing variable rate prescription maps for pesticide management, may also be of interest for future research.
- Since UAV-derived data can be used to address multiple themes, the development of decision support tools that can simultaneously address multiple objectives should be explored further.
- Advances in freely-available geospatial cloud-computing platforms, such as Google Earth Engine (GEE) have created new and exciting opportunities for the processing, analysis, dissemination and visualisation of remote sensing data. Although the platform has largely been utilised for analysing satellite-earth observation data, its functionality can extend seamlessly to UAV-derived data.
- Satellite-earth observation and UAV technologies are typically utilised mutually exclusive, yet these platforms can often provide complementary data for various applications. Therefore, more research is required into developing methods to unlock the untapped potential synergies.
- Several studies have explored and evaluated the methods that rely on using in-situ measurements to develop models to estimate variables of interest. However, more emphasis should be placed on developing and evaluating approaches that can guide decision-making without in-situ data.

For example, Ellsaßer et al. (2020) developed an approach to estimate ET that only requires remotely-sensed thermal data as an input to their ET estimation model. In addition, Chew et al. (2020) and Tseng et al. (2022) demonstrated how transfer learning can overcome data scarcity challenges, when performing image classification.

- UAVs have been identified as a lower-cost alternative to traditional satellite-based remote sensing techniques to guide and inform PA practices. However, to adequately quantify the benefits that UAVs may provide, the cost of ownership, maintenance and operation of UAVs and other state-of-the art technologies should be examined, to determine whether they provide acceptable returns on the investment (Rejeb et al., 2022).
- Since women play such a prominent and integral role within smallholder agriculture, the adoption of PA practices facilitated by UAV technologies can significantly improve the productivity of their farms. This will contribute immensely to their upliftment and empowerment, by enhancing their capacity to deal with challenges that they have traditionally faced, or are likely to face in the future.
- The modernised nature of UAV-based PA is likely to aid in changing negative perceptions of being involved or employed within the agricultural sector, which may serve as a catalyst to stimulate interest among the youth and to accelerate their involvement within this sector, ultimately contributing to improving its longevity and resilience (Kwakye et al., 2021; Henning et al., 2022).

2.5 Conclusions

PA agricultural applications that are facilitated by UAVs have the potential to transform the fortunes of smallholder farmers, as the adoption of these technologies to guide their decision-making can enhance their agricultural productivity, whilst promoting the optimal and sustainable utilisation of critical resources. This, in turn, promotes improved food security and their socio-economic well-being, and it equips these farmers and communities better to adapt and build resilience to the impacts of climate change. Considering these potential benefits, this study aimed to examine the state-of-play regarding the application of UAVs to facilitate PA on smallholder farms.

To this end, we employed bibliometric techniques to summarise and analyse the literature relating to this research focus area. This analysis yielded useful insights on the general trends, influential publications, journals and authors, as well as the current challenges and opportunities for the future. However, it should be noted that the findings detailed in our study may be limited in their representation, due to the subjective criteria and methods that were used to source and evaluate the literature. Nevertheless, this review serves as a useful complement to the existing knowledge base and it will stimulate greater interest in this emerging and topical research area in the future.

2.6 References

ABAFE EA, BAHTA YT and JORDAAN H (2022) Exploring Biblioshiny for historical assessment of global research on the sustainable use of water in agriculture. *Sustainability* **14** (17).

ABBAS A, WASEEM M, AHMAD R, KHAN KA, ZHAO C and ZHOU J (2022) Sensitivity analysis of greenhouse gas emissions at farm level: case study of grain and cash crops. *Environmental Science and Pollution Research* **29** 82559–82573.

ABBAS A, ZHAO C, WASEEM M, KHAN KA and AHMAD R (2022) Analysis of energy input–output of farms and assessment of greenhouse gas emissions: a case study of cotton growers. *Frontiers in Environmental Science* **9**.

ADEWOPO J, PETER H, MOHAMMED I, KAMARA A, CRAUFURD P and VANLAUWE, B (2020) Can a combination of UAV-derived vegetation indices with biophysical variables improve yield variability assessment in smallholder farms? *Agronomy* **10** (12).

AGIDEW AA and SINGH, KN (2017) The implications of land use and land cover changes for rural household food insecurity in the North-eastern highlands of Ethiopia: the case of the Teleyayen sub-watershed. *Agriculture & Food Security* **6**.

ARGENTO F, ANKEN T, ABT F, VOGELSANGER E, WALTER A and LIEBSICH F (2021) Site-specific nitrogen management in winter wheat supported by low-altitude remote sensing and soil data. *Precision Agriculture* **22** 364–386.

ARIA M and CUCCURULLO C (2017) Bibliometrix: An R-tool for comprehensive science mapping analysis. *Journal of Informetrics* **11** 959–975.

BHAGAT PR, NAZ F and MAGDA R (2022) Artificial intelligence solutions enabling sustainable agriculture: A bibliometric analysis. *PLoS One* **17** (6).

BLAES X, CHOMÉ G, LAMBERT M, TRAORÉ PS, SCHUT AGT and DEFOURNY P (2016) Quantifying fertiliser application response variability with VHR satellite NDVI time series in a rainfed smallholder cropping system of Mali. *Remote Sensing* **8** (6).

BOLLAS N, KOKINOU E and POLYCHRONOS V (2021) Comparison of Sentinel-2 and UAV multispectral data for use in precision agriculture: an application from northern Greece. *Drones* **5** (2).

BOURSIANIS AD, PAPADOPOULOU MS, DIAMANTOULAKIS P, LIOPA-TSAKALIDI A, BAROUCHAS P, SALAHAS G, KARAGIANNIDIS G, WAN S and GOUDOS SK (2020) Internet of Things (IoT) and Agricultural Unmanned Aerial Vehicles (UAVs) in smart farming: A comprehensive review. IEEE Internet Things.

BREUNIG FM, GALVÃO LS, DALAGNOL R, SANTI AL, FLORA DPD and CHEN S (2020) Assessing the effect of spatial resolution on the delineation of management zones for smallholder farming in southern Brazil. *Remote Sensing Applications: Society and Environment* **19**.

BREWER K, CLULOW A, SIBANDA M, GOKOOL S, NAIKEN V and MABHAUDHI T (2022a) Predicting the chlorophyll content of maize over phenotyping as a proxy for crop health in smallholder farming systems. *Remote Sensing* **14** (3).

BREWER K, CLULOW A, SIBANDA M, GOKOOL S, ODINDI J, MUTANGA O, NAIKEN, V, CHIMONYO VGP and MABHAUDHI T (2022b) Estimation of maize foliar temperature and stomatal conductance as indicators of water stress based on optical and thermal imagery acquired using an Unmanned Aerial Vehicle (UAV) platform. *Drones* **6** (7).

BRIKA SKM, ALGAMDI A, CHERGUI K, MUSA AA and ZOUAGHI R (2021) Quality of higher education: a bibliometric review study. *Frontiers in Education* **6**.

BUKOWIECKI J, ROSE T and KAGE H (2021) Sentinel-2 Data for Precision Agriculture-A UAV-Based assessment. *Sensors* **21** (8).

CHEW R, RINEER J, BEACH R, O'NEIL M, UJENEZA N, LAPIDUS D, MIANO T, HEGARTY-CRAVER M, POLLY J and TEMPLE DS (2020) Deep Neural Networks and Transfer Learning for food crop identification in UAV images. *Drones* **4** (1).

CUCHO-PADIN G, LOAYZA H, PALACIOUS S, BALCAZAR M, CARBAJAL M and QUIROZ R (2020) Development of low-cost remote sensing tools and methods for supporting smallholder agriculture. *Applied Geomatics* **12** 247–263.

DA COSTA TP, GILLESPIE J, CAMA-MONCUNILL X, WARD S, CONDELL J, RAMANATHAN R and MURPHY F (2023) A systematic review of real-time monitoring technologies and its potential application to reduce food loss and waste: key elements of food supply chains and IOT technologies. *Sustainability* **15** (1).

DEFOURNY P, BONTEMPS S, BELLEMANS N, CARA C, DEDIEU G, GUZZONATO E, HAGOLLE O, INGLADA J, NICOLA L, RABAUTE T, SAVINAUD M, UDROIU C, VALERO S, BÉGUÉ A, DEJOUX JF, EL HARTI A, EZZAHAR J, KUSSUL N, LABBASI K, LEBOURGEOIS V, MIAO Z, NEWBY T, NYAMUGAMA A, SALH N, SHELESTOV A, SIMONNEAUX V, TRAORE PS, TRAORE SS and KOETZ B (2019) Near real-time agriculture monitoring at national scale at parcel resolution: Performance assessment of the Sen2-Agri automated system in various cropping systems around the world. *Remote Sensing of Environment* **221** 551–568.

ELAHI E, KHALID Z, TAUNI MZ, ZHANG H and LIRONG X (2022) Extreme weather events risk to crop-production and the adaptation of innovative management strategies to mitigate the risk: A retrospective survey of rural Punjab, Pakistan. *Technovation* **117**.

ELAHI E and KHALID Z (2022) Estimating smart energy inputs packages using hybrid optimisation techniques to mitigate environmental emissions of commercial fish farms. *Applied Energy* **326**.

ELAHI E, KHALID Z and ZHANG Z (2022) Understanding farmers' intention and willingness to install renewable energy technology: A solution to reduce the environmental emissions of agriculture. *Applied Energy* **309**.

EL-HENDAWY SE, AL-SUHAIBANI NA, ELSAYED S, HASSAN WM, DEWIR YH, REFAY Y, ABDELLA K (2019) Potential of the existing and novel spectral reflectance indices for estimating the leaf water status and grain yield of spring wheat exposed to different irrigation rates. *Agricultural Water Management* **217** 356–373.

ELLSAßER F, ROLL A, STIEGLER C, HENDRAYNATO and HOLSCHER D (2020) Introducing QWaterModel, a QGIS plug-in for predicting evapotranspiration from land surface temperatures. Environmental Modelling and Software.

ESPOSITO, CRIMALDI M, CIRILLO V, SARGHINI F and MAGGIO A (2021) Drone and sensor technology for sustainable weed management: a review. *Chemical and Biological Technologies in Agriculture* **8**.

FAO (FOOD AND AGRICULTURE ORGANIZATION OF THE UNITED NATIONS), INTERNATIONAL FUND FOR AGRICULTURAL DEVELOPMENT (IFAD), UNITED NATIONS CHILDREN'S FUND (UNICEF), WORLD FOOD PROGRAMME (WFP) AND WORLD HEALTH ORGANIZATION (WHO) (2021) The state of food security and nutrition in the world 2021. Transforming food systems for food security, improved nutrition and affordable healthy diets for all. Rome, FAO.

GRACIA-ROMERO A, KEFAUVER SC, VERGARA-DÍAZ O, HAMADZIRIP E, ZAMAN-ALLAH MA, THIERFELDER C, PRASSANA BM, CAIRNS JE and ARAUS JL (2020) Leaf versus whole-canopy remote sensing methodologies for crop monitoring under conservation agriculture: a case of study with maize in Zimbabwe. *Scientific Reports* **10**.

GUO L, FU P, SHI T, CHEN Y, ZHANG H, MENG R and WANG S (2020) Mapping field-scale soil organic carbon with un-manned aircraft system-acquired time series multispectral images. *Soil and Tillage Research* **196**.

HALL C, DAWSON TP, MACDIARMID JI, MATTHEW RB and SMITH P (2017) The impact of population growth and climate change on food security in Africa: looking ahead to 2050. *International Journal of Agricultural Sustainability* **15** (2) 124–135.

HALL O, DAHLIN S, MARSTOP H, BUSTOS MFA, ÖBORN I and JIRSTRÖM M (2018) Classification of Maize in Complex Smallholder Farming Systems Using UAV *Imagery Drones* **2** (3).

HENNING JIF, MATTHEWS N, AUGUST M and MADENDE P (2022) Youths' perceptions and aspiration towards participating in the agricultural sector: a South African case study. *Social Sciences* **11**.

JIANG J, ATKINSON PM, ZHANG J, LU R, ZHOU Y, CAO Q, TIAN Y, ZHU Y, CAO W and LIU X (2022) Combining fixed-wing UAV multispectral imagery and machine learning to diagnose winter wheat nitrogen status at the farm scale. *European Journal of Agronomy* **138**.

KAMARA A, CONTEH A, RHODES ER and COOKE RA (2019) The relevance of smallholder farming to African agricultural growth and development. *African Journal of Food, Agriculture, Nutrition and Development* **19** (1) 14043–14065.

KAWAMURA K, ASAI H, YASUDA T, SOISOUVANH S and PHONGCHANMIXAY S (2021) Discriminating crops/weeds in an upland rice field from UAV images with the SLIC-RF algorithm. *Plant Production Science* **24** (2) 198–215.

KWAKYE BD, BRENYA R, CUDJOE DA, SAMPENE AK and AGYEMAN FO (2021) Agriculture technology as a tool to influence youth farming in Ghana. *Open Journal of Applied Sciences* **11** 885–898.

LINNENLUECKE MK, MARRONE M and SINGH AK (2020) Conducting systematic literature reviews and bibliometric analyses. *Australian Journal of Management* **45** (2) 175–194.

MATTON N, SEPULCRE CG, WALDNER F, VALERO S, MORIN D, INGLADA J, ARIAS M, BONTEMPS S, KOETZ B and DEFOURNY P (2015) An automated method for annual cropland mapping along the season for various agrosystems globally distributed using spatial and temporal high resolution time series. *Remote Sensing* **7** 13208–13232.

MÜHL DD and DE OLIVEIRA L (2022) A bibliometric and thematic approach to agriculture 4.0. *Heliyon* **8** (5).

NDLOVU S, ODINDI J, SIBANDA M, MUTANGA O, CLULOW A, CHIMONYO VGP and MABHAUDHI T (2021) A comparative estimation of maize leaf water content using machine learning techniques and Unmanned Aerial Vehicle (UAV)-based proximal and remotely sensed data. *Remote Sensing* **13** (20).

NHAMO L, MAGIDI J, NYAMUGAMA A, CLULOW AD, SIBANDA M, CHIMONYO VGP and MABHAUDHI T (2020) Prospects of improving agricultural and water productivity through unmanned aerial vehicles. Agriculture **10** (256).

NIU H, ZHAO T, WANG D and CHEN Y (2022) Estimating evapotranspiration of pomegranate trees using Stochastic Con-figuration Networks (SCN) and UAV multispectral imagery. *Journal of Intelligent and Robotic Systems* **104** (66).

PALOMA SGY, RIESGO L and LOUHICHI K (2020) The role of smallholder farms in food and nutrition security. Impact analysis of agri-food policies on food and nutrition security in SSA.

PANDAY US, PRATIHAST A, ARYAL J and KAYASTHA RB (2020) A review on drone-based data solutions for cereal crops. *Drones* **4** (41).

PETER BG, MESSINA JP, CARROLL JW, ZHI J, CHIMONYO V, LIN S and SNAPP SS (2020) Multi-spatial resolution satellite and sUAS imagery for precision agriculture on smallholder farms in Malawi. *American Society for Photogrammetry and Remote Sensing* **86**(2) 107–119.

RADOGLOU-GRAMMATIKIS P, SARIGIANNIDIS P, LAGKAS T and MOSCHOLIOS I (2020) A compilation of UAV applications for precision agriculture. *Computer Networks* **17**.

RANJBARI M, ESFANDABADI ZS, SHEVCHENKO T, SCAGNELLI SD, LAM SS, VARJANI S, AGHBASHLO M, PAN J and TABATABAEI M (2022) An inclusive trend study of techno-economic analyses of biofuel supply chains. *Chemosphere* **309** (2).

REJEB A, ABDOLLAHI A, REJEB K and TREIBLMAIER H (2022) Drones in agriculture: a review and bibliometric analysis. *Computers and Electronics in Agriculture* **198**.

SCHUT AGT, TRAORE PCS, BLAES X and DE BY RA (2018) Assessing yield and fertiliser response in heterogeneous smallholder fields with UAVs and satellites. *Field Crops Research* **221** 98–107.

SEGARRA J, BUCHAILLOT ML, ARAUS JL and KEFAUVER FC (2020) Remote sensing for precision agriculture: Sentinel-2 improved features and applications. *Agronomy* **10** (641).

SIBANDA M, MUTANGA O, CHIMONYO VGP, CLULOW AD, SHOKO C, MAZVIMAVI D, DUBE T and MABHAUDHI T (2021) Application of drone technologies in surface water resources monitoring and assessment: a systematic review of progress, challenges, and opportunities in the global south. *Drones* **5** (84).

SISHODIA RP, RAY RL and SINGH SK (2020) Applications of remote sensing in precision agriculture: a review. *Remote Sensing* **12** (3136).

TRICCO AC, LILLIE E, ZARIN W, O'BRIEN KK, COLQUHOUN H, LEVAC D, MOHER D, PETERS MD, HORSLEY T, WEEKS L, HEMPEL S (2018) PRISMA extension for scoping reviews (PRISMAScR): checklist and explanation. *Ann Intern Med* **169** 467–473.

TSENG HH, YANG MD, SAMINATHAN R, HSU YC, YANG CY and WU DH (2022) Rice seedling detection in UAV images using transfer learning and machine learning. *Remote Sensing* **14**.

VAN ECK NJ and WALTMAN L (2010) Software survey: VOSviewer, a computer program for bibliometric mapping. *Scientometrics* **84**: 523–538.

WAHAB I, HALL, O and JIRSTRÖM M (2018) Remote sensing of yields: application of UAV imagery-derived NDVI for estimating maize vigor and yields in complex farming systems in sub-saharan Africa. *Drones* **2**(3).

WALTMAN L, VAN ECK NJ and NOYONS ECM (2010) A unified approach to mapping and clustering of bibliometric networks. http://arxiv.org/abs/1006.1032. Accessed 07 November 2010.

XUE J and SUE B (2017) Significant remote sensing vegetation indices: a review of developments and applications. *Journal of Sensors*. **2017**(2017): 1–17. doi.org/10.1155/2017/1353691.

YEOM J, JUNG J, CHANG A, MAEDA M and LANDIVAR J (2018) Automated open cotton boll detection for yield estimation using Unmanned Aircraft Vehicle (UAV) data. *Remote Sensing* **10** (12).

YONAH IB, MOURICE SK, TUMBO SD, MBILINYI BP and DEMPEWOLF J (2018) Unmanned aerial vehicle-based remote sensing in monitoring smallholder, heterogeneous crop fields in Tanzania. *International Journal of Remote Sensing* **39** (15-16).

ZHANG Z, LI Y, ELAHI E and WANG Y (2022) Comprehensive Evaluation of Agricultural Modernization Levels. *Sustainability* **14** (9).

ZHAO J, ZHONG Y, HU X, WEI L and ZHANG L (2020) A robust spectral-spatial approach to identifying heterogeneous crops using remote sensing imagery with high spectral and spatial resolutions. *Remote Sensing of Environment* **239**.

3 STUDY SITE DESCRIPTION

The study site is situated within the communal area of Swayimane, which is located in KwaZulu-Natal, South Africa (29°31′24″ S; 30°41′37″ E), spanning from July 2023 to May 2024 (Figures 3.1 and 3.2). This geographic region falls under the jurisdiction of the uMshwathi Local Municipality and encompasses an approximate area of 36 km^2. The residents of Swayimane predominantly engage in semi-subsistence agricultural practices, which constitute a vital source of sustenance, livelihood and food security. According to Brewer et al. (2022), the dominant crop varieties cultivated in this locale include white and yellow maize, sugarcane, tomatoes, amadumbe (taro) and sweet potatoes.

Agricultural plots are typically managed by using manual methods, such as hand-weeding and applying herbicides via knapsack sprayers, while the harvesting process commonly entails manual, labour-intensive techniques. Presently, most smallholder farmers in this region rely on rainfed agriculture. However, with the adverse projected impacts of climate threatening the community's food security and long-term livelihoods, there may be a need for these farmers to consider adopting irrigation practices, in order to ensure sustained crop productivity (Adaptation Fund, 2014). A sugarcane field situated within Swayimane was selected to perform the various investigations undertaken in this study. The sugarcane crop underwent successive harvests, with the latest round of planting commencing on 30th of November 2022. Following the ratoon crop's harvest, and prior to planting in November 2022, debris clearance and weed control were achieved through controlled burning.

Although the new crop emerged from the existing root system, soil amelioration was necessary to create an optimal growth milieu. This involved shallow tillage by using manual implements, such as hand hoes, to reduce soil compaction and incorporate organic amendments, with local indigenous labourers from the Swayimane community being engaged in these preparatory activities. The application of a balanced Nitrogen, Phosphorous and Potassium (NPK) fertiliser from Omnia Nutriology enhanced the crop vigour and productivity. This formulation contained 6.7% nitrogen, 10% phosphorus and 13.3% potassium, which ensured t hat the crops received the essential nutrients for their robust development and improved yield potential.

Effective weed management was essential to minimise the competition with emerging sugarcane shoots. Mechanised approaches, particularly herbicide application, were employed during the early growth to control weed proliferation. The herbicide Gramazone, produced by Syngenta, was used to suppress the annual grasses and broadleaf weeds in the field. Following these land preparation and management practices, the systematic monitoring of meteorological parameters and ET dynamics was initiated, which covered the sugarcane growth cycle.

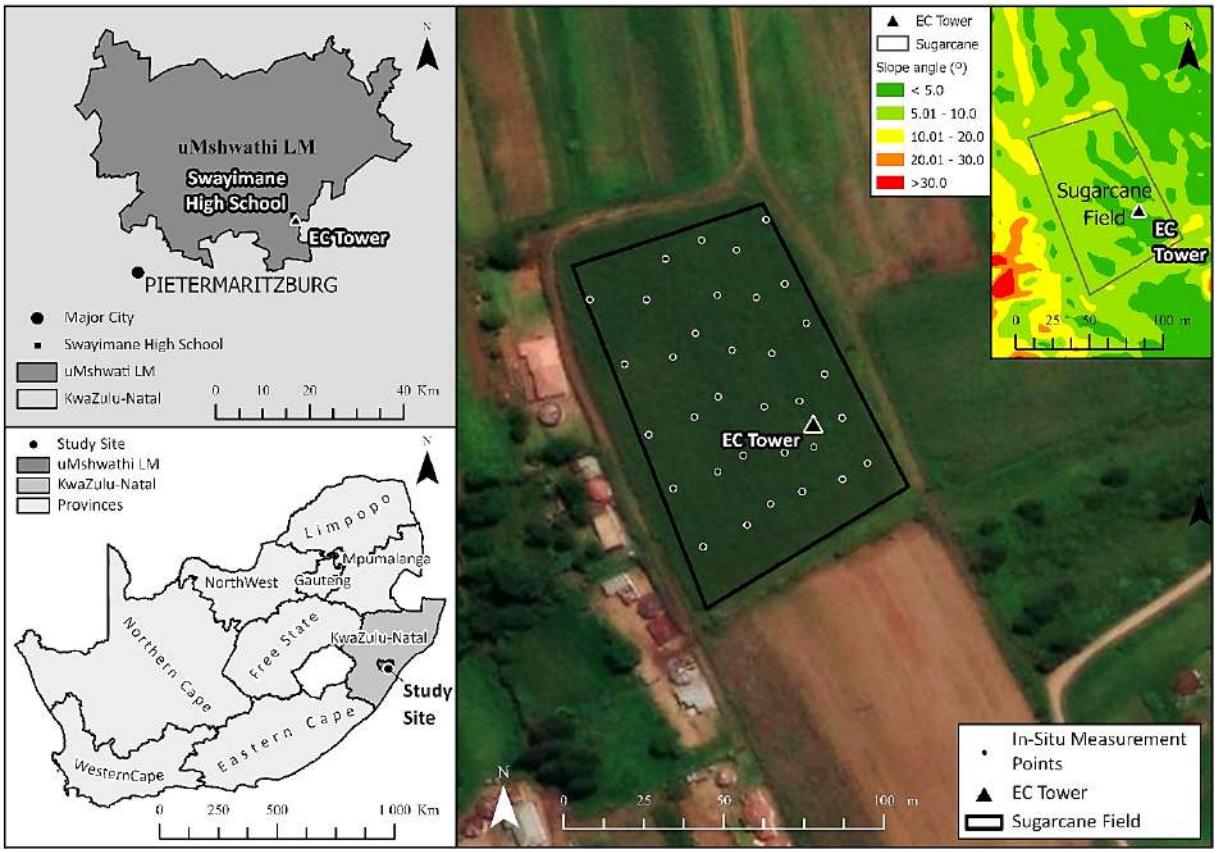

Figure 3.1 Study area map of smallholder sugarcane field in Swayimane, KwaZulu-Natal, South Africa

Data collection began seven months post-planting, from 01 July 2023 to 15 May 2024. An Automatic Weather Station (AWS) that continuously records weather conditions was situated at a high school near the study site. Due to the proximity of the AWS to the smallholder farm (approximately 1.05 km), it was deemed suitable for recording the meteorological conditions at the study site. During the data collection period, Swayimane had an average daily air temperature of 17.85°C and a total rainfall of 1190.46 mm. In addition, the average wind speed, relative humidity and solar irradiance were measured at 1.86 m s^{-1}, 80.45% and 13.69 MJ m^{-2}, respectively.

Figure 3.2 Photographs depicting the smallholder sugarcane field: (a) ground-level perspective, (b) aerial viewpoint, and (c) bird's-eye view of EC flux tower

The study site had also been instrumented with a meteorological flux tower that was equipped with sensors for measuring the various components of the shortened energy balance equation, as well as meteorological variables, including, inter alia, the precipitation (mm), wind speed (m s^{-1}), solar irradiance (MJ m^{-2}) and air temperature (˚C). Moreover, these measurements were conducted over a small-scale sugarcane field that was characterised by sloping terrain, with elevations ranging from 843.24 to 850.95 m and that encompassed an area of 7253.74 m^2 (ESRI, 2024).

4 CROP MAPPING IN SMALLHOLDER FARMS USING UNMANNED AERIAL VEHICLE IMAGERY AND GEOSPATIAL CLOUD COMPUTING INFRASTRUCTURE

4.1 Introduction

Quantifying spatiotemporal LULC dynamics within smallholder farms can play an important role in managing their resources more effectively and enhancing the productivity of these farms, as it facilitates changes in the agricultural crop types, management practices, climatic influences, water use efficiency and vegetation health that are to be assessed in near-real-time, which allows for quick and decisive operational management actions to be taken (Midekisa et al., 2017; Alabi et al., 2020; Chew et al., 2020; Ketema et al., 2020; Kpienbaareh et al., 2021; Rao et al., 2021; Ren et al., 2022). Several studies have demonstrated the potential of using remote sensing technologies for agricultural applications, such as cropland mapping (Cucho-Padin et al., 2020; Sishodia et al., 2020; Zhao et al., 2020; Rao et al., 2021; Ren et al., 2022). Satellite-earth observation datasets and their associated products can provide information at various spatial, spectral and temporal resolutions. However, their application in a smallholder farm setting is limited (Rao et al., 2021).

The spatial resolution of these open-access datasets, or products, is often too coarse to capture the spatial heterogeneity that is generally found on smallholder farms (Cucho-Padin et al., 2020; Nhamo et al., 2020; Rao et al., 2021). Whereas more advanced satellite-earth observation systems and manned aerial vehicles that can capture data at finer spatial resolutions (meter to sub-meter spatial resolution) are often too costly for widespread and long-term smallholder agricultural applications (Cucho-Padin et al., 2020). Furthermore, satellite revisit and repeat cycles, coupled with the influence of cloud cover, reduces the frequency at which data can be captured and processed (Manfreda et al., 2018; Nhamo et al., 2020).

Precision agricultural practices facilitated by UAVs have recently gained traction in the agricultural sector (Cucho-Padin et al., 2020; Radoglou-Grammatikis et al., 2020; Delavarpour et al., 2021). UAVs have been shown to hold vast potential for agricultural applications, as their low flight altitudes can potentially capture very high spatial resolution data at various spectral resolutions (depending on the optical-properties of the on-board camera).

Moreover, data can be captured at user-determined intervals, and they are less severely impacted by the effects of cloud cover, which allows data to be captured more frequently than the satellite-based approaches (Torres-Sánchez et al., 2014; Manfreda et al., 2018; Bennet et al., 2020; Cucho-Padin et al., 2020). The aforementioned features and the relatively lower costs of UAVs have seen them emerge as a promising tool for smallholder agricultural applications (Salamí et al., 2014; Cucho-Padin et al., 2020). Furthermore, with advances in geospatial cloud computing platforms, such as GEE, many more users are now able to implement sophisticated image analysis techniques without being limited by computational power and access to specialised proprietary software (Gorelick et al., 2017; Huang et al., 2018; Tamiminia et al., 2020). According to Bennet et al. (2020), with the increased use of UAVs for various applications and the growing popularity of utilising cloud-based computing platforms for image analysis, it is important to develop reproducible, adaptable and distributable techniques that can facilitate the more efficient analysis of UAV imagery for future applications.

Despite, their immense potential for accurately mapping crops on smallholder farms, as shown by Hall et al. (2018), Chew et al. (2020) and Alabi et al. (2020), the application of UAV and cloud-computing technologies in such settings is limited (Chew et al., 2020; Gokool et al., 2023). Considering that the potential of the aforementioned technologies remains largely untapped for smallholder farm applications, this study aims to explore and demonstrate the utility of using GEE to develop a semi-automated workflow, in order to: (i) process multi-spectral UAV imagery for the purpose of mapping LULC within smallholder rural farms at a localised level, and (ii) widely share these results in a simplified manner through a user-friendly interactive data visualisation web-based app.

4.2 Materials and methods

4.2.1 Data acquisition and processing

The images for the study area were collected by using a consumer-grade DJI Matrice 300 (M-300) UAV, which was fitted with a Micasense Altum multispectral sensor and Downwelling Light Sensor 2 (DLS-2). The Altum imaging sensor captures both multi-spectral (blue, green, red, red-edge and near infrared) and thermal data (https://micasense.com/altum/). It should be noted that the thermal band was not used in this study. The Altum imaging sensor was configured to capture images that have a side and front overlap of 70 and 80%, respectively, across the study area.

The boundary of the study area, which covered a geographic extent of approximately 0.11 km^2, was digitised within Google Earth and saved as a Keyhole Markup Language (kml) file, which was then imported into a DJI smart controller connected to the internet, following the DJI user account creation. The kml file was used to design an optimal flight path to acquire images covering the entire study area. The DJI Matrice 300 was configured to fly at an altitude of 100 m, which was sufficient to capture data at a 0.07 m pixel resolution for the entire study area. Light intensity changes during the day were accounted for through calibration, before and after each flight mission, using the MicaSense Altum Calibrated Reflectance Panel (CRP).

The UAV images were acquired between 8:00 and 10:00 am UTC on the 28th of April 2021. All images that were captured were pre-processed, using Pix4D fields software (Version 1.8) before further analysis. The pre-processing of the UAV images essentially involved performing atmospheric and radiometric corrections, with the corrected images then being mosaicked to create a single georeferenced orthomosaic. The orthomosaic was saved in a GeoTIFF file format, as this is the format that is required for uploading to GEE. The GeoTIFF orthomosaic image was uploaded and imported in GEE for further processing. All the spectral bands captured by the UAV on-board sensor, as well as nine vegetation indices (Table 4.1) for each of the training and validation points, were extracted and used as covariates, in order to train the classification algorithm (Midekisa et al., 2017). The selection of Vegetation Indices (VIs) to be used was subjective and it was guided by their frequency of application and performance in the literature (Xue et al., 2017; Bolyn et al., 2018; Yeom et al., 2019; de Castro et al., 2021; Rebelo et al., 2021; Wei et al., 2022). However, it should be noted that the methods implemented in this study allow for additional VIs to be included, or feature selection (to optimise the combination of bands and VIs) to be employed during the classification.

Table 4.1 List of vegetation indices used in this study

Name	Equation
normalised difference vegetation index	$\frac{NIR - Red}{NIR + Red}$
green normalised difference vegetation index	$\frac{NIR - Green}{NIR + Green}$
red-edge normalised difference vegetation index	$\frac{NIR - Red_{edge}}{NIR + Red_{edge}}$
enhanced vegetation index	$2.5 * \left(\frac{(NIR - Red)}{(NIR + 6 * Red - 7.5 * Blue) + 1}\right)$
soil adjusted vegetation index	$\frac{(Red_{edge} - RED)}{(Red_{edge} + RED + 0.5) * 1.5}$
simple blue and red-edge ratio	$\frac{BLUE}{Red_{edge}}$
simple near infrared and red-edge ratio	$\frac{NIR}{Red_{edge}}$
simple near infrared ratio	$\frac{NIR}{Red}$
green chlorophyll index	$\frac{NIR}{Green} - 1$

The training data points that were used for the image classification were acquired through a mix of data that were collected in the field and a visual inspection of the GeoTIFF orthomosaic (Midekisa et al., 2017). Five broad LULCs were identified, and training data were collected by identifying pixels within the image that completely contained one of these classes (Table 4.2). The selection of these pixels was guided by an *a-priori* knowledge of the study area acquired from multiple site visits. A total of 150 points were randomly captured for each class. A total of 750 points were available for model training (70%) and the validation (30%) of the classification accuracy (Odindi et al., 2016; Midekisa et al., 2017). For each of the training and validation data points, covariates (UAV spectral bands and VIs) were extracted from the image captured on the 28th of April 2021.

Table 4.2 A description of the LULC classes that were identified and categorised for mapping

Broad LULC classes	LULC present in each broad LULC class
1. Buildings and infrastructure	Buildings, roads, water tanks and solar panels
2. Bare ground	Bare soil, harvested crops, dirt roads
3. Crops	Maize, sugarcane, amadumbe, sweet potato and butternut
4. Grassland	Grassland
5. Trees and shrubs	Intermediate and tall trees or shrubs

In order to model and predict the five broad LULC classes, some of the commonly-used machine learning classification algorithms were deployed, namely (i) Classification and Regression Tree (CART), (ii) Support Vector Machine (SVM), (iii) Random Forest (RF), and (iv) Gradient Tree Boost (GTB), which are available in GEE (Orieschnig et al., 2021). Default hyper-parameter values for each of the aforementioned classification algorithms were used during model development and validation. However, the number of decision trees (n = 10) was specified for the RF and GTB classifiers, as this is a requirement when using these classification algorithms in GEE. The performance of each classification algorithm was then determined by comparing the Overall Accuracy (OA), the User Accuracy (UA), the Producer Accuracy (PA) and the kappa coefficient.

The model that achieved the highest accuracy scores across all the performance metrics was then selected to perform the image classification. Once the best-performing classifier had been established and applied for the original image (0.07 m), the spatial resolution of the original UAV image was resampled in GEE, by using bilinear interpolation to produce lower resolution images (0.50, 1.00 and 5.00 m). The classification process was then repeated by using the best-performing classifier and these images, to identify the optimal resolution for mapping the LULC within the study area. Once the optimal spatial resolution had been established, a final classification was performed (C1) using all of the previously-collected training data points, the best-performing classifier and the optimal spatial resolution. An overview of the classification workflow is provided in Figure 4.1.

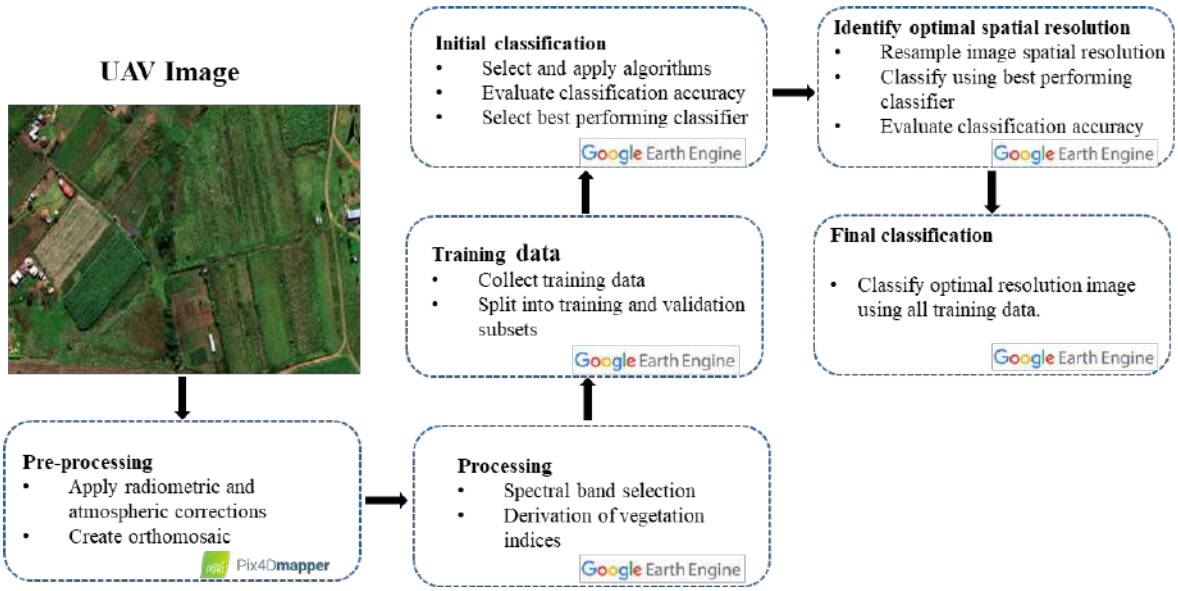

Figure 4.1 A conceptual representation of the classification workflow used to create the LULC maps for the study area

4.3 Results

4.3.1 Identifying the best-performing classifier for the original image

The best performing classification algorithm was the RF classifier, which marginally outperformed the GTB classifier. The LULC classification, using the RF model, achieved an OA of 86%, as shown in Table 4.3. The average class-specific PA and UA for the RF classification were 85.40% (± 8.30) and 85.20% (± 8.32). The buildings and infrastructure class was most accurately predicted within the RF classification, whereas the crops class was least accurately predicted.

Table 4.3 Classification accuracies for the original spatial resolution (0.07m) UAV image classified using the various classification algorithms available in GEE

Accuracy Assessment								
Classification algorithm	**CART**		**SVM**		**RF**		**GTB**	
Overall Accuracy (%)	81		83		86		85	
Kappa Coefficient	0.77		0.79		0.82		0.81	
	PA (%)	UA (%)	PA (%)	UA (%)	PA (%)	UA (%)	PA (%)	UA (%)
Buildings and infrastructure	98	88	88	100	98	93	98	91
Bare ground	85	100	100	89	93	97	88	97
Crops	80	69	67	77	78	78	84	79
Grassland	69	79	78	73	80	80	76	80
Trees & shrubs	76	76	86	80	81	81	81	79

4.3.2 Comparison of the best-performing classifier at different spatial resolutions

The classification results for each of the different spatial resolution UAV images that were classified by using the RF classification algorithm, are shown in Table 4.4. An interactive web-based app to visualise the differences between the classifications at the various spatial resolutions can be accessed from here. The overall classification accuracy and kappa coefficient for each of these classifications was relatively high. However, the highest level of accuracy was achieved by using a spatial resolution of 0.50 m, whereas the lowest classification accuracy was obtained at a spatial resolution of 5.00 m. The classification using the 0.50 m spatial resolution image achieved an OA of 91.00%, with an average PA and UA of 92 ± 7.31% and 91.20 ± 8.70%, respectively. The buildings and infrastructure, as well as the bare-ground classes were most accurately predicted within this classification, whereas crops were the least-accurately predicted. Following the analyses and results of identifying the optimal classifier and spatial resolution for mapping LULC in the study area, the original UAV image (0.07 m) was resampled to a 0.50 m spatial resolution, prior to performing the final LULC classifications by using the RF model (Figure 4.4).

Table 4.4 Classification accuracies for the UAV images at differing spatial resolutions classified using the GTB classification algorithm

Accuracy Assessment								
Spatial resolution	**0.07 m**		**0.50 m**		**1.00 m**		**5.00 m**	
OA (%)	86		91		88		81	
Kappa Coefficient	0.82		0.89		0.84		0.77	
	PA (%)	UA (%)	PA (%)	UA (%)	PA (%)	UA (%)	PA (%)	UA (%)
Buildings and infrastructure	98	93	96	100	97	93	87	84
Bare ground	93	97	100	95	90	100	77	69
Crops	78	78	87	77	78	76	84	86
Grassland	80	80	82	94	88	84	89	87
Trees & shrubs	81	81	95	90	85	88	71	82

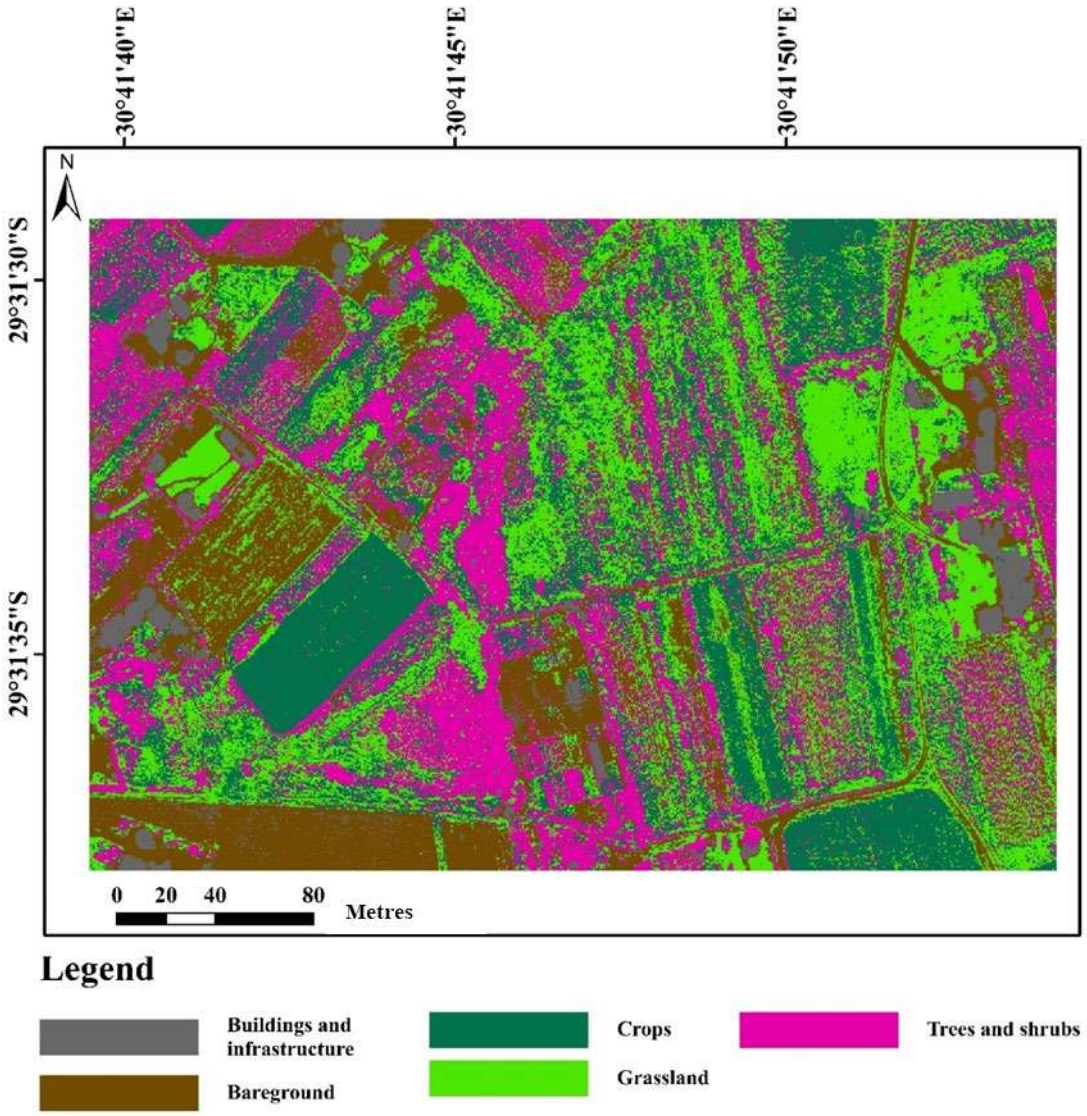

Figure 4.2 LULC classification result across the study area at a 0.50-meter spatial resolution for the 28th April 2021

4.4 Discussion

This study explored the utility of using the GEE geospatial cloud-computing platform to process and analyse a multi-spectral UAV image to map LULC within smallholder rural farms, with a particular focus on croplands. In general, we were able to map LULC at a relatively high accuracy, to capture the spatial heterogeneity within the study area and to adequately distinguish between crops and other LULC classes. The average PAs and UAs for crops across the various classification algorithms for the original UAV image (0.07 m) was approximately 75%.

However, once the best-performing classifier and an optimal spatial resolution for mapping had been identified and applied, the average PA and UA for crops increased to approximately 82%, which is relatively close to the 85% target accuracy, as specified by McNairn et al. (2009). These results are consistent and within the range of values reported in similar studies (Hall et al., 2018; Alabi et al., 2020; Chew et al., 2020). Overall, the C1 classification was able to adequately capture the spatial heterogeneity within the study area and to fairly accurately distinguish the crops from other LULC classes.

Considering the choice of classification algorithm on the classification accuracy, we found that the various machine learning algorithms available within GEE performed relatively well at mapping LULC within the study area (OA $\geq$ 75%). However, it should be noted that the training and evaluation of these algorithms were performed using data that were largely collected from visual inspection of the UAV true colour image. The collection of training data from a visual inspection of the UAV true colour image does promote the ease of application and expedites the classification process. However, this may contribute to the occurrence of misclassifications. Some of the data points may be incorrectly identified or may not adequately represent the unique spectral properties for each of the classes that are to be mapped. Therefore, it is recommended that, where possible, more ground truth data should be included in the training and evaluation process, so that a more accurate and objective assessment of the performance of these classification algorithms can be ascertained (Midekisa et al., 2017).

Furthermore, since there was no Real Time Kinematic (RTK) or Post-Processing Kinematic (PPK) corrections performed on the images, positional inaccuracies of the pixels within the image may exist. This may also contribute to the occurrence of misclassifications, as the spectral signature extracted for a particular training point from the image may not correspond with the LULC class on the ground. Therefore, it is recommended that the use of Ground Control Points (GCPs) to georeference the image or the implementation of PPK or RTK corrections, be applied where possible, in order to minimise the impact of potential positional inaccuracies (Martínez Carricondo et al., 2023). During the initial classifications when trying to establish the best-performing classifier, the classification accuracy of each LULC class ranged between 67-100%. The major source of inaccuracy in these classifications was generally due to the confusion between crops, grasslands, as well as trees and shrubs. This confusion may largely be a consequence of the limited training data that were used during the classification process.

The training data for crops were collected mainly from sugarcane and maize, since these are the dominant crops that cover the largest geographic extent within the study area. Consequently, fewer training points were used for the other crops, which may have resulted in them being incorrectly classified and contributing to the overall classification inaccuracy for this broad LULC class. Comparisons between the various classification algorithms showed that the ensemble-machine learning algorithms (RF and GTB) performed the best, with similar findings being reported in Orieschnig et al. (2021). This may have been due to the ability of these ensemble-machine learning methods to combine several predictive models to create a single model that can improve the predictive performance by decreasing the variance and bias, while significantly improving the classification accuracy, relative to other machine learning models (Wagle et al., 2020; Orieschnig et al., 2021). Furthermore, these models are generally less sensitive to input data and are better suited for generalised LULC applications (Orieschnig et al., 2021). While the RF and GTB models were shown to perform better than the SVM and CART models, the accuracies that have been presented in this study may not represent the possible maximum, as these values will largely be influenced by the user-specified parameter choices for each algorithm (Abdi, 2020).

While it was not within the scope of this study, Abdi (2020) recommends that an unbiased evaluation of each algorithm's performance is undertaken through an equally robust hyper-parameter selection, where possible, so as not to introduce bias into the performance of the model. During this process, these algorithms should be evaluated with respect to their overall accuracy and their ability to adequately represent each LULC class (Abdi, 2020). Considering the influence of the spatial resolution on the classification accuracy, we found that, as the spatial resolution decreased from 0.07-1.00 m, there was an increase in the OA and kappa coefficients. The OA and kappa coefficient then decreased to its lowest value when the spatial resolution decreased from one to five metres.

These results are consistent with the findings presented in Zhao et al. (2019) and Liu et al. (2020), which indicates that the use of the finest spatial resolution image available does not necessarily translate into an improved classification accuracy; however, there is a limit to which the spatial resolution can be reduced. Instead, an intermediate spatial resolution, where the spectral intra-class variation and the mixed-pixel effect are minimised, will be most appropriate for LULC mapping (Liu et al., 2020).

While the 0.50 m spatial resolution image produced the highest overall and individual class accuracies, this spatial resolution should not be viewed as a generalised optimal spatial resolution, as it may vary for specific LULC classes, or agricultural applications (Zhao et al., 2019; Liu et al., 2020). Although the C1 classification was not the highest spatial resolution image that could have been used for the mapping of LULC within the study area, this spatial resolution more than adequately captures the spatial heterogeneity within the study area.

We elected to define and map five broad LULC classes within the study area. However, in order for the landcover map to be applicable to a wider range of potential applications, it would be advantageous to map the LULC in greater detail (for example, identifying individual crop types). The relatively low spectral resolution of the UAV on-board sensor may pose a challenge to this, as it may prove difficult to distinguish between certain features that are spectrally similar (Böhler et al., 2018; Liu et al., 2020). The acquisition and use of higher spectral resolution imaging sensors can address this limitation, but these sensors are accompanied by a higher cost.

The fusion of high spatial resolution UAV imagery with freely-available higher spectral resolution satellite imagery, does present an alternate and more pragmatic approach for potentially addressing the aforementioned challenges and reducing the costs; however, further testing is advocated before these can be readily implemented (Adão et al., 2017; Böhler et al., 2018; Zhao et al., 2019). Overall, the investigations in this study could have benefited from the availability of more training data, higher spectral resolution data or model hyper-parameter tuning. However, the results were quite promising and can serve as a foundation for the development of improved LULC maps for the study area in the future.

In addition, the use of Object-Based Image Analysis (OBIA) techniques may potentially prove to be a more suitable alternative to the traditional pixel-based approaches (such as those applied in this study) for the classification of high-resolution imagery. Similarly, deep learning algorithms have shown much promise for producing accurate crop type maps. The application of these approaches, although more complex and computationally intensive, may represent useful alternatives for improving the classification accuracy (Tassi et al., 2020; Kpienbaareh et al., 2021).

The ability to accurately map the crop location and spatial distribution can play a pivotal role in improving the management of smallholder farms (Timmermans, 2018; Nhamo et al., 2020). Given the unique characteristics of UAVs and UAV imagery, these technologies are well-suited for mapping the LULC within smallholder farms, as demonstrated in this study. However, their application in smallholder farming has been relatively limited, largely due to their perceived high costs, coupled with a lack of the technical skills to operate and derive meaningful information from the acquired images (Nhamo et al., 2020). Because of creative ownership solutions and a decrease in acquisition and operational costs, UAV technologies are now more accessible to various users (Nhamo et al., 2020). Furthermore, the use of freely-available open-source UAV image processing software, such as OpenDroneMap and geospatial cloud computing platforms such as GEE, can be used to develop automated or semi-automated processing and analysis procedures (rather than the proprietary software that was used in this study), as they can be shared and used by expert and non-expert users. This may serve to further reduce the operational costs and improve the efficiency with which the tasks are executed.

Despite the favourable attributes associated with GEE, the use of the platform for non-commercial or research purposes does possess limitations. These include: (i) the limited selection of ML algorithms that can be utilised, (ii) user quotas, which limit the computational capacity, or (iii) the amount of data that can be uploaded and stored in GEE (15 Gb of data shared across all Google applications, unless additional storage capacity is purchased). While the commercial version of GEE does enable users to overcome many of these issues, its associated costs can amount to hundreds of dollars per month, which renders this technology unfeasible for application in developing and resource-poor regions.

Nevertheless, the use of GEE for non-commercial or research purposes still provides impressive computational power and also allows for the development of dynamic web-based apps that can be used to freely and rapidly communicate results in an aesthetically appealing and comprehendible manner to a wide range of users (Tamiminia et al., 2020). Considering these advancements and innovative solutions, local government, agricultural authorities and researchers are now better placed to assist smallholder farmers to exploit the benefits of modern agricultural practices and to overcome many of the limitations that they have traditionally faced.

4.5 Conclusions

In recent times, the use of UAVs has been gaining traction in the agricultural sector. With the emergence of geospatial cloud computing platforms, there are now greater opportunities for local governments, agricultural authorities and researchers in developing countries to integrate the technological advances into agricultural practices, and to use them to assist smallholder farmers to optimise their productivity. The synergistic application of these technologies offers the opportunity to develop bespoke, innovative and lower-cost solutions, which can facilitate improved agricultural management within smallholder farms.

Considering these developments, we aimed to demonstrate how GEE can be leveraged to maximise the potential of UAVs for mapping the LULC in smallholder farms. The results of these investigations demonstrated that LULC could be mapped fairly accurately, with the resulting map also adequately representing the spatial heterogeneity within the study area. Furthermore, it was shown that it is possible to sacrifice spatial resolution up to a point, in order to expedite data collection and image processing, or to reduce costs by purchasing cheaper, lower spatial resolution imaging sensors, without greatly sacrificing classification accuracy. Notwithstanding the limitations of this study, GEE was found to be particularly useful for performing a computationally-intensive and advanced image analysis on a UAV image. The availability of such an approach is particularly beneficial for data-scarce and resource-poor regions, as it provides a wide-range of users with a powerful tool to guide and support their decision making. This, in turn, can serve to ensure that smallholder farmers in developing countries are not excluded from the big data revolution in agriculture.

4.6 References

ABDI AM (2020) Land cover and land use classification performance of machine learning algorithms in a boreal landscape using Sentinel-2 data. *GIScience & Remote Sensing* **57** (1) 1–20.

ADÃO T, HRUŠKA J, PÁDUA L, BESSA J, PERES E, MORAIS R and SOUSA JJ (2017) Hyperspectral imaging: a review on UAV-based sensors, data processing and applications for agriculture and forestry. *Remote Sensing* **9**.

AGIDEW AA and SINGH KN (2017) The implications of land use and land cover changes for rural household food insecurity in the north-eastern highlands of Ethiopia: the case of the Teleyayen sub-watershed. *Agriculture & Food Security* **6**.

ALABI TR, ADEWOPO J, DUKE OP and KUMAR PL (2020) Banana mapping in heterogenous smallholder farming systems using high-resolution remote sensing imagery and machine learning models with implications for Banana Bunchy Top Disease Surveillance. *Remote Sensing* **14**.

BENNET MK, YOUNES N and JOYCE K (2020) Automating drone image processing to map coral reef substrates using the Google Earth engine. 2020. Drones **4** (3).

BÖHLER JE, SCHAEPMAN ME and KNEUBÜHLER M (2018) Crop classification in a heterogeneous arable landscape using uncalibrated UAV data. *Remote Sensing* **10** (8).

BOLYN C, MICHEZ A, GAUCHER P, LEJEUNE P and BONNET S (2018) Forest mapping and species composition using supervised per pixel classification of Sentinel-2 imagery. *Biotechnology, Agronomy, Society and Environment* **22** 172–187.

BREWER K, CLULOW A, SIBANDA M, GOKOOL S NAIKEN V and MABHAUDHI T (2022) Predicting the chlorophyll content of maize over phenotyping as a proxy for crop health in smallholder farming systems. *Remote Sensing* **14** (3).

CHEW R, RINEER J, BEACH R, O'NEIL M, UJENEZA N, LAPIDUS D, MIANO T, HEGARTY-CRAVER M, POLLY J and TEMPLE DS (2020) Deep neural networks and transfer learning for food crop identification in UAV images. *Drones* **4** (7).

CUCHO-PADIN G, LOAYZA H, PALACIOUS S, BALCAZAR M, CARBAJAL M and QUIROZ R (2020) Development of low-cost remote sensing tools and methods for supporting smallholder agriculture. *Applied Geomatics* **12** 247–263.

DE CASTRO AI, SHI Y, MAJA JM and PEÑA JM (2021) UAVs for vegetation monitoring: overview and recent scientific contributions. *Remote Sensing* **13**.

DELAVARPOUR N, KOPARAN C, NOWATZKI J, BAJWA S and SUN X (2021) A technical study on UAV characteristics for precision agriculture applications and associated practical challenges. *Remote Sensing* **13**.

DEPARTMENT OF AGRICULTURE, FORESTRY and FISHERIES (DAFF) (2012) A framework for the development of smallholder farmers through cooperatives development. Directorate Co-operative and Enterprise Development, Department of Agriculture, Forestry and Fisheries, South Africa.

GOKOOL S, MAHOMED M, KUNZ R, CLULOW A, SIBANDA M, NAIKEN V, CHETTY K and MABHAUDHI T (2023) Crop monitoring in smallholder farms using unmanned aerial vehicles to facilitate precision agriculture practices: a scoping review and bibliometric analysis. *Sustainability* **15** (4).

GORELICK N, HANCHER M, DIXON M, ILYUSCHENKO S, THAU D and MOORE R (2017) Google Earth Engine: planetary-scale geospatial analysis for everyone. *Remote Sensing of Environment* **202** 18–27.

HALL O, DAHLIN S, MARSTORP H, BUSTOS MFA, ÖBORN I and JIRSTRÖM M (2018) Classification of maize in complex smallholder farming systems using UAV imagery. *Drones* **2** (3) 22.

HUANG Y, ZHONG-XIN C, TAO Y, XIANG-ZHI H and XING-FA G () Agricultural remote sensing big data: management and applications. *Journal of Integrative Agriculture* **17** (9) 1915–1931.

KAMARA A, CONTEH A, RHODES ER and COOKE RA (2019) The relevance of smallholder farming to African agricultural growth and development. *African Journal of Food, Agriculture, Nutrition and Development* **19** (1) 14043–14065.

KETEMA H, WEI W, LEGESSE A, WOLDE Z, TEMESGEN H, YIMER F and MAMO A (2020) Quantifying smallholder farmers' managed land use/land cover dynamics and its drivers in contrasting agro-ecological zones of the East African Rift. *Global Ecology and Conservation* **21**.

KPIENBAAREH D, SUN X, WANG J, LUGINAAH I, KERR RB, LUPAFYA E and DAKISHONI L (2021) Crop type and land cover mapping in northern Malawi using the integration of Sentinel-1, Sentinel-2 and PlanetScope satellite data. *Remote Sensing* **13**.

LIU M, YU T, GU X, SUN, YANG G, ZHANG Z, MI X, CAO W and LI J (2020) The impact of spatial resolution on the classification of vegetation types in highly fragmented planting areas based on unmanned aerial vehicle hyperspectral images. *Remote Sensing* **12** (1).

LOWDER S, SKOET J and SINGH S (2014) What do we really know about the number and distribution of farms and family farms in the world? Background paper for the state of food and agriculture 2014, ESA working paper 14–02 (Rome: Food and Agriculture Organization of the United Nations (FAO), Agricultural Development Economics Division, 2014).

MAHOMED M, CLULOW AD, STRYDOM S, MABHAUDHI T and SAVAGE MJ (2021) Assessment of a ground-based lightning detection and near-real-time warning system in the rural community of Swayimane, KwaZulu-Natal, South Africa. *Weather, Climate and Society* **13** (3) 605–621.

MANFREDA S, MCCABE M, MILLER P, LUCAS R, PAJUELO MV, MALLINIS G, BEN DOR E, HELMAN D, ESTES L, CIRAOLO G, MÜLLEROVÁ J, TAURO F, DE LIMA MI, DE LIMA JLMP, MALTESE A, FRANCES F, CAYLOR K, KOHV M, PERKS M, RUIZ-PÉREZ G, SU Z, VICO G and TOTH B (2018) On the use of unmanned aerial systems for environmental monitoring. *Remote Sensing* **10**.

MARTÍNEZ-CARRICONDO P, AGÜERA-VEGA and CARVAJAL-RAMÍREZ F (2023) Accuracy assessment of RTK/PPK UAV-photogrammetry projects using differential corrections from multiple GNSS fixed-base stations. *Geocarto International* **38** (1).

MCNAIRN H, CHAMPAGNE C, SHANG J, HOLMSTROM DA and REICHERT G (2009) Integration of optical and Synthetic Aperture Radar (SAR) imagery for delivering operational annual crop inventories. *ISPRS Journal of Photogrammetry and Remote Sensing* **64** 434–449.

MIDEKISA A, HOLL F, SAVORY DJ, ANDRADE-PACHECO R, GETHING PW, BENNETT A and STURROCK HJW (2017) Mapping land cover change over continental Africa using Landsat and Google Earth Engine cloud computing. *PLoS ONE* **12** (9).

NHAMO L, MAGIDI J, NYAMUGAMA A, CLULOW AD, SIBANDA M, CHIMONYO VGP and MABHAUDHI T (2020) Prospects of improving agricultural and water productivity through unmanned aerial vehicles. *Agriculture* **10**.

ODINDI J, MUTANGA O, ROUGET M and HLANGUZA N (2016) Mapping alien and indigenous vegetation in the KwaZulu-Natal sandstone sourveld using remotely-sensed data. *Bothalia* **46** (2).

ORIESCHNIG CA, BELAUD G, VENOT JP, MASSUEL S and OGILVIE A (2021) Input imagery, classifiers, and cloud computing: Insights from multi-temporal LULC mapping in the Cambodian Mekong Delta. *European Journal of Remote Sensing* **54** (1) 398–416.

RADOGLOU-GRAMMATIKIS P, SARIGIANNIDIS P, LAGKAS T and MOSCHOLIOS I (2020) A compilation of UAV applications for precision agriculture. *Computer Networks* **172**.

RAO P, ZHOU W, BHATTARAI N, SRIVASTAVA AK, SINGH B, POONIA S, LOBELL DB and JAIN M (2021) Using Sentinel-1, Sentinel-2 and Planet Imagery to map crop type of smallholder farms. *Remote Sensing* **13** (10).

REBELO A, GOKOOL S, HOLDEN P and NEW M (2021) Can Sentinel-2 be used to detect invasive alien trees and shrubs in savanna and grassland biomes? *Remote Sensing Applications: Society and Environment* **23**.

REN T, XU H, CAI X, YU S and QI J (2022) Smallholder crop type mapping and rotation monitoring in mountainous areas with Sentinel-1/2 imagery. *Remote Sensing* **14**.

SALAMÍ E, BARRADO C and PASTOR E (2014) UAV flight experiments applied to the remote sensing of vegetated areas. *Remote Sensing* **6** 11051–11081.

SISHODIA R, RAY RL and SINGH SK (2020) Applications of remote sensing in precision agriculture: a review. *Remote Sensing* **12**.

TAMIMINIA H, SALEHI B, MAHDIANPARI M, QUACKENBUSH L, ADELI S and BRISCO B (2020) Google Earth Engine for geo-big data applications: A meta-analysis and systematic review. *ISPRS Journal of Photogrammetry and Remote Sensing* **164** 152–170.

TASSI A and VIZZARI M (2020) Object-Oriented LULC Classification in Google Earth Engine combining SNIC, GLCM and machine learning algorithms. *Remote Sensing* **12**.

TIMMERMANS A (2018) Mapping cropland in smallholder farmer systems in South Africa using Sentinel-2 imagery. MSc Dissertation in Environmental Bioengineering, Faculté des Bioingénieurs, Université Catholique de Louvain, Belgium.

TORRES-SÁNCHEZ J, PEÑA JM, DE CASTRO AI and LÓPEZ-GRANADOS F (2014) Multi-temporal mapping of the vegetation fraction in early-season wheat fields using images from UAV. *Computers and Electronics in Agriculture* **103** 104–113.

UMNGENI RESILIENCE PROJECT (URP) (2014) Building resilience in the greater uMngeni Catchment, South Africa. Adaptation Fund. Accessed 10 June 2021. https://www.adaptation-fund.org/project/building-resilience-in-the-greater-umngeni-catchment/.

WAGLE N, ACHARYA TD, KOLLURU V, HUANG H and LEE DH (2020) Multi-temporal land cover change mapping using Google Earth Engine and Ensemble learning methods. *Applied Sciences* **10**.

WEI H, GRAFTON M, BRETHERTON M, IRWIN M and SANDOVAL E (2022) Evaluation of the use of UAV-derived vegetation indices and environmental variables for grapevine water status monitoring based on machine learning algorithms and SHAP Analysis. *Remote Sensing* **14** (23).

WOLFENSON K (2013) Coping with the food and agriculture challenge: smallholders' agenda. Food and Agriculture Organization of the United Nations, Rome, Italy.

XUE J and BAOFANG S (2017) Significant remote sensing vegetation indices: a review of developments and applications. *Journal of Sensors* 353691.

YEOM J, JUNG J, CHANG A, ASHAPURE A, MAEDA M, MAEDA A and LANDIVAR J (2019) Comparison of vegetation indices derived from UAV data for differentiation of tillage effects in agriculture. *Remote Sensing* **11**.

ZHAO J, ZHONG Y, HU X, WEI L and ZHANG L (2020) A robust spectral-spatial approach to identifying heterogeneous crops using remote sensing imagery with high spectral and spatial resolutions. *Remote Sensing of Environment* **239**.

ZHAO L, SHI Y, LIU B, HOVIS C, DUAN Y and SHI Z (2019) Finer classification of crops by fusing UAV images and Sentinel-2A data. *Remote Sensing* **11**.

5 EVALUATING THE POTENTIAL OF UNMANNED AERIAL VEHICLE-DERIVED DATA FOR EVAPOTRANSPIRATION ESTIMATION ON SMALLHOLDER FARMS

5.1 Introduction

Smallholder farms are essential for achieving food security objectives, by significantly strengthening agricultural productivity, supporting livelihoods, and fostering socio-economic advancement, particularly within developing regions (Kamara et al., 2019). Nonetheless, persistent climatic variability and limited access to critical resources pose formidable challenges to smallholder farming practices in SSA, which leads to diminished productivity and profitability (Adisa et al., 2018; Brewer et al., 2022). The sugarcane industry is crucial in South Africa's agricultural sector, as it provides substantial employment opportunities and promotes rural development and food security (Hess et al., 2016).

Numerous small-scale farmers practice dryland sugarcane cultivation, due to limited access to irrigation resources, and this impacts their capacity to maximise their production and achieve competitive yields (Adisa et al., 2018; Madamombe et al., 2024). Their reliance on precipitation entails a substantial threat to their agricultural yields, as reduced seasonal rainfall and the occurrence of extreme weather can detrimentally impact crop vitality, biochemical functions and physical development (Walker and Schulze, 2006; Muzari et al., 2012; Okonya et al., 2013). Furthermore, erratic fluctuations in the precipitation patterns may compel a heightened dependence on irrigation methods, in order to sustain their agricultural yields in future years. Thus, it becomes crucial to delve into efficient and environmentally-sound irrigation methodologies, in order to accommodate the shifting climatic dynamics. Therefore, acquiring precise estimates of their crop water requirements is essential for efficient and effective irrigation planning and management.

Several in-situ and remote sensing-based approaches have been developed and implemented, in order to quantify the ET fairly accurately. Some of the most widely-utilised approaches include the weighing lysimeter, the Bowen Ratio, surface renewal, pan evaporation, sap flow, eddy covariance and the scintillometer (Bastiaanssen et al., 2012; Sur et al., 2015; Minacapilli et al., 2016; Tian et al., 2017).

However, the feasibility of adopting these approaches within a smallholder farm setting is constrained by the costs and the skilled expertise that is required to install and operate these instruments. Given the limitations of these techniques, which are primarily applicable on a local scale and lack the scalability for broader coverage, RS-based approaches have become a popular alternative for ET estimation, as they are able to provide extensive data coverage across large geographical scales, including remote and data-scarce regions (Bachour, 2013). Several remote sensing-based approaches have been extensively applied globally and have been shown to produce reliable estimates of ET. However, a vast majority of these techniques have relied upon the use of data captured from space-borne sensors. This can prove to be problematic for smallholder farm applications, due to either the spatial resolution of freely-available satellite imagery, or the exorbitant costs of suitable commercially-available products.

With the emergence of UAV technologies as a relatively cost-effective approach to collect very high spatial resolution imagery at user-defined intervals, there has been a growing interest and recognition of the potential that these technologies can provide to facilitate PA applications, particularly within the smallholder farm setting (Hoffmann et al., 2016; Messina & Modica, 2020; Hu et al., 2021; Gokool et al., 2023). Despite the increasing interest in the use of UAVs to facilitate PA, there remains a notable lack of consensus regarding the most suitable or pragmatic UAV-based approach for estimating ET (Yacoob et al., 2024). As Yacoob et al. (2024) noted, UAV-based ET estimation approaches can be broadly classified into two categories, namely, (i) the thermal band-based energy-balance approach, and (ii) empirical VI models (Tang et al., 2019). While the former approach may be favoured, due to its stronger physically-based conceptualisation, these techniques require a greater level of expertise, in order to modify and/or apply these models, using UAV-derived inputs. These approaches are further limited by the need for the extensive in-situ forcing data that are required for their successful implementation, which is often unavailable, particularly in a smallholder farm setting (Yacoob et al., 2024).

While empirical VI models that utilise the relationship between the crop coefficient (Kc) and reference ET (ETo) to estimate ET offer an arguably simpler and less data-intensive alternative for providing fairly accurate estimates of ET (Hunsaker et al., 2003; Nouri et al., 2014; French et al., 2018; Filgueiras et al., 2019; Nouri et al., 2020; Abbasi et al., 2021; Shao et al., 2021; Nagler et al., 2022; Niu et al., 2022), these approaches may also be limited by their need for in-situ measurements, in orderr to adequately define the relationship between VIs and Kc.

However, Abbassi et al. (2023) and Woldemariam et al. (2024) have shown that the use of Vis, as a proxy for Kc, can still yield fairly accurate ET estimates, without utilising the aforementioned in-situ measurements. Considering the potential of this approach, particularly in data-scarce environments, we aimed to estimate the ET by using UAV-acquired data and to evaluate these estimates against the in-situ measurements of ET. For this purpose, five VI-based ET estimation models were applied and evaluated. While Abbassi et al. (2023) and Woldemariam et al. (2024) have demonstrated the potential of their VI-based ET estimation approach, their studies have not been undertaken in a smallholder farm setting or utilised UAV-acquired data and validated the data against field-based measurements. Therefore, the results presented in this study can serve to provide further insights into the suitability and feasibility of adopting this approach, in order to potentially facilitate precision water management on smallholder farms.

5.2 Materials and methods

5.2.1 In-situ data collection

The water use of sugarcane was measured by using the Eddy Covariance (EC) approach. A 4-metre meteorological flux tower was installed within the sugarcane field, with the instrumentation being oriented to the prevailing wind direction (Figure 5.1a). These instruments enabled the calculation of the shortened energy balance equation. The installation of the meteorological flux tower adhered to the stringent eligibility criteria, to ensure methodological rigour, including: (i) representativeness, in terms of spatial variability, topography and land use; (ii) homogeneity, regarding land cover; (iii) fetch distance and (iv) sensor heights.

The EC system was comprised of an integrated open-path infrared gas analyser and 3D sonic anemometer (IRGASON, Campbell Scientific, Logan, UT, USA) that was mounted at a height of approximately 2 m above the plant canopy and captured data at 10 Hz, which enabled the direct measurement of the Latent Heat Flux (LE). The Sensible Heat Flux (H) was calculated by using a 3D sonic anemometer (CSAT3A, Campbell Scientific, Logan, UT, USA). A net radiometer (CNR4-L, Campbell Scientific, Logan, UT, USA) was incorporated, in order to compute the net radiation (Rn). At the same time, the soil heat flux (G) was measured within-row and inter-row, by using two soil Heat Flux Plates (HFPs) at a depth of 0.06 m (HFP01-L, Hukseflux, Delft, The Netherlands) (Figure 5.1b).

Each location also included four soil averaging thermocouples (TCAV, Campbell Scientific, Logan, UT, USA), for monitoring the soil temperature at depths of 0.04 and 0.08 m, as well as a water content reflectometer (CS616, Campbell Scientific, Logan, UT, USA), for measuring the volumetric water content in the top 0.08 m of the soil. Additional measurements at 0.30, 0.60 and 0.90 m depths were obtained by using CS616 probes.

The air temperature and relative humidity were recorded by using two integrated probes (H2CS3, Campbell Scientific, Logan, UT, USA) that were positioned near the IRGASON, which was supplemented by fine-wire thermocouples, for additional temperature data. A rain gauge (TE525MM-L, Campbell Scientific, Logan, UT, USA) was mounted on the structure, and an infrared radiometer (IRR, Apogee SI-111, Apogee Instruments Inc., Logan, UT, USA) was installed to monitor the canopy temperature. All instruments underwent calibration before deployment, to ensure their accuracy. Data loggers (CR3000 and CR1000, Campbell Scientific, Logan, UT, USA) collected measurements at 30-minute intervals (Figure 5.1c). The Easy Flux™ DL software facilitated the acquisition of fully-corrected fluxes from the EC system, including CO_2, LE, H, G and momentum, which integrated the optional energy balance sensors.

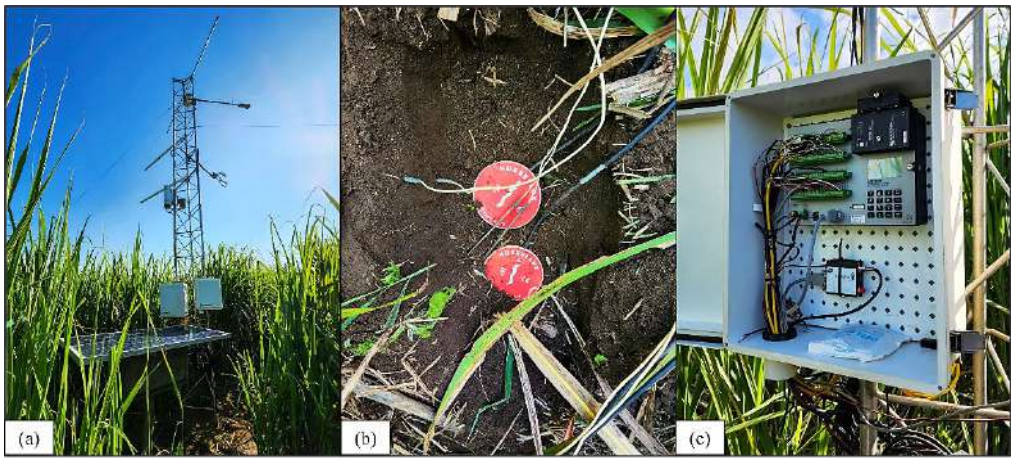

Figure 5.1 (a) EC system, (b) installation of the soil HFPs, and (c) CR3000 datalogger

Data processing procedures were performed using Microsoft Excel and by following a structured approach. A time-based filter was applied to the flux data, including only the measurements taken between 6:00 AM and 6:00 PM (SAST), as daytime solar radiation is essential for the energy balance equation. The negative values for Rn and G were excluded, particularly in instances where G exceeded Rn.

Due to missing data, a correction factor for G was applied from September 16 to October 26, 2023. This was determined by the mean ratio of G to Rn calculated between July 1 and September 15, 2023, which yielded a value of 6.64%. Data corresponding to quality assurance Grades 6-9 were excluded (Savage et al., 2017). An AWS (Climavue 50, Campbell Scientific, Logan, UT, USA) that continuously records the weather conditions was situated at a high school near the study site. Due to the proximity of the AWS to the smallholder farm (approximately 1.05 km), it was deemed to be suitable for recording the meteorological conditions at the study site. During data collection, Swayimane had an average daily air temperature of 17.9°C and a total rainfall of 1190 mm. In addition, the average wind speed, relative humidity and solar irradiance were measured at 1.86 m s^{-1}, 80.45% and 13.69 MJ m^{-2}, respectively.

5.2.2 UAV: DJI Matrice 300 and MicaSense Altum camera

The DJI Matrice 300 (M-300) platform, equipped with a MicaSense Altum camera and a Downwelling Light Sensor (DLS-2), enabled the capture of very high spatial resolution imagery of the smallholder cropland (Figures 5.2a and 5.2b) (Vélez et al., 2023; Khormizi et al., 2024). The four-rotor M-300, which featured vertical take-off and landing (VTOL) capabilities, is well-suited for aerial operations in rural areas adjacent to populated regions (Brewer et al., 2022). Notable features include a transmission range of up to 15 kilometres, a maximum operational altitude of 7000 m, obstacle detection and avoidance systems, flight path planning functions, as well as an integrated GPS tracker. With the Altum camera, the M-300 achieves a maximum flight duration of approximately 42 minutes and reaches speeds of up to 27 m s^{-1} (Brewer et al., 2022).

The MicaSense Altum camera integrates the optical and thermal infrared functionalities (Zarzar et al., 2020), which encompasses five narrow high-resolution spectral bands: blue, green, red, red-edge and near-infrared, along with a radiometric longwave infrared thermal sensor (Table 5.1) (Seiche et al., 2024). It features a global shutter mechanism that ensures high spatial resolution and alignment at a capture rate of up to one image per second (Hutton et al., 2020). The optical bands deliver a sensor resolution of 2064 × 1544 pixels. The corresponding Ground Sample Distance (GSD) at a flying height of 120 m measures 0.052 m per pixel (Brewer et al., 2022). Furthermore, the thermal infrared camera exhibits a sensor resolution of 160 × 120 pixels, with a GSD of 0.81 m per pixel at 120 metres (Brewer et al., 2022).

Figure 5.2 (a) DJI-M300 series platform, (b) MicaSense Altum camera

Table 5.1 Specifications of the MicaSense Altum camera (after Brewer et al., 2022)

Band	Spectral colour	Band centre/range (nm)	GSD at a flying height of 120 m (m pixel^{-1})
1	Blue	475	0.052
2	Green	560	0.052
3	Red	668	0.052
4	Red Edge	717	0.052
5	Near-infrared (NIR)	842	0.052
6	Thermal infrared	8000-14 000	0.81

5.2.3 UAV: image acquisition and processing

The flight area was delineated on the UAV console to define the geographical boundaries of the Swayimane study area (Figure 5.3a), enabling semi-autonomous flight operations (refer to Table 5.2). The UAV flights were scheduled on days with minimal cloud cover, in order to optimise the data acquisition conditions. A CRP was employed to calibrate the MicaSense Altum camera pre- and post-flight (Figure 5.3b) (Brewer et al., 2022). The CRP, functioning as a radiometric calibration target, is designed to provide consistent reflectance properties across the light spectrum captured by the Altum device (Sibanda et al., 2023). Additionally, the CRP facilitated the acquisition of absolute reflectance values, which allowed for a comparative data analysis across multiple flights (Kapari et al., 2024).

Following each flight, the acquired aerial imagery was processed by using Pix4Dfields photogrammetry software (version 1.8.0, Pix4D Inc., San Francisco, California, USA). This workflow involved radiometric corrections and the generation of mosaics, and it resulted in the creation of an orthomosaic image that was exported in GeoTIFF format.

Table 5.2 Flight specifications for the DJI-M300

Parameters	Specifications
Altitude	100 m
GSD	0.07 m pixel^{-1}
Speed	10 m s^{-1}
Flight duration	36 m 32 s
Image overlap	80%
Camera system	MicaSense Altum

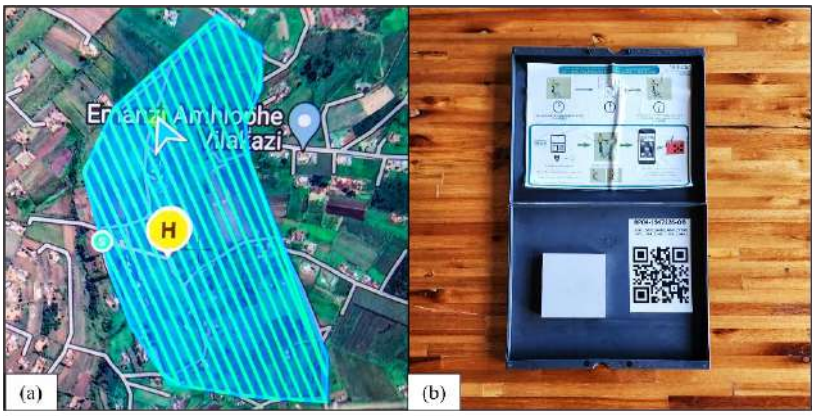

Figure 5.3 Conceptual flow diagram delineating the sequential processes involved in deriving ET-VIs

5.2.4 Vegetation index-based actual evapotranspiration estimation from UAV imagery and GEE processing

The UAV imagery was processed by using Pix4Dfields photogrammetry software (version 1.8.0, Pix4D Inc., San Francisco, California, USA). In total, 15 orthomosaic GeoTIFF files (representing the UAV flights conducted between July 2023 and March 2024) were created and resampled to a spatial resolution of 0.07 m, for further processing. To facilitate a quick and easy analysis, a data processing and visualisation app was developed in GEE to visualise and extract the data that were necessary for the estimation of the ETa.

The Google Earth Engine (GEE) is a cloud-based platform that is characterised by its user-friendly interface and extensive computational resources, and it is designed for processing large volumes of geospatial data (Senay et al., 2022). Importantly, the GEE enables users to generate systematic data products or to develop interactive applications by utilising their algorithms, without requiring expertise in application development or web programming (Gorelick et al., 2017). This investigation evaluates the effectiveness of GEE's advanced image processing capabilities for analysing the high-resolution multispectral imagery obtained from UAVs in small-scale agricultural operations. A data visualisation and processing tool was developed and utilised within GEE to compute spatially-explicit NDVI, EVI and EVI2 across the study site, by using a UAV image collection that was uploaded to the platform. The UAV-derived data and the visualisation app can be accessed here.

This investigation employed three distinct NDVI-based proxies, namely NDVI, NDVIscaled, and NDVIKc, as well as two EVI-based proxies, namely ET-EVI and ET-EVI2, to derive the Kc values for estimating the ET-NDVIs and ET-EVIs. According to the FAO56 methodology, the computation of ETa involves multiplying the Ks, Kc and ETo (Allen et al., 1998). Consequently, the VIs serve as proxies for the product of Ks and Kc (Equation 5.1) (Abbasi et al., 2023):

$$ET_a = K_c \times K_s \times ET_o \quad \text{or}$$

$$ET_a = VI \times ET_0 \qquad 5.1$$

Under sufficient moisture conditions and the absence of stress, the maximum Kc may approach 1.2, whereas the NDVI is limited to a maximum of 1 (Abbasi et al., 2023).

Therefore, adjustments to the NDVI values are necessary, in order to align them with the Kc range (Equation 5.2). Furthermore, numerous studies have documented a generalisable association between NDVI and Kc across various crops (Equation 5.3) (Belmonte et al., 2005; D'Urso, 2010; Akdim et al., 2014).

$$\mathrm{NDVI_{scaled}} = 1.2 \times \mathrm{NDVI} \quad 5.2$$

$$\mathrm{NDVI_{Kc}} = (1.25 \times \mathrm{NDVI}) + 0.2 \quad 5.3$$

The subsequent step involved retrieving VI values from the GEE application. However, it was observed that the mean NDVI values from two drone flights conducted on September 28 and October 26, 2023, were anomalously low at 0.31 and 0.26, respectively. In addition, the RGB images from these flights exhibited visible abnormalities. These occurrences may be attributed to factors, such as the timing of the flight, improper radiometric calibration, illumination variability during the flight or between calibration and data acquisition, as well as the misalignment of the spectral bands. These flights were therefore excluded from further analysis, which resulted in a final collection of 13 images. Due to the bi-weekly collection of UAV images, the UAV-derived VI values were aggregated into monthly averages, based on the respective VI values that were obtained each month. These monthly UAV-derived VIs served as inputs for the various VI-based models to estimate the monthly Kc. In line with the methodology outlined by Gokool et al. (2024), the monthly Kc estimates were utilisutilised alongside the daily Eto to calculate the daily Eta, by using each of the five models. The EVI and EVI2 were calculated by using Equations 5.4 and 5.5.

$$\mathrm{EVI} = 2.5 \times \left(\frac{\mathrm{NIR} - \mathrm{RED}}{\mathrm{NIR} + 6\mathrm{RED} - 7.5\mathrm{BLUE} + 1}\right) \quad 5.4$$

$$\mathrm{EVI2} = 2.5 \times \left(\frac{\mathrm{NIR} - \mathrm{RED}}{\mathrm{NIR} + \mathrm{RED} + 1}\right) \quad 5.5$$

Subsequently, five iterations of ETa were computed by multiplying pixel-specific estimates of Kc values (NDVI, NDVIscaled, NDVIKc, EVI and EVI2), with the corresponding ETo values, as specified in Equations 5.6-5.10 (see Figure 5.4).

$$\mathrm{ET_{NDVI}} = \mathrm{ET}_o \times \mathrm{NDVI} \quad 5.6$$

$$\mathrm{ET_{NDVIscaled}} = \mathrm{ETo} \times \mathrm{NDVI_{scaled}} \quad 5.7$$

$$\mathrm{ET_{NDVIKc}} = \mathrm{ETo} \times \mathrm{NDVI_{Kc}} \quad 5.8$$

$$\mathrm{ET_{EVI}} = \mathrm{ETo} \times \mathrm{EVI} \quad 5.9$$

$$ET_{EVI2} = ETo \times EVI2 \quad (5.10)$$

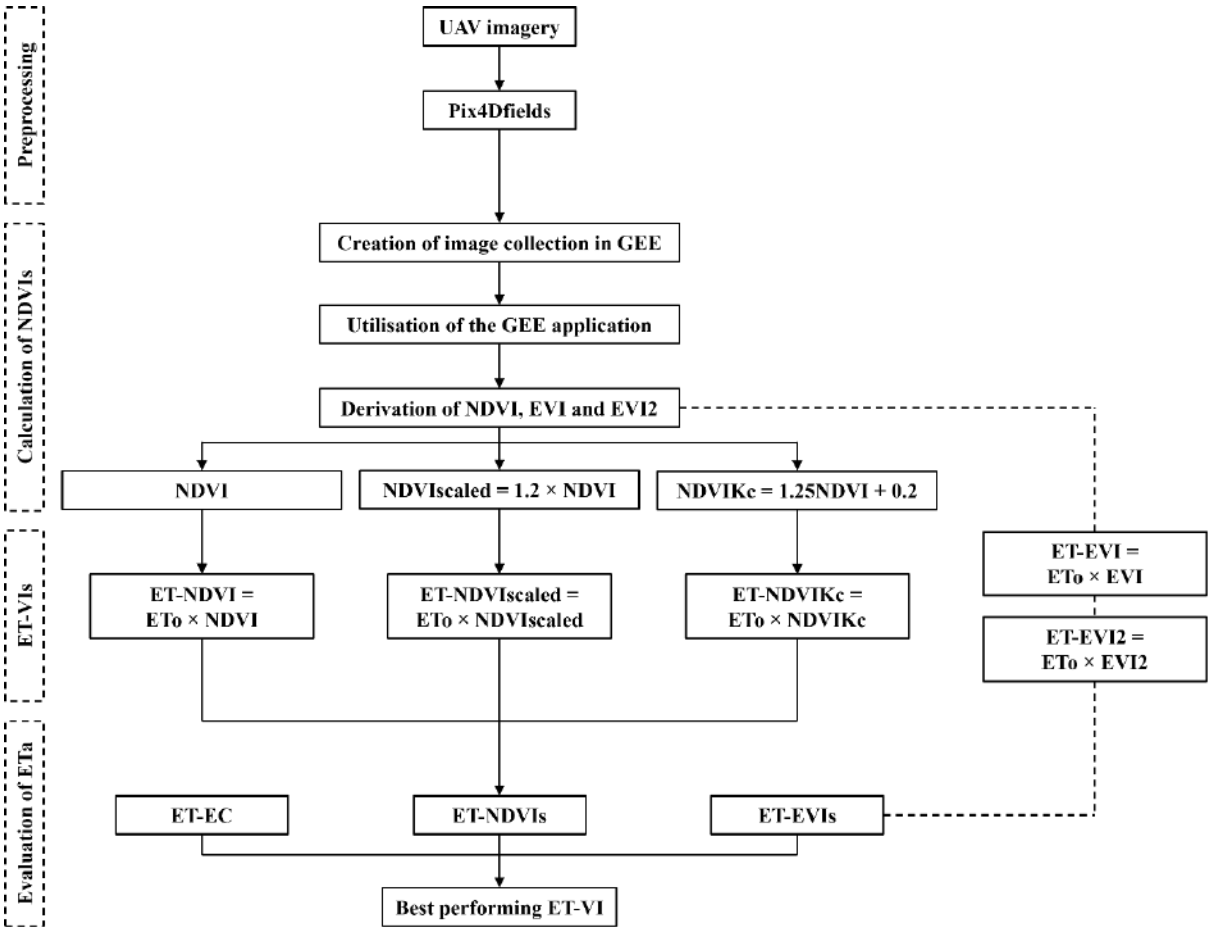

Figure 5.3 Conceptual flow diagram delineating the sequential processes involved in deriving ET-VIs

5.2.5 Assessing the quality of in-situ ET measurements and performance evaluation of VI-based ET estimates

Prior to the evaluation of the accuracy of the VI-based ET estimates, the potential level of uncertainty in the in-situ eddy covariance ET (ET-EC) measurements first needed to be established. For this purpose, a regression analysis between the turbulent energy fluxes (H + LE) and available energy (Rn - G) was undertaken to quantify the degree of energy balance closure (Baldocchi et al., 2000; Twine et al., 2000; Wilson et al., 2002).

Following the assessment of the energy balance closure, the accuracy of the daily VI-based ET estimates was ascertained by means of comparisons against the daily ET-EC, using a range of summary statistics and performance metrics, such as R^2, RMSE and MAE.

5.3 Results

5.3.1 Energy balance closure and daily ET

The precision of the EC system in quantifying turbulent fluxes was assessed by means of an Energy Balance Closure (EBC) analysis. Energy balance closure involves a linear regression between the turbulent energy fluxes (H + LE) and the available energy (Rn - G) (Baldocchi et al., 2000; Twine et al., 2000; Wilson et al., 2002). Jin et al. (2022) stated that a perfect energy balance closure requires the slope of the regression line to equal one and the intercept to be zero. Accordingly, the analyses constrained the intercept to zero (Jin et al., 2022). The findings revealed that turbulent fluxes were approximately 27% and 24% lower than the available energy for the 30-minute and daily intervals, respectively (Figure 5.5). These results indicate s a satisfactory EBC, which is consistent with previous studies that reported deficits ranging from 10% to 30% (Baldocchi et al., 2000; Twine et al., 2000; Testi et al., 2003; Poblete-Echeverría & Ortega-Farias, 2013). In addition, the R^2 values were 0.98 for the 30-minute time-step and 0.99 for the daily time-step, which further supports the reliability of the measurements.

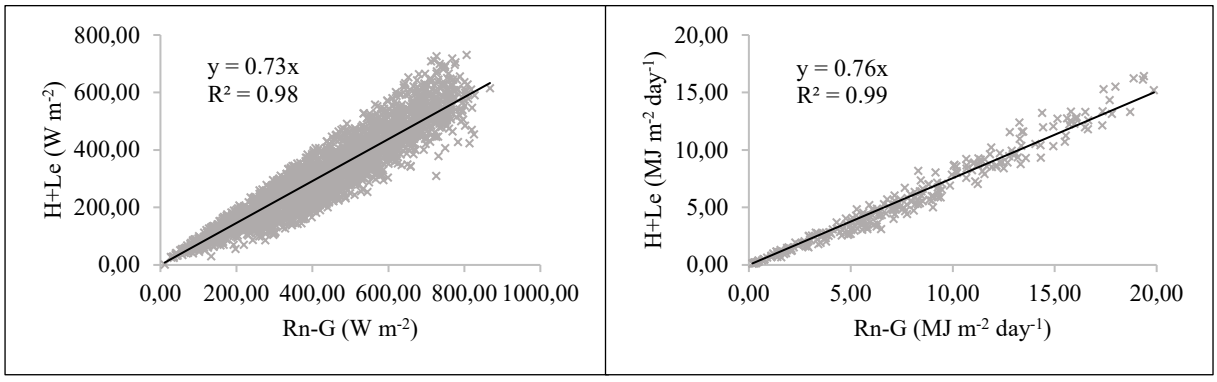

Figure 5.4 Scatter plots of Rn–G vs H+LE from the Swayimane flux tower, showing EBC gradients at 30-minute (left, W m^{-2}) and daily (right, MJ m^{-2} day^{-1}) temporal resolutions

A time-series comparison of the ETo and ET-EC across the data collection period reveals distinct seasonal and growth-phase trends (Figure 5.6). The ETo is consistently greater than the ET-EC across the observation period, with both variables exhibiting distinct seasonal variations. The daily values reached their lowest in June, they peaked in December, and gradually decreased through to May. This cyclical pattern is consistent with the expected seasonal climate changes, as warmer temperatures, increased rainfall and solar radiation during summer favour higher evapotranspiration rates, as opposed to the cooler and drier conditions that are experienced during winter. ET-EC is approximately 588 mm lower than the ETo across the entire data collection period and it is, on average, approximately 2.12 mm d^{-1} lower than the ETo (Table 5.3).

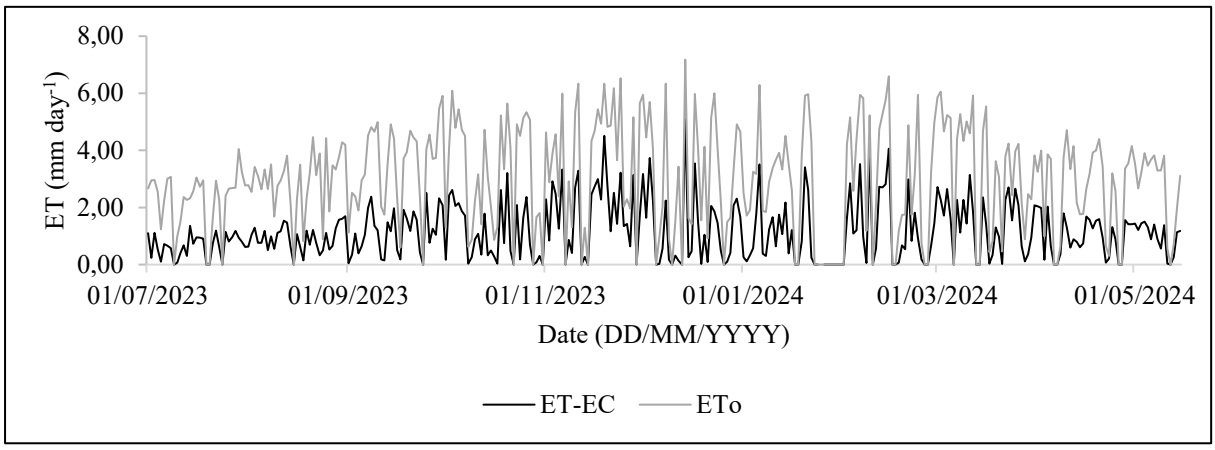

Figure 5.5 Daily ET-EC (mm day^{-1}) with ET_o (mm day^{-1}) during the sugarcane-growing season

Table 5.3 Summary of daily ET-EC (mm day^{-1}) and ET_o (mm day^{-1}) measured during the 2023-2024 growing season at the study site in Swayimane

	ET-EC	ET_o
Minimum (mm day^{-1})	0.02	0.31
Maximum (mm day^{-1})	5.09	7.18
Mean (mm day^{-1})	1.30	3.42
Median (mm day^{-1})	1.16	3.35
Std. dev. (mm day^{-1})	0.95	1.51
Sum (mm)	361.75	949.38

5.3.2 Comparative analysis of evapotranspiration-vegetation index products against eddy covariance measurements

The frequency and range of the modelled and measured daily ET estimates are presented in Figure 5.8. In general, the results indicate that the VI-based ET models tend to over-estimate the ET, when compared with ET-EC.

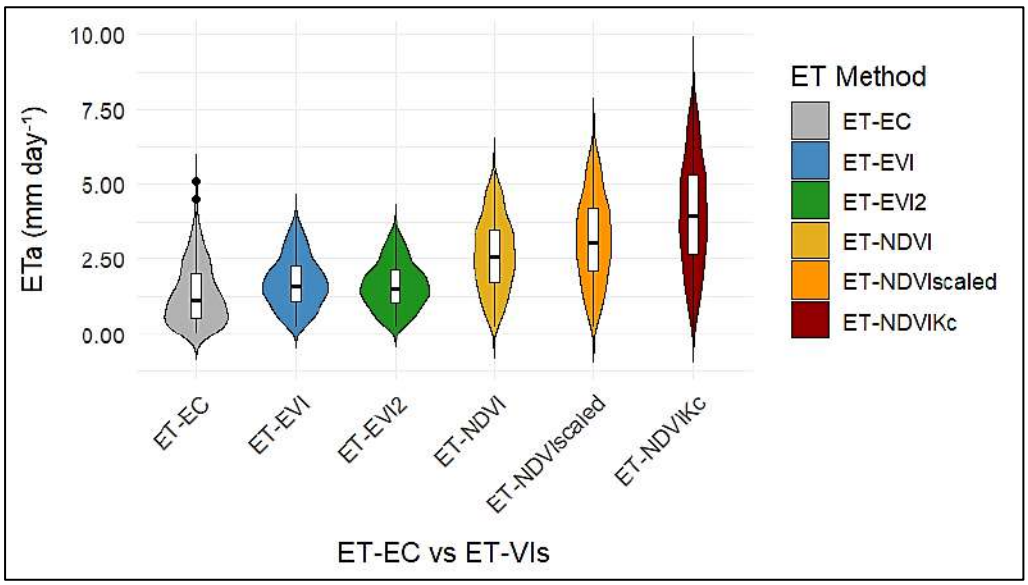

Figure 5.6 Violin plots illustrating the distribution of daily ET-EC (mm day^{-1}) and ET-VIs (mm day^{-1}) during the SE and M growth phases of sugarcane

The EVI-based (EVI and EVI2) ET estimation models demonstrating the closest association to ET-EC. As shown in Table 5.4, across the entire data collection period, the degree of over-estimation, when compared with ET-EC, was the greatest for ET estimates that were derived through the implementation of ET-NDVIKc (441 mm). Conversely, ET estimates that were derived through the implementation of ET-EVI2 exhibited the slightest degree of overestimation (71 mm), and this was closely followed by ET-EVI (94 mm). These observations are reaffirmed by the performance metrics presented in Figure 5.8, with the EVI-based ET estimation models producing similar R^2 values, but noticeably lower RMSE and MAE values, in comparison to the NDVI-based ET estimation models, when compared to those of the ET-EC. The time-series comparison (Figure 5.10) between the EVI-based ET estimation models and ET-EC also demonstrates that these modelled ET estimates are able to adequately capture the seasonal and growth-phase ET dynamics.

Table 5.4 Descriptive statistics for measured ET-EC and predicted ET-VI variants

	ET-EC	ET-NDVI	ET-NDVIscaled	ET-NDVIKc	ET-EVI	ET-EVI2
Minimum (mm day^{-1})	0.02	0.36	0.43	0.53	0.25	0.24
Maximum (mm day^{-1})	5.09	5.48	6.57	8.28	3.92	3.65
Mean (mm day^{-1})	1.34	2.66	3.19	4.02	1.73	1.63
Median (mm day^{-1})	1.12	2.58	3.09	3.95	1.62	1.55
Std. Deviation (mm day^{-1})	1.00	1.19	1.43	1.79	0.83	0.78
Total (mm)	317.73	632.64	759.17	956.97	412.39	388.53

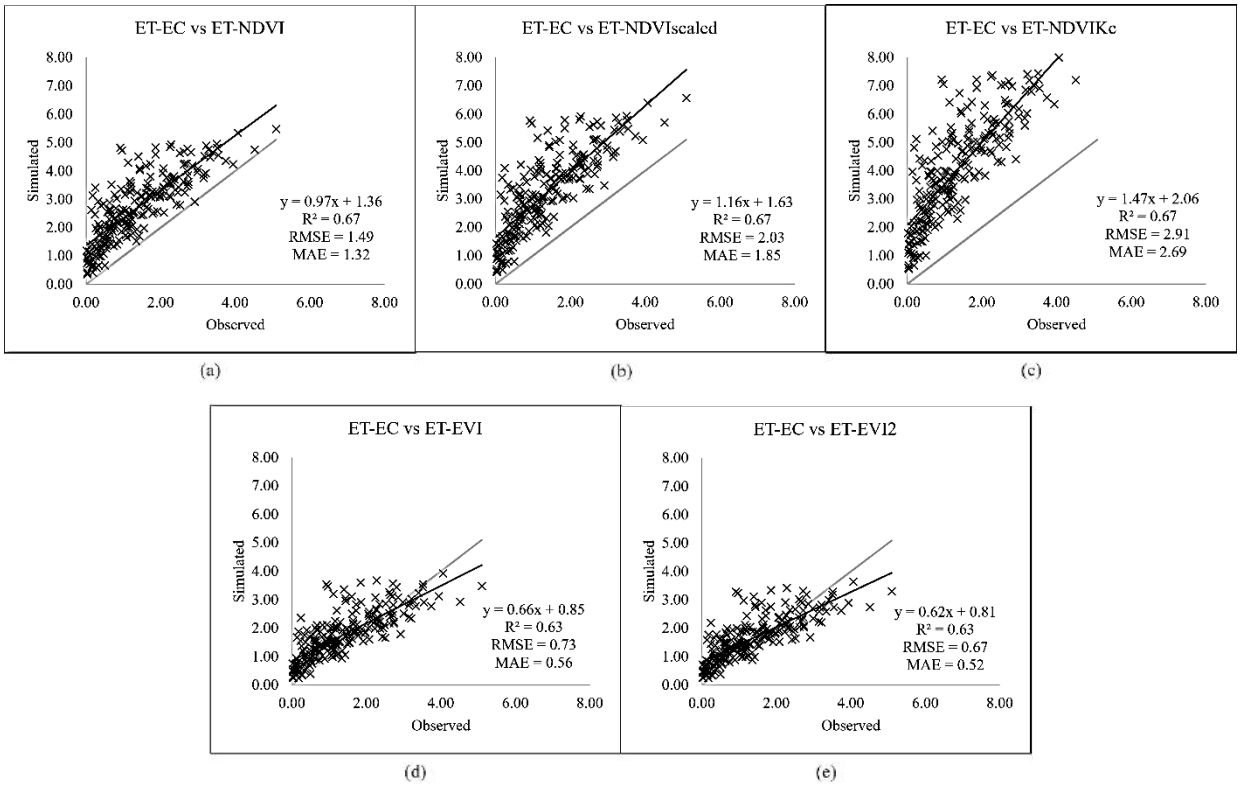

Figure 5.7 Regression analysis of ET-EC against simulated ET-VIs: (a) ET-NDVI, (b) ET-NDVIscaled, (c) ET-NDVIKc, (d) ET-EVI, and (e) ET-EVI2. The solid black line represents the regression line, while the grey line indicates perfect agreement between observed and simulated ETa values

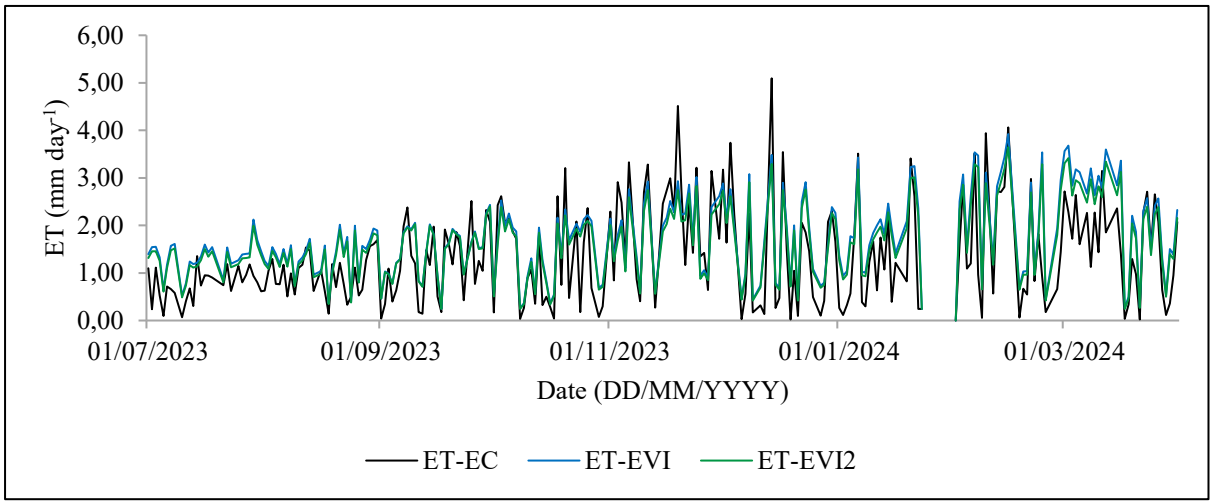

Figure 5.8 Comparison of EVI-based daily ET across the entire data collection period

5.3.3 Spatial distribution of sugarcane water-use across the study site

Spatially explicit ET maps (Figures 5.10 and 5.11) for the sugarcane cropland were generated for selected dates during the cooler and drier winter (18 July 2023) and the warmer and wetter summer (6 February 2024), by utilising the ET-VI approach. For the winter ET maps, the mean ET ranged from 1.45 mm day^{-1} (using the ET-EVI2 method) to 3.65 mm day^{-1} (using the NDVIKc method). The summer ET maps show noticeably higher ET values, with mean ET values ranging from 3.29 mm day^{-1} (using the ET-EVI2) to 7.21 mm day^{-1} (using the ET-NDVIKc). These findings demonstrate a significant rise in ET from winter to summer, which corresponds to the increased water usage during the warmer season.

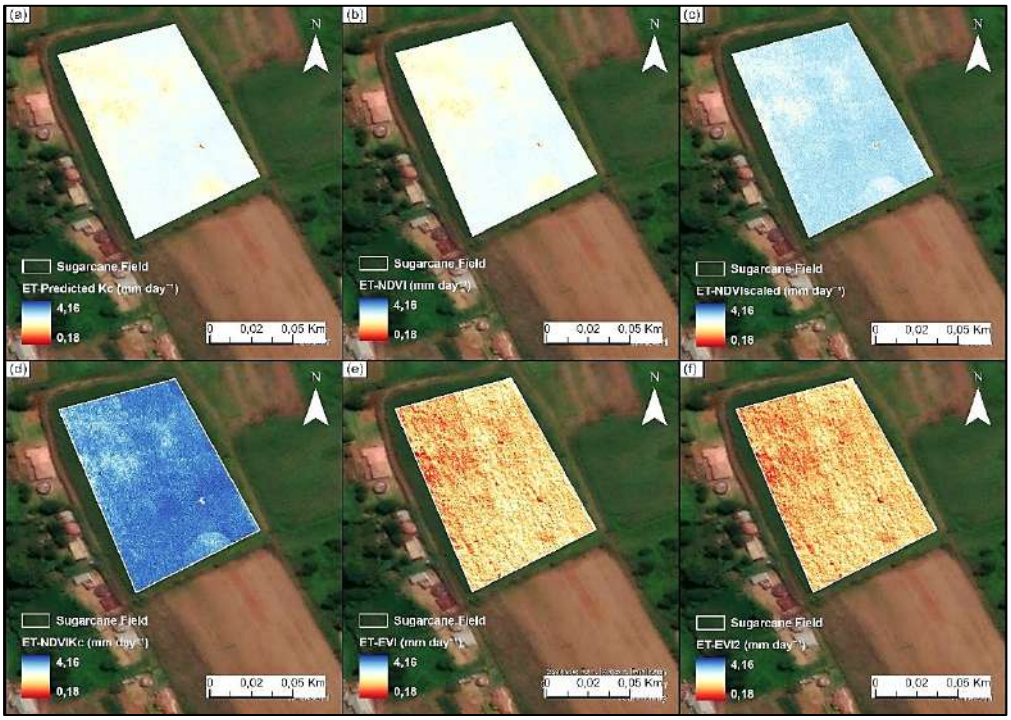

Figure 5.9 Modelled ETa maps (mm day^{-1}) for (a) ET-Predicted Kc, (b) ET-NDVI, (c) ET-NDVIscaled, (d) ET-NDVIKc, (e) ET-EVI, and (f) ET-EVI2 on July 18, 2023

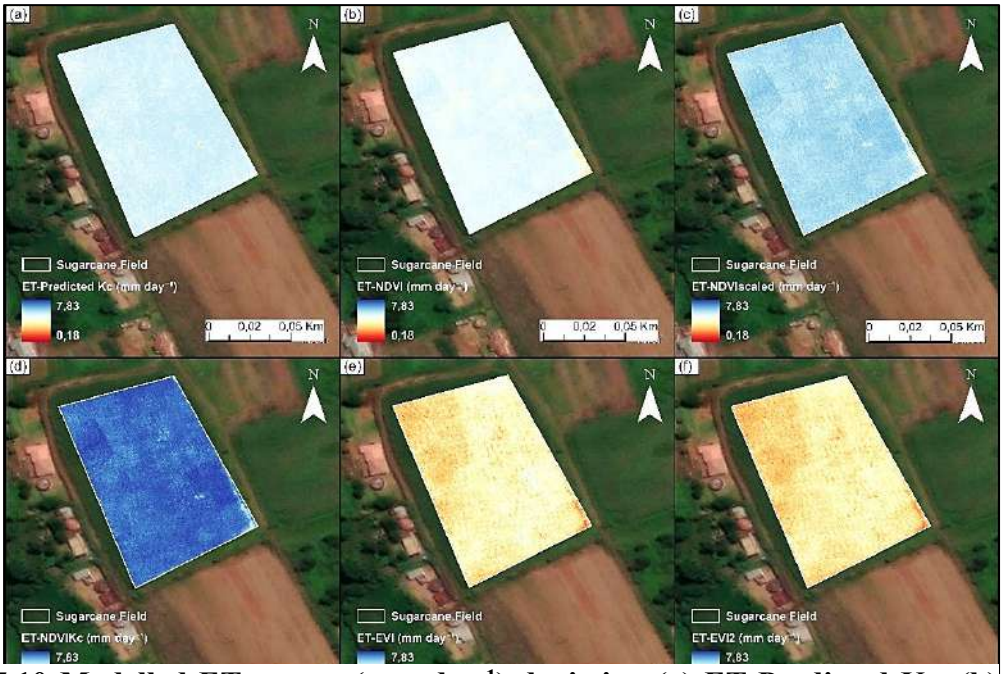

Figure 5.10 Modelled ETa maps (mm day^{-1}) depicting (a) ET-Predicted Kc, (b) ET-NDVI, (c) ET-NDVIscaled, (d) ET-NDVIKc, (e) ET-EVI, and (f) ET-EVI2, observed on February 6, 2024

5.4 Discussion

5.4.1 Assessing the quality of in-situ evapotranspiration measurements

While the EC system was set up to ensure that the level of uncertainty in the measurements is minimised, the results of the energy balance closure assessment revealed that there was a lack of closure, both at the 30-minute and daily time-steps. According to Mauder et al. (2020) and Jin et al. (2022), the lack of closure can be attributed to the combined influence of several factors, such as measurement and data processing errors, the lack of adequate turbulence development and low wind velocities. Furthermore, the averaging time of flux measurements can also influence the level of closure, with longer time steps usually displaying improved closure. Despite, the lack of perfect closure in our measurements, the level of closure for both the 30-minute and daily time steps was within acceptable limits, indicating that the in-situ ET measurements could be used as a reference to compare the UAV-derived ET estimates against.

5.4.2 Comparative analysis of evapotranspiration-vegetation index products against eddy covariance measurements

Over the course of the data collection period, the results of the analyses revealed consistently-higher ET values across all VI approaches, compared to ET-EC. While the degree of overestimation was highest for the NDVI-based ET models (ET-NDVI, ET-NDVIscaled and ET-NDVIKc), when compared to ET-EC, the EVI-based ET models (ET-EVI, ET-EVI2) exhibited greater resilience to canopy saturation and soil variation. ET-NDVIKc and ET-NDVIscaled displayed the poorest performance, which highlights the limitations of NDVI at a high biomass, where saturation reduces its sensitivity to vegetation changes. The inclusion of a blue band in the EVI and its coefficients mitigate the atmospheric and soil background effects, which improves its robustness (Jiang et al., 2008).

Consistent with Woldemariam et al. (2024), the EVI-based models outperformed the NDVI-based models, which emphasises the superior sensitivity of the EVI to biophysical changes that are crucial for monitoring sugarcane growth (Woldemariam et al., 2024). This aligns with previous research, and it highlights the superiority of EVI and EVI2 in estimating ET in semi-arid regions (Nouri et al., 2020; Abbasi et al., 2023).

These findings underline the potential of the ET-VI approach for sustainable water and resource management in agriculture. Despite the good performance of EVI-based ET models, it should be noted that all the VI-based ET models overestimated the ET, when compared to ET-EC. However, the level of overestimation may have been exaggerated to some degree by the lack of energy balance closure, which may have contributed to an underrepresentation of the ET within the observed data record.

5.4.3 Limitations and recommendations for future research

In-situ EC measurements were utilised to evaluate the accuracy of the ET estimates produced by the various ET-VI methodologies. However, due to the time-frame of the study, these in-situ measurements only captured a portion of the sugarcane growth cycle. To further understand the capabilities of these ET-VI based models, it is advisable to utilise a larger and more representative dataset that encompasses the entire sugarcane growth cycle, beyond the 10-month period of this study. This dataset should incorporate a broader spectrum of soil moisture levels and diverse sugarcane genotypes across various regions, in order to better capture the variability in crop responses and environmental interactions, which will ultimately improve our understanding of the models' robustness and applicability across different climatic and environmental settings.

Despite their perceived simplicity (Glenn et al., 2010), VI-based methodologies are prone to inaccuracies and biases. NIR and R-reflectance from the visible band typically yield a higher resolution than thermal bands (Nagler et al., 2005; French et al., 2020). However, these spectral bands are insufficient for capturing soil evaporation following irrigation and precipitation events, which complicates drought and water stress assessments. Although the immediate effects of water scarcity on plant characteristics are generally minimal (Moran et al., 1994), NDVI saturation in densely vegetated regions limits its reliability as an indicator of short-term variations in plant water stress.

EVI has proven to be more effective in alleviating NDVI saturation, particularly in dense vegetation, by mitigating atmospheric influences and demonstrating reduced sensitivity to background noise (Huete et al., 2002). However, EVI's dependence on a blue band may lead to low signal-to-noise ratios and potential instability. Consequently, EVI2 was introduced as a supplementary metric, which circumvents the need for a blue band and offers greater noise resilience, thus enhancing its reliability as an index (Jiang et al., 2007; Jiang et al., 2008).

While the use of alternate or multiple vegetation indices can overcome some of the aforementioned challenges, the costs associated with multi-spectral sensors that are used to captured the requisite data to derive these indices, as well as the expertise and software required for data processing, can limit the feasibility of adopting these approaches for smallholder farm applications. To improve the accessibility for smallholder farmers, future studies should evaluate the potential of adopting similar VI-based ET estimation approaches by using RGB sensors, as these are generally more affordable. Nevertheless, the findings presented in this study show promise in the use of UAV-based approaches to quantify crop water use in a smallholder farm setting. This, in turn, can facilitate PA practices, particularly precision water management, which can potentially improve agricultural water management and productivity within these smallholder farms.

5.5 Conclusion

The focus of this study was to explore the potential of utilising UAV-acquired data to accurately estimate crop water use, in order to facilitate precision water management within the smallholder farm context. Of the various approaches that were evaluated, the EVI-based approaches showed the greatest promise. This finding has also been documented in several studies, which underscores its potential as a viable UAV-based approach for crop water use estimation. While the uptake in the use of these technologies for smallholder farm applications remains in its infancy, due to capacity constraints, it is envisaged that these challenges will become less obtrusive in the future, which will increase the accessibility and viability of adopting UAV-based approaches to guide and inform agricultural management decisions.

5.6 References

ADISA O, BOTAI CM, BOTAI JO, HASSEN A, DARKEY D, TESFAMARIAM EH, ADISA AF, ADEOLA AM and NCONGWANE KP (2018) Analysis of agro-climatic parameters and their influence on maize production in South Africa. *Theoretical and Applied Climatology* **134** 991–1004.

AKDIM N, ALFIERI SM, HABIB A, CHOUKRI A, CHERUIYOT EK, LABBASSI K and MENENTI M (2014) Monitoring of irrigation schemes by remote sensing: phenology versus retrieval of biophysical variables. *Remote Sensing* **6** 5815–5851.

BACHOUR R (2013) Evapotranspiration modelling and forecasting for efficient management of irrigation command areas. Unpublished thesis, Department of Civil and Environmental Engineering, Utah State University, Logan, Utah.

BALDOCCHI DD, LAW BE and ANTHONI PM (2000) On measuring and modeling energy fluxes above the floor of a homogeneous and heterogeneous conifer forest. *Agricultural and Forest Meteorology* **102**(2) 187–206.

BASTIAANSSEN WGM, CHEEMA MJM, IMMERZEEL WW, MILTENBURG IJ and PELGRUM H (2012) Surface energy balance and actual evapotranspiration of the transboundary Indus Basin estimated from satellite measurements and the ETLook model. Water Resources Research **48** (11).

BELMONTE AC, JOCHUM AM, GARCÍA AC, RODRÍGUEZ AM and FUSTER PL (2005) Irrigation management from space: Towards user-friendly products. *Irrigation and Drainage Systems* **19** (3) 337–353.

BREWER K, CLULOW A, SIBANDA M, GOKOOL S, ODINDI J, MUTANGA O, NAIKEN V, CHIMONYO VGP and MABHAUDHI T (2022) Estimation of maize foliar temperature and stomatal conductance as indicators of water stress based on optical and thermal imagery acquired using an unmanned aerial vehicle (UAV) platform. *Drones* **6** (7).

D'URSO G (2010) Current status and perspectives for the estimation of crop water requirements from earth observation. *Italian Journal of Agronomy* **5**.

FILGUEIRAS R, MANTOVANI E, ALTHOFF D, BALIEIRO RIBEIRO R, VENANCIO L and ARGOLO DOS SANTOS R (2019) Dynamics of actual crop evapotranspiration based in the comparative analysis of SEBAL and METRIC-EEFLUX. *IRRIGA* **1** 72–80.

FRENCH AN, HUNSAKER DJ, BOUNOUA L, KARNIELI A, LUCKETT WE and STRAND RJ (2018) Remote sensing of evapotranspiration over the Central Arizona irrigation and drainage district, USA. *Agronomy* **8** (12) 278.

GLENN EP, JARCHOW CJ and WAUGH WJ (2016) Evapotranspiration dynamics and effects on groundwater recharge and discharge at an arid waste disposal site. *Journal of Arid Environments* **133** 1-9.

GOKOOL S, MAHOMED M, KUNZ R, CLULOW A, SIBANDA M, NAIKEN V, CHETTY K and MABHAUDHI T (2023) Crop monitoring in smallholder farms using unmanned aerial vehicles to facilitate precision agriculture practices: A scoping review and bibliometric analysis. *Sustainability* **15** (4).

GORELICK N, HANCHER M, DIXON M, ILYUSHCHENKO S, THAU D and MOORE R (2017) Google Earth Engine: Planetary-scale geospatial analysis for everyone. *Remote Sensing of Environment* **202** 18–27.

HESS TM, SUMBERG J, BIGGS T, GEORGESCU M, HARO-MONTEAGUDO D, JEWITT, G, OZDOGAN M, MARSHALL M, THENKABAIL P, DACCACHE A, MARIN F and KNOX JW (2016) A sweet deal? Sugarcane, water and agricultural transformation in Sub-Saharan Africa. *Global Environmental Change* **39** 181–94.

HOFFMANN H, NIETO H, JENSEN R, GUZINSKI R, ZARCO-TEJADA P and FRIBORG T (2016) Estimating evaporation with thermal UAV data and two-source energy balance models. *Hydrol. Earth Syst. Sci.* **20** (2) 697–713.

HU P, CHAPMAN S and ZHENG B (2021) Coupling of machine learning methods to improve estimation of ground coverage from unmanned aerial vehicle (UAV) imagery for high-throughput phenotyping of crops. *Functional Plant Biology* **48**.

HUNSAKER DJ, PINTER P, BARNES EM and KIMBALL BA (2003) Estimating cotton evapotranspiration crop coefficients with a multispectral vegetation index. *Irrigation Science* **22** 95–104.

HUTTON JJS, LIPA G, BAUSTIAN D, SULIK JJ and BRUCE RW (2020) High accuracy direct georeferencing of the altum multi-spectral uav camera and its application to high throughput plant phenotyping. ISPRS - International Archives of the Photogrammetry, *Remote Sensing and Spatial Information Sciences*. 451-456. 10.5194/isprs-archives-XLIII-B1-2020-451-2020.

JIANG Z, HUETE A, KIM Y and DIDAN K (2007) 2-Band enhanced vegetation index without a blue band and its application to AVHRR data. Proceedings of SPIE - The International Society for Optical Engineering 6679.

JIANG Z, HUETE AR, DIDAN K and MIURA T (2008) Development of a two-band enhanced vegetation index without a blue band. *Remote Sensing of Environment* **112** (10) 3833–3845.

JIN Y, LIU Y, LIU J and ZHANG X (2022) Energy balance closure problem over a tropical seasonal rainforest in Xishuangbanna, south-west China: Role of Latent Heat Flux. Water **14** (3).

KAMARA A, CONTEH AR, RHODES E and COOKE R (2019) The relevance of smallholder farming to African agricultural growth and development. *African Journal of Food, Agriculture, Nutrition and Development* **19** 14043–14065.

KUSANGAYA S, WARBURTON TOUCHER M, ARCHER E and JEWITT G (2013) Impacts of climate change on water resources in southern Africa: A review. *Physics and Chemistry of the Earth Parts A/B/C* **67-69**.

MADAMOMBE S, KARANJA S, OBORN I, GEORGE N, CHIRINDA N, KIHARA J and LIBÈRE N (2024) Climate change awareness and adaptation strategies by smallholder farmers in semi-arid areas of Zimbabwe. *International Journal of Agricultural Sustainability* **22.**

MATTON N, SEPULCRE CG, WALDNER F, VALERO S, MORIN D, INGLADA J, ARIAS, M, BONTEMPS S, KOETZ B and DEFOURNY P (2015) An automated method for annual cropland mapping along the season for various agrosystems globally distributed using spatial and temporal high resolution time series. *Remote Sensing* **7** 13208–13232.

MAUDER M, FOKEN T and CUXART J (2020) Surface-energy-balance closure over land: A review. *Boundary-Layer Meteorology* **177** 395-426.

MESSINA G and MODICA G (2020) Applications of UAV thermal imagery in precision agriculture: State of the art and future research outlook. *Remote Sensing* **12** 1491.

MINACAPILLI M, CONSOLI S, VANELLA D, CIRAOLO G and MOTISI A (2016) A time domain triangle method approach to estimate actual evapotranspiration: Application in a Mediterranean region using MODIS and MSG-SEVIRI products. *Remote Sensing of Environment* **174** 10-23.

MORAN MS, CLARKE TR, INOUE Y and VIDAL A (1994) Estimating crop water deficit using the relation between surface-air temperature and spectral vegetation index. *Remote Sensing of Environment* **49** (3) 246-263.

MUZARI W, GATSI W and MUVHUNZI S (2012) The impacts of technology adoption on smallholder agricultural productivity in sub-Saharan Africa: A review. *Journal of Sustainable Development* **5**.

NAGLER P, SALL I, BARRETO-MUÑOZ A, GÓMEZ-SAPIENS M, NOURI H, CHAVOSHI BORUJENI S and DIDAN K (2022) Effect of restoration on plant greenness and water use in relation to drought in the riparian corridor of the Colorado River delta. *JAWRA Journal of the American Water Resources Association* **58** (5) 746–784.

NAGLER PL, SCOTT RL, WESTENBURG C, CLEVERLY JR, GLENN EP and HUETE AR (2005) Evapotranspiration on western U.S. rivers estimated using the Enhanced Vegetation Index from MODIS and data from eddy covariance and Bowen ratio flux towers. *Remote Sensing of Environment* **97** (3) 337–351.

NIU H, ZHAO T, WANG D and CHEN Y (2022) Estimating evapotranspiration of pomegranate trees using stochastic configuration networks (SCN) and UAV multispectral imagery. *Journal of Intelligent & Robotic Systems* **104**.

NOURI H, BEECHAM S, ANDERSON S and NAGLER P (2014) High spatial resolution WorldView-2 imagery for mapping NDVI and its relationship to temporal urban landscape evapotranspiration factors. *Remote Sensing* **6** (1) 580–602.

NOURI H, NAGLER P, CHAVOSHI BORUJENI S, BARRETO MUNEZ A, ALAGHMAND S, NOORI B, GALINDO A and DIDAN K (2020) Effect of spatial resolution of satellite images on estimating the greenness and evapotranspiration of urban green spaces. *Hydrological Processes* **34** (15) 3183–3199.

OKONYA J, SYNDIKUS K and KROSCHEL J (2013) Farmers' perception of and coping strategies to climate change: evidence from six agro-ecological zones of Uganda. *Journal of Agricultural Science* **5** 252–262.

ORTEGA-FARIAS S, IRMAK S and CUENCA RH (2009) Special issue on evapotranspiration measurement and modeling. *Irrigation Science* **28** (1) 1–3.

PANDAY US, PRATIHAST A, ARYAL J and KAYASTHA, RB (2020) A review on drone-based data solutions for cereal crops. *Drones* **4** (41).

POBLETE-ECHEVERRÍA C and ORTEGA-FARIAS S (2013) Evaluation of single and dual crop coefficients over a drip-irrigated Merlot vineyard (*Vitis vinifera* L.) using combined measurements of sap flow sensors and an eddy covariance system. *Australian Journal of Grape and Wine Research* **19** 249–260.

SCHULZE R (2011) Climate proofing the South African Water Sector 2: An initial study on practical suggestions for adaptation to climate change. Water Research Commission, Pretoria, South Africa. In: Schulze RE (Ed), A 2011 Perspective on Climate Change and the South African Water Sector, Chapter 9.3, 311-366. WRC Report TT 518/12, Water Research Commission, Pretoria, RSA.

SEGARRA J, BUCHAILLOT ML, ARAUS JL and KEFAUVER FC (2020) Remote sensing for precision agriculture: Sentinel-2 improved features and applications. *Agronomy* **10** (641).

SENAY G, FRIEDRICHS M, MORTON C, PARRISH G, SCHAUER M, KHAND K, KAGONE S, BOIKO O and HUNTINGTON J (2022) Mapping actual evapotranspiration using Landsat for the conterminous United States: Google Earth Engine implementation and assessment of the SSEBop model. *Remote Sensing of Environment* **275** 113011.

SHAO G, HAN W, ZHANG H, LIU S, WANG Y, ZHANG L and CUI X (2021) Mapping maize crop coefficient Kc using random forest algorithm based on leaf area index and UAV-based multispectral vegetation indices. *Agricultural Water Management* **252** 106906.

SUR C, KANG S, KIM J-S and CHOI M (2015) Remote sensing-based evapotranspiration algorithm: a case study of all sky conditions on a regional scale. *GIScience & Remote Sensing* **52** (5) 627–642.

TANG J, HAN W and ZHANG L (2019) UAV multispectral imagery combined with the FAO-56 dual approach for maize evapotranspiration mapping in the North China Plain. *Remote Sensing* **11** (21) 2519.

TESTI L, VILLALOBOS F and ORGAZ F (2003) Evapotranspiration of a young irrigated olive orchard in southern Spain. *Agricultural and Forest Meteorology* **121** 1–18.

TIAN X, YAN M, TOL C, LI Z, SU B, ERXUE C, LI L, WANG X, PAN X, GAO L and HAN Z (2017) Modeling forest above-ground biomass dynamics using multi-source data and incorporated models: A case study over the qilian mountains. *Agricultural and Forest Meteorology* **246** 1–14.

TWINE T, KUSTAS WP, NORMAN J, COOK D, HOUSER P, TEYERS TP, PRUEGER J, STARKS P and WESELY M (2000) Correcting eddy-covariance flux underestimates over a grassland. *Agricultural and Forest Meteorology* **103**.

WAGNER W, FRANCISCO JP, FLUMIGNAN DL, MARIN FR and FOLEGATTI MV (2022) Optimised algorithm for evapotranspiration retrieval via remote sensing. *Agricultural Water Management* **262** 107390.

WALKER NJ and SCHULZE RE (2006) An assessment of sustainable maize production under different management and climate scenarios for smallholder agro-ecosystems in KwaZulu-Natal, South Africa. Physics and Chemistry of the Earth, Parts A/B/C **31**(15) 995–1002.

WILSON K, GOLDSTEIN A, FALGE E, AUBINET M, BALDOCCHI D, BERBIGIER P, BERNHOFER C, CEULEMANS R, DOLMAN H, FIELD C, GRELLE A, IBROM A, LAW BE, KOWALSKI A, MEYERS T, MONCRIEFF J, MONSON R, OECHEL W, TENHUNEN J, VALENTINI R and VERMA S (2002) Energy balance closure at FLUXNET sites. *Agricultural and Forest Meteorology* **113** (1) 223–243.

WOLDEMARIAM G, GESSESSE AB and VARGAS MARETTO R (2024) Remote sensing vegetation indices-driven models for sugarcane evapotranspiration estimation in the semiarid Ethiopian Rift Valley. *ISPRS Journal of Photogrammetry and Remote Sensing* **215** 136-156.

YACOOB A, GOKOOL S, CLULOW A, MAHOMED M and MABHAUDHI T (2024) Leveraging unmanned aerial vehicle technologies to facilitate precision water management in smallholder farms: A scoping review and bibliometric analysis. *Drones* **8** (9) 476.

6 A MACHINE LEARNING APPROACH FOR QUANTIFYING CROP WATER STRESS IN SMALLHOLDER FARMS, USING UNMANNED AERIAL VEHICLE MULTISPECTRAL IMAGERY

6.1 Introduction

Widespread water scarcity, erratic weather patterns and arid conditions increasingly compromise agricultural productivity across the Southern African Development Community (SADC) region (Lickley & Solomon, 2018; Brewer et al., 2022). This crisis disproportionately affects many smallholder farmers within the region, who cultivate less than two hectares of land and predominantly practice dryland agriculture, which leads to significant water-related challenges, due to the unpredictable precipitation (Rockstrom, 2000; Adisa et al., 2018; Gokool et al., 2023). Consequently, livelihoods and food security remain acutely threatened.

South Africa, a key player in the SADC region, which collectively contributes nearly 58% of Africa's sugar production and exports, over 1.2 million tons annually, faces increasing pressure to sustain its agricultural output amid environmental challenges (Ngcobo, 2023). Limited access to financial resources, technology and appropriate irrigation systems causes substantial socio-economic hardships among these smallholder farmers (Gokool et al., 2023). This situation is severely exacerbated by the high water demand of sugarcane (approximately 850 mm per growth cycle for sustainable rainfed production) (Carr & Knox, 2011; Jones et al., 2015) and the effects of climate change, which include an increased drought frequency, reduced water availability, and amplified precipitation variability (Knox et al., 2010; Archer et al., 2019; IPCC, 2019). While various factors may influence crop growth, water stress frequently emerges as the primary constraint on plant development (Haarhoff et al., 2020; Zaib et al., 2023). Water deficits can induce stomatal closure, which reduces transpiration and increases the leaf temperature, due to decreased evaporative cooling (Jackson, 1982; Saseendran et al., 2015).

The urgent need for adequate water stress detection and mitigation strategies in South Africa is evident, as the lack of comprehensive assessment tools hinders the implementation of such measures (Bezuidenhout & Singels, 2007; Andersson et al., 2009; Dunkelberg et al., 2014; Olivier & Singels, 2015; Lu et al., 2017).

Traditional methods for evaluating crop water stress, namely, relying on in-situ measurements, the soil moisture content or climatic factors, are often time-consuming, expensive and labour-intensive (González-Dugo et al., 2006; Safdar et al., 2023), particularly in regions like South Africa, where security concerns further compromise their effectiveness (Gray et al., 2022). RS techniques, which utilise specific regions of the electromagnetic spectrum to indirectly measure the crop water content via the biochemical properties of leaves, offer a promising alternative and have become crucial for the monitoring of crop conditions and water stress in PA (Brewer et al., 2022a; Liu et al., 2023; Safdar et al., 2023). RS-based techniques often rely upon the use of the data acquired from the visible, near-infrared (NIR) and thermal infrared (TIR) regions of the electromagnetic spectrum to detect the plant physiological changes that are associated with water stress.

Narrow-band indices, particularly those using visible and red-edge spectral regions, have been proven to be effective in detecting crop water stress (Zarco-Tejada et al., 2013; Zhao et al., 2015), and they are often preferred to the TIR methods. Vegetation Indices (Vis), which are derived from leaf reflectance in the visible and NIR spectrum, are widely used to evaluate the crop health and water status (Brewer et al., 2022a). These include indices, such as the NDVI, green NDVI (GNDVI) and the Optimised Soil Adjusted Vegetation Index (OSAVI) (Roujean & Breon, 1995; Allen et al., 1998; Haboudane et al., 2002; Bajwa & Vories, 2006; Baluja et al., 2012; Jones, 2014; Zhao et al., 2015; Leroux et al., 2016; Ihuoma & Madramootoo, 2017). Water indices that directly assess the vegetation and soil water content, offer significant advantages over the aforementioned traditional VIs for water stress detection (Virnodkar et al., 2020). The Normalised Difference Water Index (NDWI), which utilises the NIR and SWIR reflectance (approximately 860 nm and 1240 nm, respectively), is particularly effective for this purpose and it is among the most frequently-applied indices that are used to detect plant water stress (Ihuoma & Madramootoo, 2017).

Although RS technologies provide a feasible alternative to traditional crop water stress detection methods, there are trade-offs between the spatiotemporal and spectral resolution of the sensors onboard the various platforms (spaceborne and airborne sensors). Freely-available satellite-earth observation products generally provide sufficient spectral detail to detect crop water stress over large geographic extents; however, they lack the spatiotemporal resolution to capture the heterogeneity that is present within a smallholder farm setting.

Whereas finer spatial resolution commercial products are far too expensive for widespread use in smallholder farm settings, UAV technologies, which have gained prominence in facilitating PA applications (e.g. crop monitoring) are able to overcome the spatiotemporal limitations of freely-available satellite-earth observation data products, and they are generally significantly cheaper than commercial satellite-earth observation products for widespread and long-term monitoring (Gokool et al., 2023). Despite these advantages, most UAVs that are utilised to facilitate PA applications utilise RGB or multispectral (MS) sensors, rather than hyperspectral sensors, due to their cost-effectiveness. However, this affordability comes at the expense of a reduced spectral resolution, as RGB and most MS sensors do not possess a SWIR band, which is typically used to detect plant water stress.

The accurate assessment of crop water stress in smallholder farming presents significant challenges, due to limitations in traditional remote sensing methods and the high cost of advanced sensor technologies. Considering the challenges of utilising each of the aforementioned remote sensing platforms independently, to quantify crop water stress within smallholder farm settings, this study proposes a novel method, which leverages the use of advanced Machine Learning Algorithms (MLAs) to exploit the synergies between these platforms to produce spatially explicit maps that can be used to assist in the identification and quantification of crop water stress.

6.2 Methodology

6.2.1 In-situ data collection techniques

Measurements of the climatic conditions (as described in Section 5.2.1) and plant physiological changes were taken within the study site to understand how potential crop water deficits affect vegetation growth dynamics and health. Data collection began ≈ 7.5 months into the growth cycle (July 18, 2023), with the crop already entering the Stalk Elongation (SE) phase by the time the measurements had commenced. The data collection period (July 18, 2023 to March 15, 2024) encompassed only the SE and M phases before the scheduled harvest in May 2024. A sampling strategy was developed to address the characteristics of sugarcane and the difficulties of traversing the field.

The sugarcane field was divided into six equal sections, with sampling points strategically arranged in a grid layout along the rows, approximately 10 metres apart. Six samples were extracted from each section, which yielded 36 samples.

However, three points were excluded from the analysis due to their proximity to the edge of the field and their location outside the designated sugarcane shapefile, which resulted in a final sample size of 33 (Figure 3.1). The chlorophyll content in sugarcane foliage was assessed by using a Konica Minolta SPAD 502 meter (Minolta Corporation, Ltd., Osaka, Japan), which provides portable, non-destructive measurements of red (650 nm) and infrared (940 nm) light transmittance through leaves. This device yields a dimensionless Soil Plant Analysis Development (SPAD) value that is indicative of the total chlorophyll concentration (Chl) (Sibanda et al., 2020; Brewer et al., 2022a). Measurements were conducted during optimal photosynthetic hours, specifically from 10:00 AM to 2:00 PM (SAST).

During the SE phase, SPAD readings were taken from the most recent fully-expanded leaf at the leaf blade-sheath junction. In the maturity phase, the focus shifted to the uppermost flag leaf, which is vital for photosynthetic efficiency. Measurements were obtained from three specific locations on a single leaf per plant, namely: mid-length near the primary vein, one-third from the apex and two-thirds from the apex. The average SPAD values from these sites enhanced the accuracy, with the device being shielded from direct sunlight during the readings (Brewer et al., 2022b). The chlorophyll measurements coincided with the UAV flight missions (as described in Sections 5.2.2 and 5.23), which facilitated a comprehensive plant health analysis. SPAD data were converted into Chl by using Equation 6.1 (Markwell et al., 1995), which resulted in an R^2 of 0.94 (Brewer et al., 2022b).

$$\mathrm{Chl} = 10^{\mathrm{M}(0.264)} \qquad (6.1)$$

Chl denotes the total chlorophyll concentration per unit leaf area measured in micromoles per square metre (μmol m^{-2}), while M, in this context, indicates the dimensionless SPAD value (Ling et al., 2011).

LAI was obtained by using the LAI-2200C sensor (Li-Cor, Inc., Lincoln, NE, USA), and the measurement protocol employed a sensor equipped with a 45° view cap (Castro-Nava et al., 2016).

To improve the accuracy of the measurement, data collection was prioritised for the early morning and late afternoon, under overcast sky conditions, in order to minimise the direct effects of sunlight, to reduce the glare and a variability in the readings (Castro-Nava et al., 2016). The LAI-2200C was positioned vertically above the sugarcane canopy, and the sensor head was aimed downward to capture the light transmission through the leaves. At each sampling point, 12 measurements were taken - four above the canopy and eight below - to account for the natural variability. Above-canopy readings were performed under various conditions for reliability, including: (i) diffuser caps in direct sunlight, (ii) diffuser caps in shaded areas, (iii) readings without a cap in shaded conditions, and (iv) conducting standard readings without any modifications or caps. The foliar temperature of the sugarcane crop was assessed by using the Testo Thermal Imager 882 (Testo SE & Co. KGaA, Lenzkirch, Germany). Readings were taken between 10:00 am and 2:00 pm (SAST) to align with the UAV flight missions (as described in Sections 5.2.2 and 5.23) and optimal photosynthetic conditions (Brewer et al., 2022a). The imager was aimed at the uppermost leaves, specifically the flag leaves, from approximately 1 metre away from the canopy, to ensure a clear line of sight.

Multiple readings were averaged from three points on each leaf: the mid-length, one-third from the apex, and two-thirds from the apex. Thermal images and numerical temperature data were documented to analyse the foliar temperature distribution across the crop (see Appendix D for measurement device details). In addition, the sugarcane height was measured by using a measuring staff that was positioned vertically alongside the main stem, which captured the distance from the ground level to the apex (the tip of the tallest leaf).

6.2.2 Water deficit index calculation

The Water Deficit Index (WDI) was used for comparative purposes to assess the ability of the UAV-derived NDWI to account for the crop water status. The WDI quantitatively illustrates the relationship between actual ET (ETa) and the potential ET (ETp) (Equation 6.2) (Moran et al., 1994; Antoniuk et al., 2021).

$$\mathrm{WDI} = 1 - \frac{\mathrm{ETa}}{\mathrm{ETp}} \tag{6.2}$$

The ETa was measured by using an EC system that provides real-time, high-accuracy assessments of the water vapour flux in the sugarcane crop (see Section 5.2.1). The ETp was estimated by multiplying the reference ET (ET_o) values by the crop coefficient (Kc) factors for each growth stage. The Penman-Monteith approach (Monteith, 1965), which is widely recognised as the leading approach for calculating ET_o, was used in this study (Equation 6.2) (Chimonyo et al., 2016; Roby et al., 2017);

$$ETo = \frac{0.408\Delta(R_n - G) + \gamma \frac{900}{T+273} u_2 (e_s - e_a)}{\Delta + \gamma(1 + 0.34u_2)} \quad (6.3)$$

where Δ represents the slope of the saturation vapour pressure curve in kPa°C^{-1}, Rn denotes the tnet radiation in MJ m^{-2} day^{-1}, and G signifies he soil heat flux density, also measured in MJ m^{-2} day^{-1}. The psychrometric constant (γ) is expressed in kPa °C^{-1}, T indicates the air temperature in °C, u_2 refers to the wind speed in m s^{-1}, e_s represents the saturation vapour pressure in kPa, and e_a indicates the actual vapour pressure in kPa. For the calculation of ETp, two Kc values were used for the two sugarcane growth phases i.e. Kc_{mid} = 1.25 during the SE phase and Kc_{end} = 0.75 for M (Allen et al., 1998).

While recognising the uncertainty in comparing WDI and NDWI is important, due to the potential impacts on the precision of water stress assessments, understanding their interaction could enhance the robustness of NDWI as an indicator of the vegetation water content. However, temperature-based indicators like the Crop Water Stress Index (CWSI) are often preferred, for their reliability in quantifying crop water stress (Zhang et al., 2019; Yacoob et al., 2024). Nevertheless, these approaches can potentially support informed decision-making in agricultural water management.

6.2.3 Remote sensing data acquisition and machine learning model development for normalised difference water index prediction

6.2.3.1 Data preparation for Sentinel-2 imagery in the Google Earth Engine

In the GEE, training data acquisition points were strategically established within the sugarcane field to ensure representation. Three rows of five points were placed, avoiding proximity to the field edges. Sentinel-2 data (1 July 2023 to 31 May 2024) were imported at 10 m (visible and near-infrared) and 20 m (red-edge and shortwave infrared) spatial resolutions.

A 20% cloud cover threshold was applied for cloud masking, to enhance the data quality by removing obscured pixels. This time-frame resulted in a dataset comprising of 28 images with 15 points per image. Relevant spectral bands from the Sentinel-2 data were selectively extracted to support a further analysis. Various VIs were computed for each image in the Sentinel-2 dataset, to enable feature extraction by using specific functions, and these VIs were integrated as bands within the image structure (refer to Table 6.1). Following this, the script progressed to a time series analysis stage by implementing the VI calculation function across the image collection, thereby enhancing each image with the computed indices.

Table 6.1 Overview of VIs and corresponding equations

Vegetation index	Abbreviation	Equation	Reference
normalised difference water index	NDWI	$\frac{(\text{NIR} - \text{SWIR})}{(\text{NIR} + \text{SWIR})}$	(Gao, 1996)
normalised difference vegetation index	NDVI	$\frac{(\text{NIR} - \text{RED})}{(\text{NIR} + \text{RED})}$	(Huang et al., 2020)
green normalised difference vegetation index	GNDVI	$\frac{(\text{NIR} - \text{GREEN})}{(\text{NIR} + \text{GREEN})}$	(Rozenstein et al., 2018)
normalised difference vegetation index for red edge	NDVIre	$\frac{(\text{NIR} - \text{RED EDGE})}{(\text{NIR} + \text{RED EDGE})}$	(Pironato Amaro et al., 2024)
soil-adjusted vegetation index	SAVI	$(1 + 0.5) \times \left(\frac{(\text{NIR} - \text{RED})}{(\text{NIR} + \text{RED} + 0.5)}\right)$	(Brewer et al., 2022a)
transformed chlorophyll absorption in reflectance index	TCARI	$3 \times ((\text{RED EDGE} - \text{RED}) - 0.2 \times (\text{RED EDGE} - \text{GREEN}) \times (\text{RED EDGE}/\text{RED}))$	(Shang et al., 2015)
optimised soil-adjusted vegetation index	OSAVI	$\frac{(\text{NIR} - \text{RED})}{(\text{NIR} + \text{RED} + 0.16)}$	(Romero Ponce et al., 2018)
transformed chlorophyll absorption in reflectance index / optimised soil-adjusted vegetation index Ratio	TO	$\frac{\text{TCARI}}{\text{OSAVI}}$	(Haboudane et al., 2002)

Temporal information was then integrated into the image collection by incorporating the data properties, which enabled the retrieval of time series data for each predefined point within the feature collection. Upon completing the time series analysis, a time series of the VI data for each specified point was exported to Google Drive as a comma-separated values (CSV) file.

6.2.3.2 Predictive modelling of NDWI using UAV-derived data in R Studio

The VI time series was imported into R Studio (Allaire, 2024) to develop and assess MLAs for predicting the NDWI by using VIs. The methodology consisted of several stages, namely, data preprocessing, model training, evaluation and prediction, using the trained models (Figure 4.8). Initially, the focus was on preprocessing Sentinel-2 data from the CSV file. The data were shuffled to introduce randomness, which optimised each model's performance in handling unseen data, thereby increasing the reliability and accuracy of the predictions. The dataset was partitioned into training and validation sets by utilising a standard 80/20 split (Gokool et al., 2022), a separating predictor and target variables for dedicated training and testing data frames.

A variety of MLAs, including the Generalised Linear Model (GLM), k-nearest neighbours (kNN), CART, RF, GTB and SVM (Kibirige et al., 2023), were implemented and assessed by using the caret package (Kuhn, 2008; Mayer, 2014). Performance metrics, such as the RMSE, R^2 and MAE were calculated to identify the most effective models for ensemble modelling (Gokool et al., 2022). The best-performing model was selected, based on these metrics, and two ensemble models were then developed by combining the predictions from multiple base models. The optimal ensemble model was applied to the validation dataset for a predictive analysis. The performance metrics were then computed, in order to evaluate the model's performance on unseen data. The study extended its analysis to predict NDWI values on the UAV-derived raster data. The same predictor variables that were used for the Sentinel-2 data to predict NDWI, using Vis, were also derived for each of the UAV images that were acquired during the course of the study (as described in Sections 5.2.2 and 5.2.3). The processed UAV-derived raster data were imported as a GeoTIFF file into R Studio and then transformed into a data frame. The previously-trained ensemble model (using Sentinel-2 data) was then used to predict the NDWI values for the UAV-derived raster data. These predicted NDWI values were added as a new column in the raster data frame, which was converted back into a raster object and saved as a GeoTIFF file, for further analysis and visualisation.

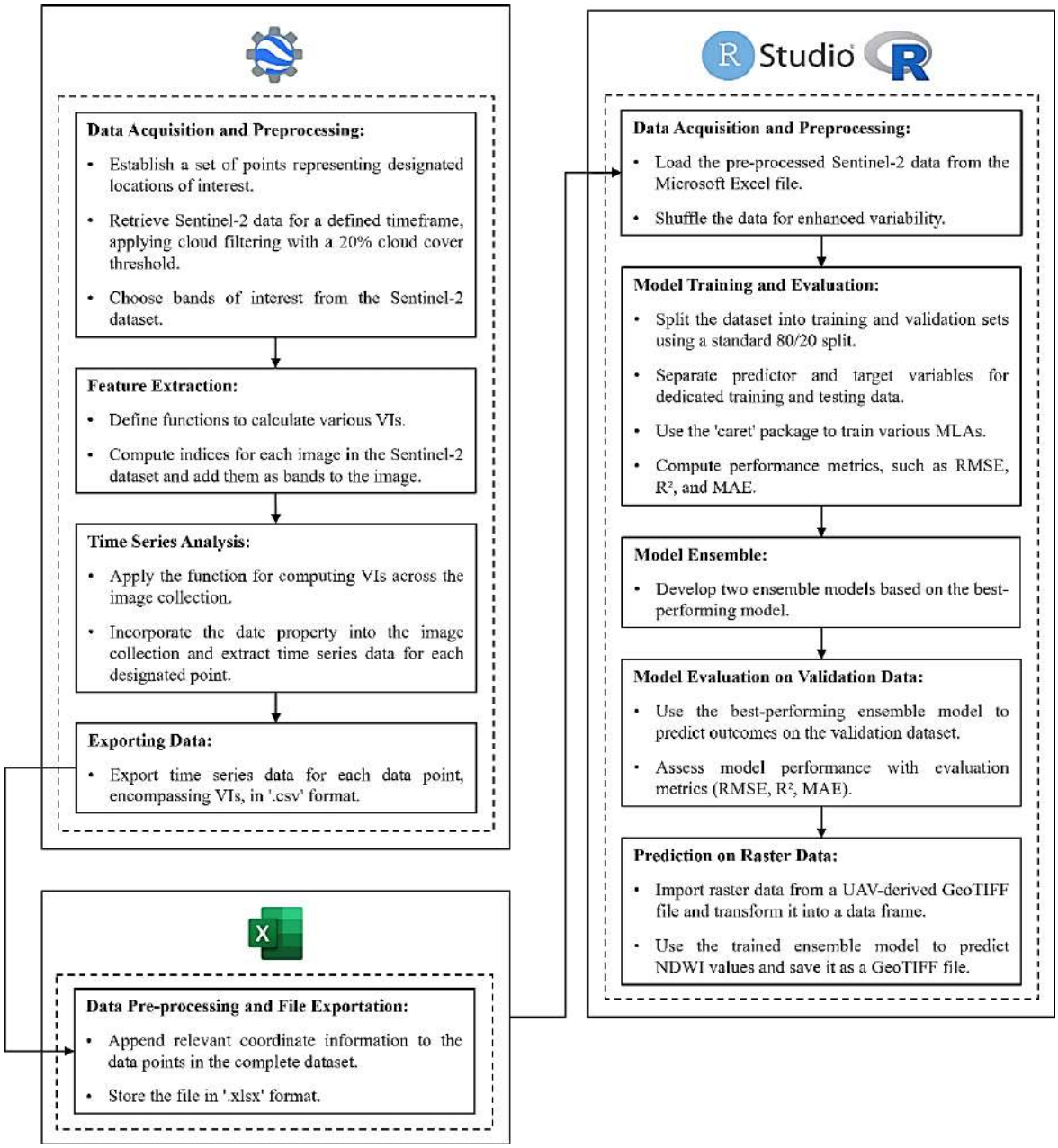

Figure 6.1 Conceptual flow diagram illustrating the methodology and framework for RS data acquisition, feature extraction and ML model development for NDWI prediction

6.3 Performance evaluation

The analysis integrated the in-situ measurements, UAV-acquired multispectral data and Sentinel-2 satellite imagery to evaluate the crop water stress dynamics. In order to compare Sentinel-2 satellite-derived VIs with in-situ measurements, the VIs were extracted by using GEE at 15 predefined sampling points across all available images, between July 2023 and May 2024. The temporal trends in the SE and early M phases of sugarcane were assessed by using descriptive statistics, including the mean, median, standard deviation, minimum and maximum values.

Corresponding in-situ measurements, namely the CC, LAI and crop height, were recorded at 33 sampling locations, as outlined in Section 6.2.1, to determine whether satellite-based indices reflected the observed physiological variations. For the UAV-based analyses, multispectral data and ensemble model-predicted NDWI were spatially linked to the in-situ sampling points. The geographic coordinates of the in-situ measurement locations were imported into ArcGIS Pro to extract UAV-derived raster values, which ensured spatial consistency across the datasets. This extraction process was uniformly applied to all subsequent analyses, including the Pearson correlation assessments and violin plots. A correlation analysis quantified the relationship between the UAV-derived VIs, the predicted NDWI and the in-situ crop parameters. Similarly, violin plots were generated to illustrate the distribution of the UAV-derived VIs, the predicted NDWI and the EC-derived ETa across the phenological stages of sugarcane.

6.4 Results

6.4.1 Comparative analysis of vegetation indices during the sugarcane growth phases: insights from Sentinel-2 imagery

Table 6.2 provides a comparative analysis of VIs for the sugarcane SE and early M phases, that were derived from Sentinel-2 imagery and analysed by using statistical measures, including the mean, median, standard deviation, minimum and maximum values.

Table 6.2 VIs derived from Sentinel-2 imagery for sugarcane SE and early M growth phases

Statistic	Phase	NDWI	NDVI	GNDVI	NDVIre	SAVI	TCARI	OSAVI	TO
Mean	SE	0.25	0.70	0.64	0.48	0.43	0.11	0.39	0.28
	M	0.34	0.78	0.70	0.57	0.49	0.10	0.48	0.22
Median	SE	0.26	0.70	0.64	0.48	0.43	0.11	0.40	0.27
	M	0.35	0.79	0.70	0.57	0.49	0.10	0.48	0.21
Std. dev.	SE	0.11	0.07	0.05	0.08	0.06	0.01	0.07	0.07
	M	0.06	0.03	0.03	0.04	0.03	0.01	0.03	0.03
Min.	SE	-0.09	0.51	0.51	0.23	0.29	0.07	0.18	0.18
	M	0.15	0.71	0.62	0.43	0.38	0.07	0.36	0.17
Max.	SE	0.45	0.85	0.74	0.63	0.55	0.14	0.53	0.70
	M	0.43	0.84	0.75	0.65	0.55	0.13	0.55	0.33

The mean values of the VIs indicate the overall crop health and water status, with the NDWI increasing from 0.25 in the SE phase, to 0.34 in the early M phase, which suggests reduced water stress, as the crop matures. Similarly, the NDVI, GNDVI and NDVI also rise from SE to early M, which reflects improved crop health over time. These indices, which are sensitive to vegetation greenness and CC, imply denser and more vigorous growth during early M. The mean increases in SAVI (0.43 to 0.49) and OSAVI (0.39 to 0.48) further support this, as they account for soil brightness and provide a clearer picture of the vegetation health. In contrast, TCARI shows a marginal decline, from 0.11 in the SE phase to 0.10 in the early M phase, which indicates a slight decrease in chlorophyll absorption as the crop matures. A slight reduction in TO (TCARI/OSAVI) (from 0.28 to 0.22) suggests subtle changes in the canopy structure, as the crop transitions from active growth to early M.

Minimum and maximum values reveal the range of the crop health and water status, with higher minimum values of NDWI, NDVI and GNDVI during the early M phase, which indicate improved conditions, even for the most stressed parts of the crop. While there are slight increases in the maximum values, particularly in NDVIre and OSAVI, which highlights the crop's enhanced health and moisture retention, the significant drop in the maximum TO, from 0.70 in the SE phase to 0.33 in early M, suggests a notable shift in the canopy structure and potential reductions in photosynthetic efficiency.

6.4.2 In-situ analysis of sugarcane physiological parameters across growth phases: correlations with satellite-derived indices

The in-situ measurements in Table 6.3 provide a detailed analysis of the physiological characteristics of sugarcane during the SE and early M phases. The parameters that were analysed include the CC, LAI and crop height, with the statistical measures offering insights into the crop's development and health. The mean values indicate improvements in the crop health, as the sugarcane transitions from SE to early M. For instance, the mean CC increases from 249.92 µmol m^{-2} in SE to 550.41 µmol m^{-2} in early M, which suggests an enhanced chlorophyll concentration, as well as improved photosynthetic activity and overall plant health. Similarly, the mean LAI rises from 3.92 to 5.13, which reflects more substantial leaf area development, which is crucial for maximising the photosynthetic efficiency. In addition, the mean crop height increases significantly, from 226 cm in SE to 273 cm in early M, which signals active vegetative growth.

Table 6.3 Descriptive statistics of sugarcane crop parameters across the SE and early M growth phases

Statistic	Phase	CC (µmol m^{-2})	LAI	Crop height (m)
Mean	SE	249.87	3.92	226
	M	550.45	5.13	273
Median	SE	247.52	3.67	225
	M	539.03	5.09	280
Std. dev.	SE	54.91	0.94	31
	M	45.23	0.69	55
Min.	SE	19.67	2.01	121
	M	249.43	3.37	130
Max.	SE	446.31	9.52	320
	M	880.52	7.72	360

The minimum values for CC and LAI show significant increases from SE to early M, which indicates improved conditions, even in the least-developed parts of the crop. For example, the minimum CC rises from 19.67 µmol m^{-2} in SE to 249.43 µmol m^{-2} in early M, which implies a better CC and health, even in the most stressed plants, as they mature. Conversely, the maximum values remain high across both phases, with slight increases from SE to early M, which highlights the potential for optimal growth during early M.

The in-situ measurements align closely with those of the satellite-derived Vis, such as NDWI, NDVI, GNDVI, NDVIre, SAVI, OSAVI, TCARI and TO. The increase in CC from SE to early M corresponds with rises in the NDVI, GNDVI and NDVIre, which are sensitive to chlorophyll and vegetation greenness. This confirms that both the in-situ and satellite data indicate healthier and more chlorophyll-rich foliage, as the crop matures. Furthermore, the LAI increases during the early M phase support the upward trends in NDWI, SAVI and OSAVI. The higher NDWI indicates an increased vegetation water content, which suggests an enhanced biomass and potentially-reduced water stress, which is consistent with the observed increases in the LAI. In summary, the in-situ measurements during the SE and early M phases, particularly regarding CC and LAI, strongly corroborate the trends that were observed in satellite-derived the VIs. Both datasets show improved crop health, density and uniformity as the sugarcane matures, and provide a thorough assessment of its development during these phases.

6.4.3 Evaluating ensemble model performance for predicting NDWI: a comparative analysis

The performance of the ensemble models for predicting NDWI was evaluated by using three performance metrics, namely, R^2, RMSE and MAE. Table 6.4 presents the comparative results of the two ensemble models. Ensemble Model 1 showed a strong predictive capability, with an R^2 of 0.87. Its RMSE and MAE values were 0.04 and 0.03, respectively, which indicate reliable accuracy. Ensemble Model 2 outperformed Model 1, achieving an R^2 of 0.95 and capturing 95% of the variance. It also had a lower RMSE (0.03) and MAE (0.02), which reflects enhanced precision and reduced errors. These findings demonstrate that Ensemble Model 2 offers more accurate and consistent NDWI predictions, which are likely due to the effective integration of the base models within the ensemble.

Table 6.4 Ensemble model results

	R^2	RMSE	MAE
Ensemble model 1	0.87	0.04	0.03
Ensemble model 2	0.95	0.03	0.02

6.4.4 Correlation analysis of predicted NDWI with UAV-derived structural indices and in-situ measurements

The Ensemble 2 model was used to derive spatially-explicit NDWI values across the study site (Figure 6.2). The correlation plot reveals the key relationships between the predicted NDWI, UAV-derived VIs and in-situ measurements, and it provides significant insights into the crop water status (Figure 6.3). A negative correlation between the NDWI and NIR (Pearson correlation R = -0.51) suggests that an increased NIR reflectance corresponds to reduced NDWI values, which indicates a possible decrease in the crop water content. This relationship underlines the sensitivity of NDWI to water stress, with the positive correlations observed between NDWI and indices, like NDVI (R = 0.51) and GNDVI (R = 0.52), suggesting that higher vegetation vigour and CC are associated with improved water status, which thus reflect healthier crop conditions.

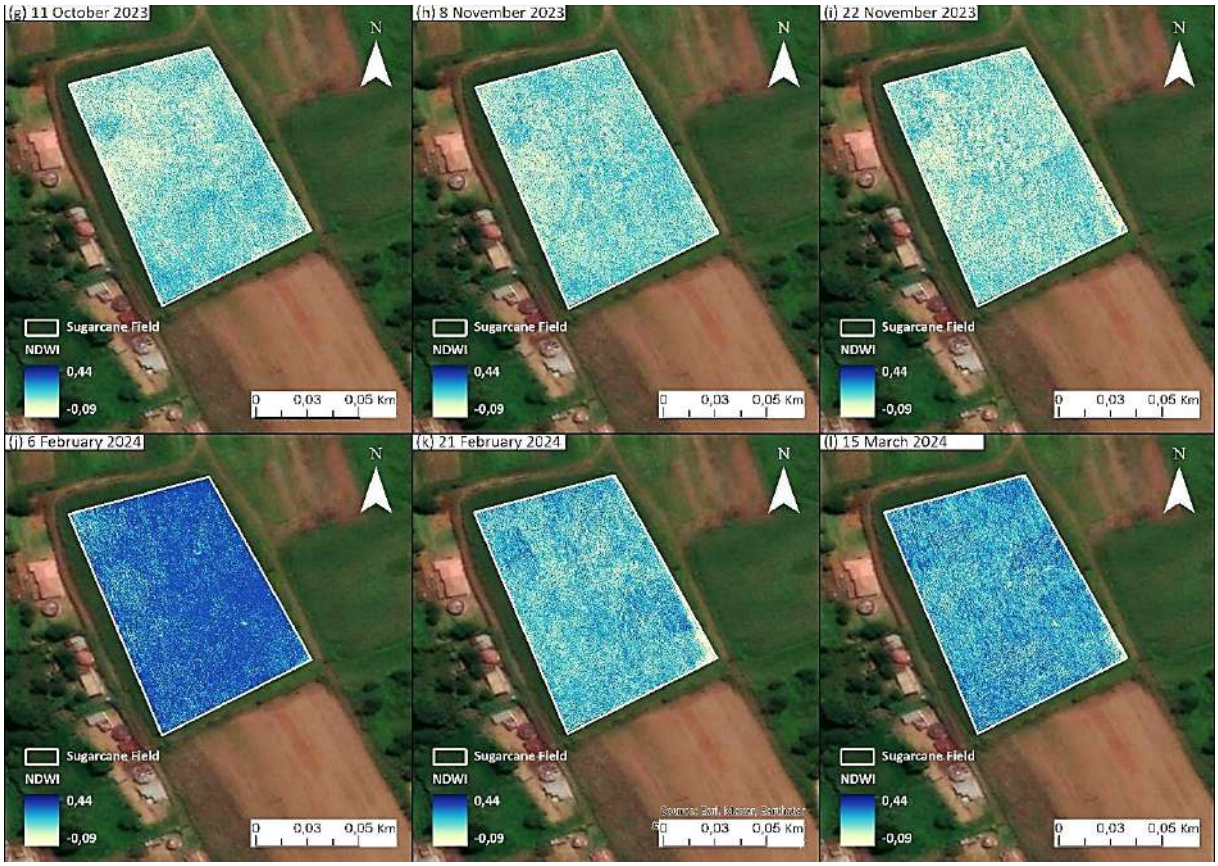

Figure 6.2 Spatio-temporal NDWI maps derived from UAV-derived data inputs to ensemble Model 2

In addition, the moderate correlation between the predicted NDWI and LAI (R = 0.41) highlights the link between the canopy structure and water availability, and it implies that a denser canopy may enhance water retention, which is critical during the growth phases. The positive, albeit weaker, correlation with the crop height (R = 0.31) indicates that taller crops, potentially resulting from an adequate water supply, may exhibit better overall growth. This finding, as well as the moderate correlation between predicted NDWI and CC (R = 0 .33), suggest that the water status, as NDWI indicates, is integral to the crop's photosynthetic efficiency and overall vitality. The minimal correlation between the predicted NDWI and the foliar temperature (R = 0.10) raises questions about the factors that influence the foliar temperature, independent of NDWI. This indicates that the external environmental conditions, or stressors, may have a greater impact on the foliar temperature than the water status. The strong positive correlation between the NDWI and OSAVI (R = 0.63) highlights the efficacy of soil-adjusted VIs in evaluating the water content. OSAVI integrates the vegetation structure and water status, and serves as a robust indicator for crop monitoring. This analysis emphasises the importance of monitoring the NDWI alongside other structural VIs and in-situ measurements, in order to comprehensively assess the crop water status and health during critical phenological stages.

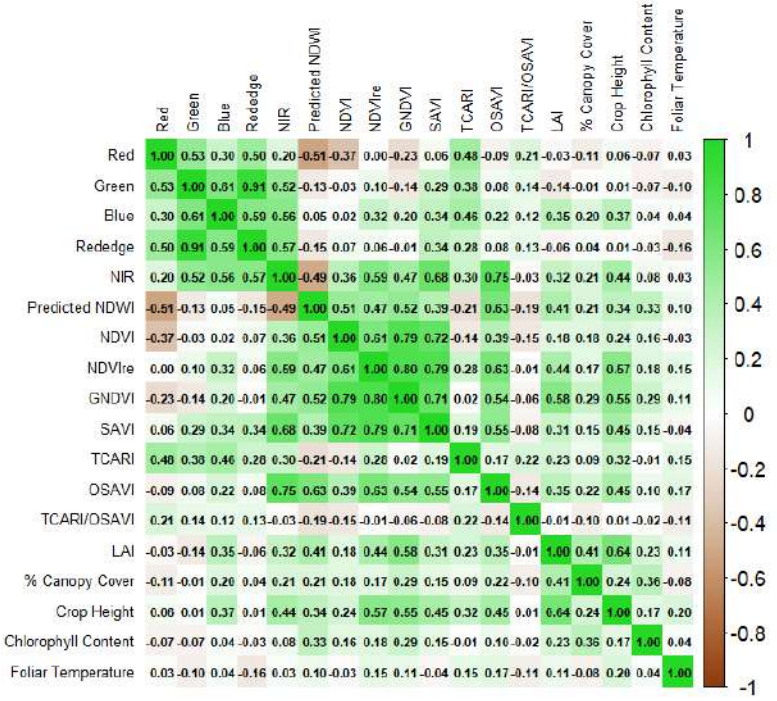

Figure 6.3 Pearson correlation (R) plot of predicted NDWI with UAV-derived VIs and in-situ measurements across the SE and early M phenological stages

6.4.5 Comparative violin plot analysis of predicted NDWI, UAV-based vegetation indices and actual evapotranspiration during the stalk elongation and early maturation phases

ET-EC distribution demonstrates a distinct pattern between the growth phases. The SE exhibits a broader range of ET-EC values, which indicates a significant variability in water loss through ETa (Figure 6.3i). Conversely, the early M phase shows a more constrained distribution, which suggests consistent ETa rates as the crop canopy fully establishes and efficiently manages its water use.

The predicted NDWI values reveal a marked increase during early M, reflecting enhanced vegetation water content as the crop matures (Figure 6.3a). The more consistent distribution during early M indicates stability in the moisture retention across the field. In contrast, SE shows a broader range of values, possibly due to the uneven plant establishment and growth rates. NDVI, GNDVI and NDVIre showcase higher and more consistent values during early M, which denotes uniformity in the canopy greenness and vigour (Figures 6.3b-d). SE displays more variability, which is likely due to the spatial differences in growth and development. This variability highlights the heterogeneity that is inherent in earlier growth stages. The SAVI and OSAVI patterns emphasise the impact of soil brightness and biomass accumulation on the VIs (Figures 6.3e and 6.3g). The early M phase shows a reduced variability in these indices, which suggests a fully-developed canopy with less soil influence on the spectral data. SE presents a broader distribution, which indicates varying degrees of canopy development.

During SE, the TCARI values are more variable, which possibly reflects the differences in CC as the crop is established (Figure 6.3f). In contrast, the early M phase shows higher mean TCARI values with a reduced variability, which indicates stabilised chlorophyll levels and a fully-developed canopy. However, TCARI/OSAVI values decrease slightly during the early M phase, which marks a shift in the canopy health as sugarcane enters the early M phase (Figure 6.3h). This decline suggests a stabilisation of the chlorophyll levels and changes in the canopy structure, which is consistent with the crop's transition from active growth to physiological maturity. The reduced variability in the early M phase also highlights the uniformity in crop conditions, as the canopy stabilises.

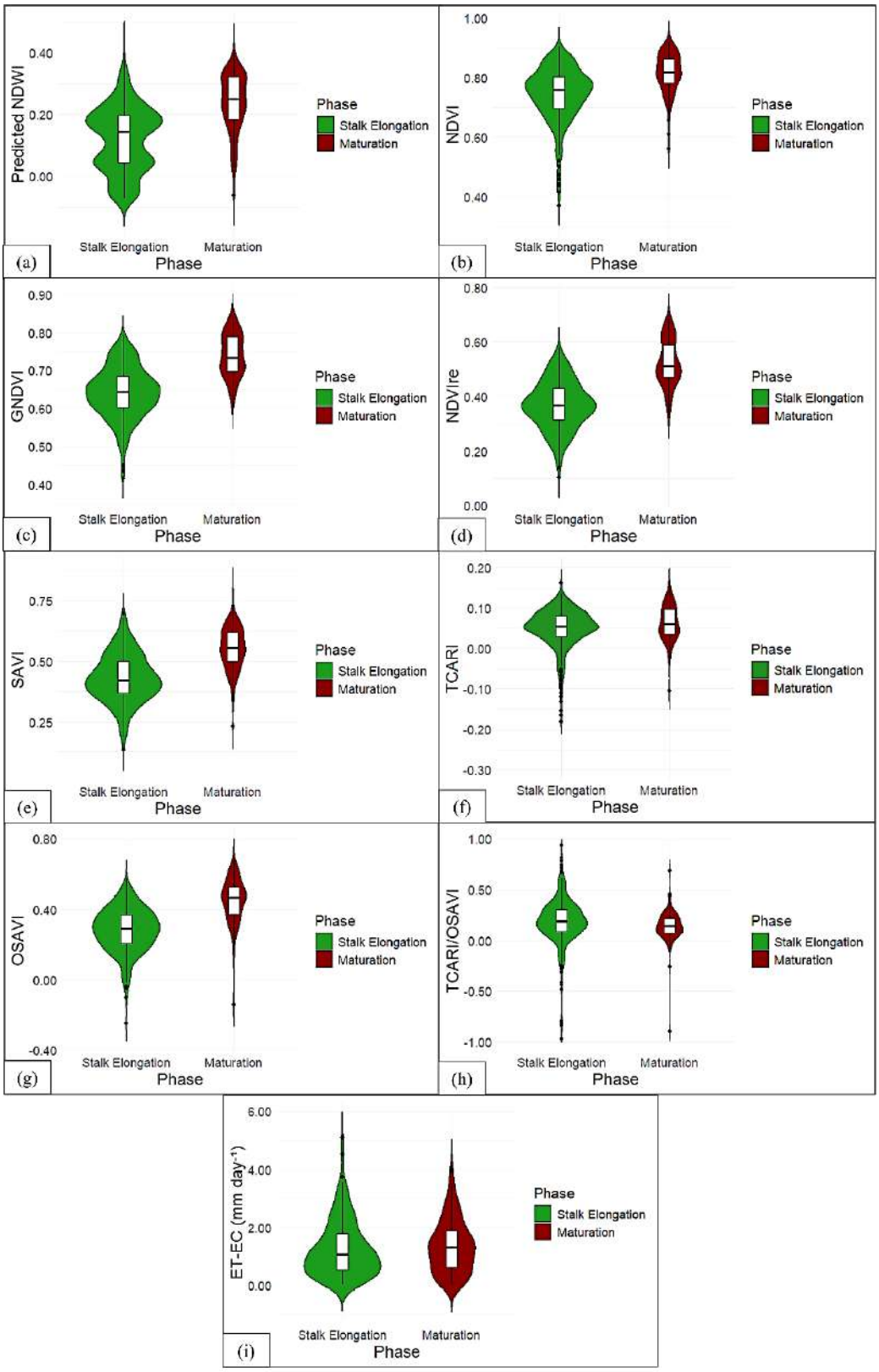

Figure 6.5 Violin plots comparing (a) Predicted NDWI, (b) NDVI, (c) GNDVI, (d) NDVIre, (e) SAVI, (f) TCARI, (g) OSAVI, (h) TCARI/OSAVI, and (i) ET-EC (mm day^{-1}) across SE and early M growth phases

6.4.6 Validation and temporal analysis of predicted NDWI against actual evapotranspiration, WDI, precipitation, air temperature and soil water metrics

Figure 6.4a analyses the relationship between the mean predicted NDWI values obtained from 12 UAV flights conducted during the study, as well as the ETa data collected from an EC system (ET-EC), spanning July 2023 to March 2024. The higher predicted NDWI values indicate an increased vegetation water content, which correlates with the elevated ET-EC rates and the potentially lower water stress in sugarcane. Conversely, the lower predicted NDWI values suggest a reduced water content, which may correspond to the heightened stress levels. The analysis reveals a strong positive correlation ($R^2 = 0.60$), which indicates that predicted NDWI fluctuations explain 60% of the ET-EC variability. This emphasises the potential of NDWI as a reliable proxy for the vegetation water content and intra-field water dynamics.

The low standard error values further enhance the accuracy of the predicted NDWI estimates, which facilitate the detection of seasonal variations and align the trends with changes in the moisture availability and crop health. Figure 6.4b presents the correlation between the mean predicted NDWI values, derived from the same 12 UAV flights, and the WDI, yielding an R^2 of 0.62. This negative correlation indicates that 62% of WDI variability is explained by the NDWI changes, which highlights the sensitivity of the index to water stress in sugarcane. The inverse relationship suggests that, as predicted NDWI decreases, the water deficit increases, which reflects the lower vegetation water content. These findings validate the predicted applicability of NDWI in assessing crop water stress and they deepen the understanding of its relationship with ET-EC.

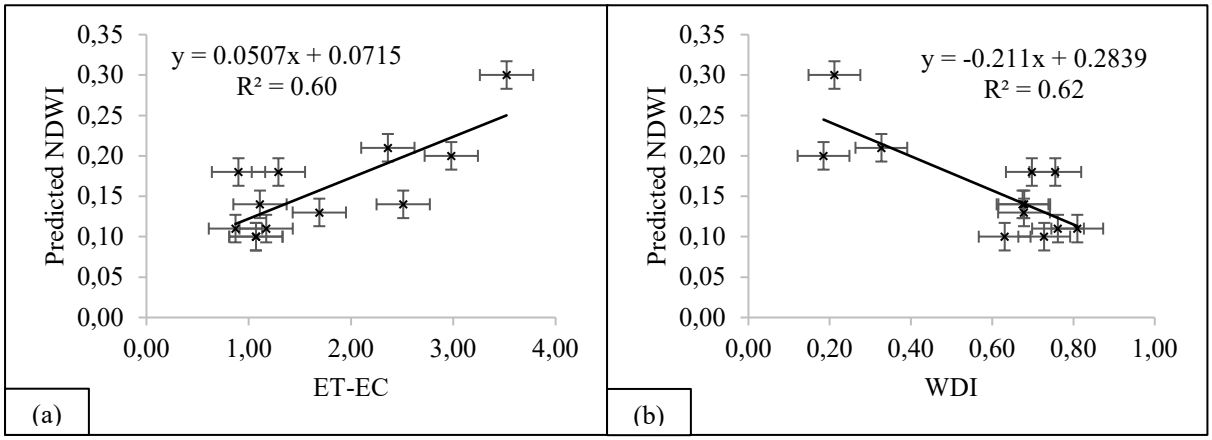

Figure 6.6 Correlation analysis between mean daily NDWI values and (a) ET-EC (mm day^{-1}) and (b) WDI for validation purposes

Figure 6.6 illustrates the interplay between the precipitation (mm), the Total Soil Water Profile (TSWP) (mm^{-1}), the average air temperature (°C), the WDI and the mean NDWI during a segment of the sugarcane phenological cycle. Rainfall events from July 2023 to March 2024 were sporadic, with notable peaks in October, December and January, indicating periods of substantial precipitation within the study area. Conversely, July and August experienced prolonged dry spells due to the seasonal climate patterns. The NDWI values ranged from 0.10 to 0.30, peaking at 0.30 on February 6. This suggests a temporal relationship between the NDWI and precipitation, particularly following the cumulative rainfall of 331 mm in December. This indicates that the vegetation absorbs water during and after rains, albeit with a delay, due to soil water infiltration and subsequent plant uptake.

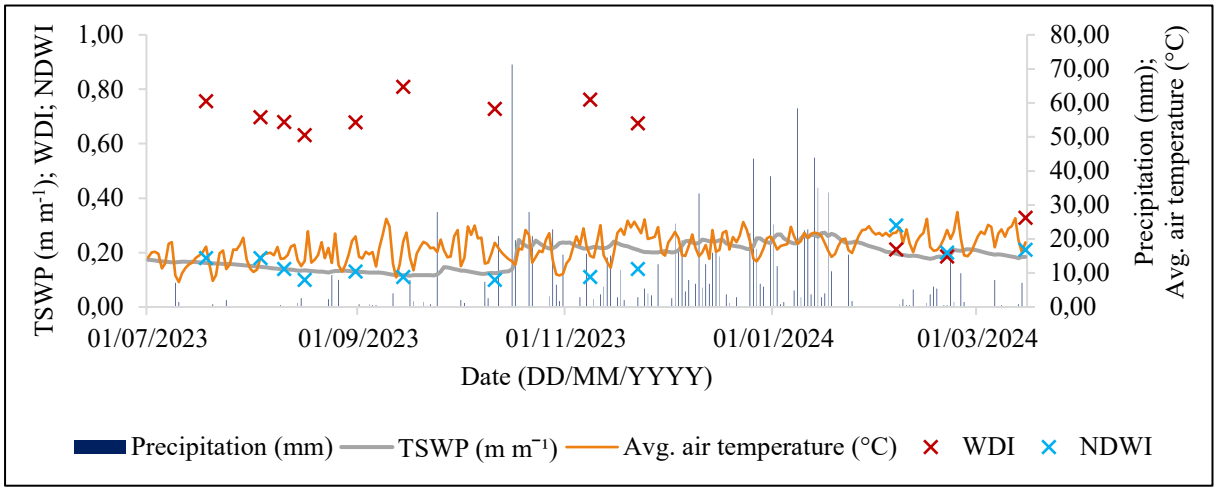

Figure 6.7 Temporal dynamics of precipitation (mm), TSWP (mm^{-1}), air temperature (°C), WDI, and NDWI during the sugarcane phenological cycle

The TSWP generally declined from July to October 2023, with increases following rainfall events, which suggests a correlation with the wet season dynamics. Notably, changes in the TSWP did not directly correspond to the rainfall amounts, which indicated potential delays influenced by the soil characteristics or ET-EC dynamics. High-stress periods, particularly from July to November, were marked by elevated WDI values (0.76 on July 18 and 0.81 on September 14), which coincided with low or zero precipitation and reduced NDWI values and signalled significant water stress. This period also shows a decline in the TSWP, which reflects the diminishing soil moisture. Elevated temperatures, reaching 20.74°C on August 31 and 19.24°C on September 14, may have further exacerbated the transpiration rates and stress levels.

In contrast, the water stress diminished from February to March, with WDI values decreasing (0.21 on February 6 and 0.18 on February 21) and NDWI values increasing, notably 0.30 on February 6. This improvement most likely resulted from the enhanced TSWP and periodic precipitation, which contributed to the reduced stress and a more stable crop environment. Overall, high-stress periods correlated with a low NDWI and TSWP, and they were compounded by minimal rainfall and elevated temperatures. In summary, the sugarcane crop experienced significant stress throughout the study, particularly during the dry months (July–November 2023), but improved conditions in February and March 2024 indicated periods of reduced stress. Despite some relief, the data suggest that the crop endured substantial water stress for much of the study.

6.5 Discussion

6.5.1 Analysis of predicted NDWI in the study area

The validation of the NDWI predictive model employed a comprehensive approach, by integrating the ground truth data and correlation analyses. Ground truth data from in-situ measurements of CC and LAI, alongside the meteorological variables, served as a benchmark for evaluating the predicted NDWI values. The ensemble model achieved a high R^2 of 0.95, which indicated the high predictive accuracy of the model to estimate NDWI, by using data captured in the visible and NIR regions of the electromagnetic spectrum. Low RMSE and MAE values of 0.03 and 0.02 reflected minimal deviations between the predicted and actual NDWI values. This validation adheres to the best practices outlined in recent research (Dong et al., 2024), assuring its prediction reliability. The model also accurately captured the increased vegetation water content during the early M phase, which correlated with the observed increases in CC and LAI.

6.5.2 Influence of climatic conditions and sugarcane phenology on the NDWI and structural vegetation index trends

Strong positive correlations were observed between the NDWI and Vis, such as NDVI and GNDVI ($r > 0.5$), which aligns with the established literature (Gao, 1996; Strashok et al., 2022). However, interpreting these trends requires careful consideration of the data collection period (July 18, 2023 to March 15, 2024), which encompasses only the SE and early M phases before harvest (May 2024).

Compared to the SE phase, increases in the NDWI and the other VIs during the early M phase reflect the favourable summer conditions (higher temperatures and increased rainfall), which fostered vigorous post-tillering growth, enhanced photosynthetic activity and biomass accumulation and improved the water status. An increased CC and LAI further support this.

Crucially, this represents only the initial M phase; the data collection period concluded before the expected peak in sucrose accumulation and the senescence of lower leaves that are characteristic of the later M phase (Stoller, 2024). Conversely, the unfavourable winter conditions during SE most likely restricted the root development and nutrient uptake, thereby hindering the SE and sucrose accumulation (Smith et al., 2005; Pierre et al., 2019), despite the drought tolerance of sugarcane (Mehdi et al., 2024). Lower NDWI and VI values during the SE may also reflect heterogeneous crop development at this earlier growth stage (Meyer et al., 2011; Xu et al., 2021), which impacted the spectral reflectance.

The SE to M transition involves a physiological shift from vegetative growth to sucrose accumulation, with the early M phase trends potentially being masked by the favourable environmental conditions. The absence of later-stage water stress may reflect relatively mild early M phase conditions; decreased LAI (Castro-Nava et al., 2016), chlorophyll (Harakotr et al., 2024) and the associated index values (Pereira et al., 2016) are typically expected in later M, due to leaf senescence and the resource reallocation towards sugar accumulation (Mehdi et al., 2024). In addition, the increased water stress during the later M phase negatively influences sugar production and flowering (Mehdi et al., 2024).

6.5.3 Canopy development, water use, and photosynthetic efficiency

Canopy development impacted the water status and plant health, as indicated by moderate correlations between the NDWI and LAI (r = 0.41), the crop height (r = 0.31), the CC (r = 0.33) and the photosynthetic indices (TCARI, TCARI/OSAVI). Improved water retention and enhanced photosynthetic activity, which are linked to the more developed canopy of the early M phase, contributed to the higher NDWI values. Compared to the SE phase, the increased consistency in NDWI and VI values during the early M phase reflects a more uniform canopy cover, resulting in a more stable water status and reduced ET-EC variability. The greater variability in ET-EC during SE may be attributed to the uneven canopy development and varying solar radiation exposure.

Higher TCARI variability during SE reflects an uneven chlorophyll distribution, which is consistent with the observed VI variability. In addition, the slightly higher and more consistent TCARI values during the early M phase suggest an improved photosynthetic efficiency and plant health, which is directly linked to the more developed and uniform canopy structure, which enhances light interception and photosynthetic activity (Haboudane et al., 2002). However, these improvements may also partly reflect favourable environmental conditions. The data do not capture the typical later-stage decline in LAI (Castro-Nava et al., 2016), CC (Harakotr et al., 2024) and the associated indices (Pereira et al., 2016), due to leaf senescence.

6.5.4 The relationship between NDWI and environmental variables

The temporal analysis of the NDWI, precipitation, air temperature and TSWP reveals a dynamic interplay that significantly influences the crop water status. A positive correlation between the NDWI and precipitation is evident, with the NDWI increasing sharply after substantial rainfall events, such as in November 2023, which indicates effective water-use for stress recovery. In contrast, prolonged dry periods (July-August 2023), which are characterised by low precipitation and reduced TSWP, resulted in decreased NDWI values, which underpins the critical role of rainfall in sustaining crop health during the essential growth phases.

Despite these fluctuations, the sugarcane crop exhibited persistent water stress throughout the monitoring period, especially from July to November 2023. The elevated WDI values during this time-frame reflect significant stress, with only brief recoveries following rainfall events. While February and March 2024 saw the increased NDWI values coinciding with the rising TSWP and precipitation, the overall data emphasise the substantial water stress that was experienced throughout the study. This situation highlights the need for effective water management strategies to enhance crop resilience against variable climatic conditions during the critical growth periods.

Further investigation reveals an intricate interplay between the NDWI and environmental variables, such as ETa and WDI, that significantly influence crop water stress. A strong positive correlation with ETa ($R^2 = 0.60$) suggests the potential of the NDWI as a proxy for assessing the sugarcane water status (Nguyen et al., 2024). However, fluctuations in NDWI due to external factors like soil moisture, solar radiation, wind speed and atmospheric demand, significantly affect the ETa rates.

Thus, low ETa values can occur even when the NDWI shows no stress. The negative correlation with WDI (R^2 = 0.62) further highlights its sensitivity to water deficits, where increased stress correlates with lower NDWI values. For sugarcane cultivation, NDWI is a valuable indicator of crop water status; however, integrating factors, such as water resource availability, climatic conditions and the overall crop health, are imperative. The increase in NDWI following rainfall events, particularly in November 2023, illustrates the significant impact of precipitation on water availability and recovery. This effect may be more pronounced during periods of high and moderate stress, which highlights the need for a holistic approach that considers a variety of environmental variables, in order to understand water stress.

6.5.5 Implications for sustainable sugarcane production in South Africa

6.5.5.1 Addressing data limitations

The results of this study demonstrate the potential of UAV-based NDWI for monitoring water stress in sugarcane; however, several limitations warrant consideration. Coarse-resolution satellite imagery requires careful processing, in order to address the mixed-pixel effect, where the high NIR reflectance of soil can artificially lower the NDWI values, obscuring the actual crop water content (Zhou et al., 2021). In addition, downscaling satellite data introduces uncertainty (Gokool et al., 2022), due to inherent sub-pixel variability and method-dependent assumptions, which necessitates cautious interpretation. Consequently, if the NDWI predictions derived from satellite data lack accuracy, they could misrepresent the severity of water stress, which would directly impact the water management decisions. Moreover, the limited number of training points in model development may compromise its robustness (Budach et al., 2022), as insufficient data might not fully capture the relationship between the NDWI and the various predictor variables.

The reliance on a single study site restricts the generalisability of the findings (Alavi et al., 2024). This limitation may not accurately reflect the diverse conditions and management practices across South Africa, which potentially skews the understanding of water dynamics. In-situ measurements may only partially capture the heterogeneity that is inherent in extensive sugarcane fields, which may introduce sampling bias (Blatchford et al., 2019).

Consequently, this bias could under-represent the variability in crop response to water stress, which may lead to misleading conclusions about the NDWI model's overall effectiveness in the broader agricultural context. In addition, the data collection period of this study encompassed only the SE and early M phases, which precluded a comprehensive assessment of the water stress dynamics throughout the growth cycle. This limitation, particularly concerning the later M stages, may affect the reliability and generalisability of the model.

In order to address these limitations, future research should prioritise the following: (i) expanding data collection across multiple sites and diverse sugarcane cultivars and cultivation methods within South Africa; (ii) employing advanced image-processing techniques, such as spectral unmixing, to correct for mixed pixels and enhance NDWI accuracy; (iii) extending the data collection period to encompass the complete sugarcane growth cycle; (iv) increasing the size of the training dataset to improve model's robustness and generalisability; and (v) exploring alternative VIs and integrating the TIR data, in order to gain a more comprehensive understanding of the complex interplay between the water stress, canopy temperature and other environmental factors. Integrating the data from multiple sources (UAV, satellite and ground-based measurements) will further enhance the reliability and application of NDWI-based water stress assessments.

6.6 Conclusion

Amid the increasing water scarcity and erratic weather patterns in South Africa, effective crop water stress monitoring is crucial, particularly for smallholder sugarcane farmers. This study addresses this need by introducing a novel ML model for accurately predicting sugarcane NDWI by using UAV-based multispectral imagery. The model's strong concordance with Sentinel-2 data and in-situ measurements validates the UAV-derived NDWI as a robust indicator of sugarcane water status, showing significant correlations with established VIs and key environmental variables. This highlights the sensitivity of the NDWI to sugarcane health, and offers substantial potential for precision water management. Accurate NDWI predictions facilitate several critical operational applications; for example, (i) spatially-explicit and timely assessments enable optimised precision irrigation, and they minimise water wastage and maximise resource allocation; (ii) continuous monitoring establishes an early warning system for proactive mitigation before significant yield loss; and (iii) data integration into decision support systems provides timely recommendations to farmers.

This enhanced adaptive capacity is crucial in the face of climate change. However, the study's reliance on a single site, its limited training dataset, as well as data collection that encompasses only the SE and early M growth phases, limits its generalisability. Challenges related to the in-situ data (sampling bias and heterogeneity) and downscaled satellite data (sub-pixel variability) further constrain its broader applicability. Future research should expand the data collection across diverse sites and cultivars, it should incorporate advanced image processing techniques (e.g. spectral unmixing), it should increase the training dataset size, and it should extend data collection to cover the entire sugarcane growth cycle. Collaboration among researchers, extension services and farming communities is vital for translating this research into user-friendly tools, which will maximise its operational value and improve water resource management and food security in vulnerable regions of South Africa.

6.7 References

ADISA O, BOTAI CM, BOTAI JO, HASSEN A, DARKEY D, TESFAMARIAM EH, ADISA AF, ADEOLA AM and NCONGWANE KP (2018) Analysis of agro-climatic parameters and their influence on maize production in South Africa. *Theoretical and Applied Climatology* **134** (1) 991–1004.

ALAVI M, ALBAJI M, GOLABI M, ALI NASERI A and HOMAYOUNI S (2024) Estimation of sugarcane evapotranspiration from remote sensing and limited meteorological variables using machine learning models. *Journal of Hydrology* **629** (1) 130605.

ALLEN R, PEREIRA L, RAES D and SMITH M (1998) Crop evapotranspiration: guidelines for computing crop water requirements. FAO Irrigation and Drainage Paper No. 56. Food and Agriculture Organization of the United Nations, Rome, Italy.

ANDERSSON JCM, ZEHNDER AJB, JEWITT GPW and YANG H (2009) Water availability, demand and reliability of in-situ water harvesting in smallholder rain-fed agriculture in the Thukela River Basin, South Africa. *Hydrology and Earth System Sciences* **13** (12) 2329-2347.

ANTONIUK V, MANEVSKI K, KØRUP K, LARSEN R, SANDHOLT I, ZHANG X and ANDERSEN MN (2021) Diurnal and seasonal mapping of water deficit index and evapotranspiration by an unmanned aerial system: a case study for winter wheat in Denmark. *Remote Sensing* **13** (15) 2998.

ARCHER E, LANDMAN W, MALHERBE J, TADROSS M Aand PRETORIUS S (2019) South Africa's winter rainfall region drought: a region in transition? *Climate Risk Management* **25** (1) 100188.

BAJWA S and VORIES E (2006) *Spectral Response of Cotton Canopy to Water Stress*. (incomplete?)

BALUJA J, DIAGO M-P, BALDA P, ZORER R, MEGGIO F, MORALES F and TARDAGUILA J (2012) Assessment of vineyard water status variability by thermal and multispectral imagery using an unmanned aerial vehicle (UAV). *Irrigation Science* **30** (1) 511-522.

BASDEW M, JIRI O and MAFONGOYA PL (2017) Integration of indigenous and scientific knowledge in climate adaptation in KwaZulu-Natal, South Africa. *Change and Adaptation in Socio-Ecological Systems* **3** (1) 56-67.

BERTALAN L, HOLB I, PATAKI A, NÉGYESI G, SZABÓ G, KUPÁSNÉ SZALÓKI A and SZABÓ S (2022) UAV-based multispectral and thermal cameras to predict soil water content – a machine learning approach. *Computers and Electronics in Agriculture* **200** 107262.

BEZUIDENHOUT CN and SINGELS A (2007) Operational forecasting of South African sugarcane production: Part 1 – System description. *Agricultural Systems* **92** (1) 23-38.

BLATCHFORD ML, MANNAERTS CM, ZENG Y, NOURI H and KARIMI P (2019) Status of accuracy in remotely sensed and in-situ agricultural water productivity estimates: a review. *Remote Sensing of Environment* **234** (1) 111413.

BREWER K, CLULOW A, SIBANDA M, GOKOOL S, ODINDI J, MUTANGA O, NAIKEN V, CHIMONYO VGP and MABHAUDHI T (2022a) Estimation of maize foliar temperature and stomatal conductance as indicators of water stress based on optical and thermal imagery acquired using an unmanned aerial vehicle (UAV) platform. *Drones* **6** (7) 169.

BREWER K, CLULOW A, SIBANDA M, GOKOOL S, NAIKEN V and MABHAUDHI T (2022b) Predicting the chlorophyll content of maize over phenotyping as a proxy for crop health in smallholder farming systems. *Remote Sensing* **14** (3) 518.

BUDACH L, FEUERPFEIL M, IHDE N, NATHANSEN A, NOACK N, PATZLAFF H, HARMOUCH H and NAUMANN F (2022) *The effects of data quality on ML-model performance*.

CARR M and KNOX J (2011) The water relations and irrigation requirements of sugarcane (Saccharum officinarum): a review. *Experimental Agriculture* **47** (1) 1-25.

CARTER G (1991) Primary and secondary effects of water content on the spectral reflectance of leaves. *American Journal of Botany* **78** (7) 916-924.

CASTRO-NAVA S, HUERTA AJ, PLÁCIDO-DE LA CRUZ JM and MIRELES-RODRÍGUEZ E (2016) Leaf growth and canopy development of three sugarcane genotypes under high temperature rainfed conditions in North-eastern Mexico. *International Journal of Agronomy* 2016 (incorrect) (1) 2561026.

CHIMONYO V, MODI A and MABHAUDHI T (2016) Assessment of sorghum-cowpea intercrop system under water-limited conditions using a decision support tool. *Water SA* **42** (2) 316-327.

COCKBURN J, COETZEE H, VAN DEN BERG J, CONLONG D and WITTHÖFT J (2014) Exploring the role of sugarcane in small-scale farmers' livelihoods in the Noodsberg Area, KwaZulu-Natal, South Africa. *The South African Journal of Agricultural Extension* **42** (1) 80-97.

DONG H, DONG J, SUN S, BAI T, ZHAO D, YIN Y, SHEN X, WANG Y, ZHANG Z and WANG Y (2024) Crop water stress detection based on UAV remote sensing systems. *Agricultural Water Management* **303** (1) 109059.

DUNKELBERG E, FINKBEINER M and HIRSCHL B (2014) Sugarcane ethanol production in Malawi: measures to optimise the carbon footprint and to avoid indirect emissions. *Biomass and Bioenergy* **71** (1) 37-45.

EDGERTON CW (1934) *Stubble deterioration of sugar cane.* Louisiana State University and Agricultural andMechanical College, Agricultural Experiment Station, 256.

FERREIRA THS, TSUNADA MS, BASSI D, ARAÚJO P, MATTIELLO L, GUIDELLI GV, RIGHETTO GL, GONÇALVES VR, LAKSHMANAN P and MENOSSI M (2017) Sugarcane water stress tolerance mechanisms and its implications on developing biotechnology solutions. *Frontiers in Plant Science* **8** (1) 1077.

GAO B-C (1996) NDWI - A normalised difference water index for remote sensing of vegetation liquid water from space. *Remote Sensing of Environment* **58** (3) 257-266.

GLASSOP D, ROESSNER U, BACIC A and BONNETT GD (2007) Changes in the sugarcane metabolome with stem development. Are they related to sucrose accumulation? *Plant and Cell Physiology* **48** (4) 573-584.

GOKOOL S, KUNZ R and WARBURTON TM (2022) Deriving moderate spatial resolution leaf area index estimates from coarser spatial resolution satellite products. *Remote Sensing Applications: Society and Environment* **26** (1) 100743.

GOKOOL S, MAHOMED M, KUNZ R, CLULOW A, SIBANDA M, NAIKEN V, CHETTY K and MABHAUDHI T (2023) Crop monitoring in smallholder farms using unmanned aerial vehicles to facilitate precision agriculture practices: a scoping review and bibliometric analysis. *Sustainability* **15** (4) 3557.

GONZÁLEZ-DUGO MP, MORAN MS, MATEOS L and BRYANT RB (2006) Canopy temperature variability as an indicator of crop water stress severity. *Irrigation Science* **24** (1) 233-240.

GRAY BA, TOUCHER ML, SAVAGE MJ and CLULOW AD (2022) Seasonal evapotranspiration over an invader vegetation (Pteridium aquilinum) in a degraded montane grassland using surface renewal. *Journal of Hydrology: Regional Studies* **40** (1) 101012.

HAARHOFF SJ, KOTZÉ T and SWANEPOEL P (2020) A prospectus for sustainability of rainfed maize production systems in South Africa. *Crop Science* **60** (1) 14-28.

HABOUDANE D, MILLER JR, TREMBLAY N, ZARCO-TEJADA PJ and DEXTRAZE L (2002) Integrated narrow-band vegetation indices for prediction of crop chlorophyll content for application to precision agriculture. *Remote Sensing of Environment* **81** (2) 416-426.

HARAKOTR P, SORNPHA W, KHONGHINTA J, GONKHAMDEE S, SONGSRI P and JONGRUNGKLANG N (2024) Correlation between rapid measurement and leaf chlorophyll content of various sugarcane genotypes at different growth phases. *Asian Journal of Plant Sciences* **23** (1) 367-376.

HUANG S, TANG L, HUPY J, WANG Y and SHAO G (2020) A commentary review on the use of Normalised Difference Vegetation Index (NDVI) in the era of popular remote sensing. *Journal of Forestry Research* **32** (1) 1-6.

IHUOMA SO and MADRAMOOTOO CA (2017) Recent advances in crop water stress detection. *Computers and Electronics in Agriculture* **141** (1) 267-275.

IHUOMA SO, MADRAMOOTOO CA and KALACSKA M (2021) Integration of satellite imagery and in-situ soil moisture data for estimating irrigation water requirements. *International Journal of Applied Earth Observation and Geoinformation* **102** (1) 102396.

INMAN-BAMBER NG (2004) Sugarcane water stress criteria for irrigation and drying off. *Field Crops Research* **89** (1) 107-122.

INMAN-BAMBER NG and SMITH DM (2005) Water relations in sugarcane and response to water deficits. *Field Crops Research* **92** (2) 185-202.

IPCC (2019) *Climate Change and Land: An IPCC Special Report on Climate Change, Desertification, Land Degradation, Sustainable Land Management, Food Security, and Greenhouse Gas Fluxes in Terrestrial Ecosystems.* Cambridge University Press, Cambridge, UK and New York, USA.

JACKSON RD (1982) Canopy temperature and crop water stress. In: ed. Hillel, D, *Advances in Irrigation*. Elsevier.

JONES HG (2014) Remote sensing of plant stresses and its use in irrigation management. 239-247. International Society for Horticultural Science (ISHS), Leuven, Belgium.

JONES MR, SINGELS A and RUANE AC (2015) Simulated impacts of climate change on water use and yield of irrigated sugarcane in South Africa. *Agricultural Systems* **139** (1) 260-270.

KHORMIZI HZ, MALAMIRI HRG and FERREIRA CSS (2024) Estimation of evaporation and drought Stress of pistachio plant using UAV multispectral images and a surface energy balance approach. *Horticulturae* **10** (5) 515.

KHUMALO S (2016) Exploring the role of women in subsistence and smallholder farming: implications for horticultural crop value chain development in Swayimane and Sweetwaters. Unpublished thesis, Agriculture and Environmental Sciences, African Centre for Food Security, University of KwaZulu-Natal, Pietermaritzburg, South Africa.

KIBIRIGE D, GOKOOL S and MKHIZE Z (2023) Estimation of soil moisture using environmental covariates and machine learning algorithms in Cathedral Peak Catchment, South Africa. *Vadose Zone Journal* **23** (3) e20289.

KNOX JW, RODRÍGUEZ DÍAZ JA, NIXON DJ and MKHWANAZI M (2010) A preliminary assessment of climate change impacts on sugarcane in Swaziland. *Agricultural Systems* **103** (2) 63-72.

KONICA MINOLTA (2025) SPAD-502Plus Chlorophyll Meter [Internet]. Konica Minolta Sensing Europe. Available from: https://sensing.konicaminolta.eu. [Accessed: 30 October 2024].

KUHN M (2008) Building predictive models in R using the caret package. *Journal of Statistical Software* **28** (5) 1-26.

LEROUX L, BARON C, ZOUNGRANA, B, TRAORÉ SB, SEEN DL and BÉGUÉ A (2016) Crop monitoring using vegetation and thermal indices for yield estimates: case study of a rainfed cereal in semi-arid west africa. *IEEE Journal of Selected Topics in Applied Earth Observations and Remote Sensing* **9** (1) 347-362.

LICKLEY M and SOLOMON S (2018) Drivers, timing and some impacts of global aridity change. *Environmental Research Letters* 13 (10) 104010.

LI-COR (2025) LAI-2200C Plant Canopy Analyser [Internet]. LI-COR Biosciences. Available from: https://www.licor.com/products/leaf-area/LAI-2200C. [Accessed: 30 October 2024].

LING Q, HUANG W and JARVIS P (2011) Use of a SPAD-502 meter to measure leaf chlorophyll concentration in Arabidopsis thaliana. *Photosynthesis Research* **107** (2) 209-214.

LIU S, PAN X, YANG Y, YUAN J, YANG Z, WANG Z, XIE W, SON, H and HAO (2023) A Crop water stress index based on remote sensing methods for monitoring drought in an arid area. *Remote Sensing Letters* **14** (1) 890-900.

LOFTON J, TUBANA B, KANKE Y, TEBOH J, VIATOR H and DALEN M (2012) Estimating sugarcane yield potential using an in-season determination of normalised difference vegetative index. *Sensors* **12** (1) 7529-7547.

LU H-D, XUE J-Q and GUO D-W (2017) Efficacy of planting date adjustment as a cultivation strategy to cope with drought stress and increase rainfed maize yield and water use efficiency. *Agricultural Water Management* **179** (1) 227-235.

MAHOMED M, CLULOW AD, STRYDOM S, MABHAUDHI T and SAVAGE MJ (2021) Assessment of a ground-based lightning detection and near-real-time warning system in the rural community of Swayimane, Kwazulu-Natal, South Africa. *Weather, Climate and Society* **13** (3) 605-621.

MARKWELL JP, OSTERMAN JC and MITCHELL JL (2004) Calibration of the Minolta SPAD-502 leaf chlorophyll meter. *Photosynthesis Research* **46** (1) 467-472.

MARTINS MTB, DE SOUZA WR, DA CUNHA BADB, BASSO MF, DE OLIVEIRA NG, VINECKY F, MARTINS PK, DE OLIVEIRA PA, ARENQUE-MUSA BC, DE SOUZA AP, BUCKERIDGE MS, KOBAYASHI AK, QUIRINO BF and MOLINARI HBC (2016) Characterisation of sugarcane (Saccharum spp.) leaf senescence: implications for biofuel production. *Biotechnology for Biofuels* **9** (1) 153.

MATSUOKA S (2012) *Sugarcane tillering and ratooning: key factors for a profitable cropping.* In: Goncalves, JF and Correia, KD (eds.), *Sugarcane: Physiology, biochemistry and functional biology.* Nova Science Publishers, Araras, Brazil.

MEHDI F, CAO Z, ZHANG S, GAN Y, CAI W, PENG L, WU Y, WANG W and YANG B (2024) Factors affecting the production of sugarcane yield and sucrose accumulation: suggested potential biological solutions. *Frontiers in Plant Science* **15** (1) 1374228.

MEYER J, REIN P, TURNER P and MATHIAS K (2011) *Good Management Practices Manual for the Cane Sugar Industry.* PGBI Sugar and Bio Energy Pty Ltd, Johannesburg, South Africa.

MISRA V, SOLOMON S, MALL AK, PRAJAPATI CP, HASHEM A, ABDALLAH EF and ANSARI MI (2020) Morphological assessment of water-stressed sugarcane: a comparison of waterlogged and drought affected crop. *Saudi Journal of Biological Sciences* **27** (1) 1228-1236.

MONTEITH JL (1965) Evaporation and environment. *Symposia of the Society for Experimental Biology* **19** (1) 205-234.

MOORE PH and BERDING N (2013) Flowering. In: *Sugarcane: Physiology, biochemistry, and functional biology*. (incomplete?)

MORAN MS, CLARKE TR, INOUE Y and VIDAL A (1994) Estimating crop water deficit using the relation between surface-air temperature and spectral vegetation index. *Remote Sensing of Environment* **49** (3) 246-263.

NDLOVU PN, THAMAGA-CHITJA JM and OJO TO (2021) Factors influencing the level of vegetable value chain participation and implications on smallholder farmers in Swayimane, KwaZulu-Natal. *Land Use Policy* **109** (1) 105611.

NGCOBO SI (2023) An assessment of the potential impacts of climate variability on sugarcane production across Southern Africa. Unpublished thesis, Discipline of Hydrology, University of KwaZulu-Natal, Pietermaritzburg, South Africa.

NGUYEN VL, DAO DT, LE MS and NGUYEN MH (2024) Assessing the correlation between spectral indices and land surface heat fluxes by remote sensing technology: a case study in Thai Binh Province, Red River Delta, Vietnam. *Remote Sensing in Earth Systems Sciences* **7** (3) 159-171.

NHAMO L, MAGIDI J, NYAMUGAMA A, CLULOW AD, SIBANDA M, CHIMONYO VGP and MABHAUDHI T (2020) Prospects of improving agricultural and water productivity through unmanned aerial vehicles. *Agriculture* **10** (7) 256.

OLIVIER FC and SINGELS A (2015) Increasing water use efficiency of irrigated sugarcane production in South Africa through better agronomic practices. *Field Crops Research* **176** (1) 87-98.

PEÑUELAS J and FILELLA I (1998) Visible and near-infrared reflectance techniques for diagnosing plant physiological status. *Trends in Plant Science* 3 (1) 151-156.

PEREIRA R, CASAROLI D, VELLAME L, JÚNIOR J and PÊGO EVANGELISTA A (2016) Sugarcane leaf area estimate obtained from the corrected Normalised Difference Vegetation Index (NDVI). *Pesquisa Agropecuaria Tropical* **46** (1) 140-148.

PIERRE JS, PERROUX JM and RAE AL (2019) Screening for sugarcane root phenes reveals that reducing tillering does not lead to an increased root mass fraction. *Frontiers in Plant Science* **10** (1) 119.

PIRONATO AMARO R, CHRISTINA M, TODOROFF P, LE MAIRE G, FIORIO P, PEREIRA E and LUCIANO A (2024) Regional model to predict sugarcane yield using Sentinel-2 imagery in São Paulo State, Brazil. *Sugar Tech*.

REJEB A, ABDOLLAHI A, REJEB K and TREIBLMAIER H (2022) Drones in agriculture: a review and bibliometric analysis. *Computers and Electronics in Agriculture* **198** (1) 107017.

RIAZ A, ALQUDAH AM, KANWAL F, PILLEN K, YE L-Z, DAI F and ZHANG G-P (2023) Advances in studies on the physiological and molecular regulation of barley tillering. *Journal of Integrative Agriculture* **22** (1) 1-13.

ROBY MC, SALAS FERNANDEZ MG, HEATON EA, MIGUEZ FE and VANLOOCKE A (2017) Biomass sorghum and maize have similar water use efficiency under non-drought conditions in the rain-fed Midwest U.S. *Agricultural and Forest Meteorology* **247** (1) 434-444.

ROCKSTROM J (2000) Water resources management in smallholder farms in Eastern and Southern Africa: an overview. *Physics and Chemistry of the Earth, Part B: Hydrology, Oceans and Atmosphere* **25** (3) 275-283.

ROMERO PM, LUO Y, SU B and FUENTES S (2018) Vineyard water status estimation using multispectral imagery from an UAV platform and machine learning algorithms for irrigation scheduling management. *Computers and Electronics in Agriculture* **147** (1) 109-117.

ROUJEAN JL and BREON, FM (1995) Estimating PAR absorbed by vegetation from bidirectional reflectance measurements. *Remote Sensing of Environment* **51** (3) 375-384.

ROZENSTEIN O, HAYMANN, N, KAPLAN G and TANNY J (2018) Estimating cotton water consumption using a time series of Sentinel-2 imagery. *Agricultural Water Management* **207** (1) 44-52.

RYU J-H, JEONG H and CHO J (2020) Performances of vegetation indices on paddy rice at elevated air temperature, heat stress, and herbicide damage. *Remote Sensing* **12** (16) 2654.

SAFDAR M, SHAHID MA, SARWAR A, RASUL F, MAJEED MD and SABIR RM (2023) Crop water stress detection using remote sensing techniques. *Environmental Sciences Proceedings* **25** (1) 20.

SAKAIGAICHI T, TERAJIMA Y, TERAUCHI T, HATTORI T, ISHIKAWA S, HATTORI I, SUGIMOTO A and MATSUOKA M (2013) Effect of stubble shaving after high-level cutting on the growth and yield of forage sugarcane, KRFo93-1, under multiple ratooning cultivation. *Plant Production Science* **16** (1) 183-190.

SASEENDRAN SA, TROUT TJ, AHUJA LR, MA L, MCMASTER GS, NIELSEN DC, ANDALES AA, CHÁVEZ JL and HAM JM (2015) Quantifying crop water stress factors from soil water measurements in a limited irrigation experiment. *Agricultural Systems* **137** (1) 191-205.

SAVAGE M, PASI J, MYENI L and CLULOW A (2017) *Open water evaporation measurement using micrometeorological methods*. TT 729/17. Water Research Commission Pretoria, South Africa.

SHANG J, LIU J, MA B, ZHAO T, JIAO X, GENG X, HUFFMAN T, KOVACS JM and WALTERS D (2015) Mapping spatial variability of crop growth conditions using RapidEye data in Northern Ontario, Canada. *Remote Sensing of Environment* **168** (1) 113-125.

SIBANDA M, MUTANGA O, DUBE T and MAFONGOYA PL (2020) Spectrometric proximally sensed data for estimating chlorophyll content of grasslands treated with complex fertiliser combinations. *Journal of Applied Remote Sensing* **14** (1) 024517-024517.

SMITH DM, INMAN-BAMBER NG and THORBURN PJ (2005) Growth and function of the sugarcane root system. *Field Crops Research* **92** (2) 169-183.

SOMARD J, ATZBERGER C, IZQUIERDO-VERDIGUIER E, VUOLO F and IMMITZER M (2021) Remote sensing applications in sugarcane cultivation: a review. *Remote Sensing* **13** (20) 4040.

STOLLER (2024) Sugarcane [Internet]. Corteva Agriscience. Available from: https://stollersouthafrica.co.za/sugarcane/. [Accessed: 14 October 2024].

STRASHOK O, ZIEMIAŃSKA M and STRASHOK V (2022) Evaluation and correlation of Sentinel-2 NDVI and NDMI in Kyiv (2017–2021). *Journal of Ecological Engineering* **23** (9) 212-218.

TESTO 2025. Testo 882 Thermal Imager [Internet]. Testo SE & Co. KGaA. Available from: https://www.testo.com/en-DK/testo-882/p/0560-0882. [Accessed: 30 October 2024].

TOPPA E, JULIANETTI A, HULSHOF T and ONO E (2011) Physiology development in the vegetative stage of sugarcane. *Applied Research & Agrotechnology* **3** (2) 177-185.

VÉLEZ S, ARIZA-SENTÍS M and VALENTE J (2023) VineLiDAR: high-resolution UAV-LiDAR vineyard dataset acquired over two years in northern Spain. *Data in Brief* **51** (1) 109686.

VIRNODKAR S, PACHGHARE V, PATIL VC and JHA S (2020) Remote sensing and machine learning for crop water stress determination in various crops: a critical review. *Precision Agriculture* **21** (13) 1121-1155.

WANG X, ZHAO C, GUO N, LI Y, JIAN S and YU K (2015) Determining the canopy water stress for spring wheat using canopy hyperspectral reflectance data in loess plateau semiarid regions. *Spectroscopy Letters* **48** (1) 492-498.

XU F, WANG Z, LU G, ZENG R and QUE Y (2021) Sugarcane ratooning ability: research status, shortcomings, and prospects. *Biology* **10** (1) 1052.

YACOOB A, GOKOOL S, CLULOW A, MAHOMED M and MABHAUDHI T (2024) Leveraging unmanned aerial vehicle technologies to facilitate precision water management in smallholder farms: a scoping review and bibliometric analysis. *Drones* **8** (9) 476.

ZAIB M, FAROOQ U, ADNAN M, ABBAS Z, HAIDER K, KHAN N, ABBAS R, NASIR A, SIDRA MM, FAROOQ T and MUHAMMAD A (2023) Water stress in crop plants, implications for sustainable agriculture: current and future prospects. *Journal of Environmental and Agricultural Science* **25** (1) 37-50.

ZARCO-TEJADA PJ, GONZÁLEZ-DUGO V, WILLIAMS LE, SUÁREZ L, BERNI JAJ, GOLDHAMER D and FERERES E (2013) A PRI-based water stress index combining structural and chlorophyll effects: assessment using diurnal narrow-band airborne imagery and the CWSI thermal index. *Remote Sensing of Environment* **138** (1) 38-50.

ZARZAR CM, DASH P, DYER JL, MOORHEAD R and HATHCOCK L (2020) Development of a simplified radiometric calibration framework for water-based and rapid deployment unmanned aerial system (UAS) operations. *Drones* **4** (2) 17.

ZHANG L, ZHANG H, NIU Y and HAN W (2019a) Mapping maize water stress based on UAV multispectral remote sensing. *Remote Sensing* **11** (1) 605.

ZHAO T, STARK B, CHEN Y, RAY A and DOLL D (2015) A detailed field study of direct correlations between ground truth crop water stress and normalised difference vegetation index (NDVI) from small unmanned aerial system (sUAS). *2015 International Conference on Unmanned Aircraft Systems, ICUAS 2015* 520-525.

ZHOU Y, LAO C, YANG Y, ZHANG Z, CHEN H, CHEN Y, CHEN J, NING J and YANG N (2021) Diagnosis of winter-wheat water stress based on UAV-borne multispectral image texture and vegetation indices. *Agricultural Water Management* **256** (1) 107076.

7 SYNTHESIS: KEY FINDINGS AND RECOMMENDATIONS FOR FUTURE INVESTIGATIONS

7.1 Introduction

Smallholder farms across Sub-Saharan Africa (SSA) form the backbone of agricultural systems within these regions, and they play a pivotal role in supporting livelihoods and advancing human well-being. While smallholder farming systems in SSA are crucial for sustaining and enhancing food security, their unique circumstances, particularly their limited access to critical resources, often results in these farms being unable to fulfil their agricultural productivity potential, thus they are unable to contribute more effectively to meeting the socio-economic development targets. Considering that the challenges that these farmers have to contend with are likely to be exacerbated in the future, due to the adverse impacts of climate change, as well as the pressure of meeting the demands of a burgeoning population, there is an urgent need to identify innovative, bespoke and cost-effective solutions that can assist them in improving their operations, so that they are not only able to fulfil their agricultural productivity potential, but also able to sustainably utilise the critical resources that are in limited supply.

The precision agriculture paradigm, which involves the use and application of state-of-the-art data collection and analytics to develop customised management interventions for improving agricultural productivity and sustainability, has been gaining momentum within the agricultural sector, and it is potentially well-suited to deliver on the above-mentioned targets. Precision agricultural practices have often been facilitated through the use of remote sensing technologies and, more recently, there has been a growing interest in the use of UAV technologies for such purposes. However, the majority of these applications have been undertaken within a commercial farm setting, with only a handful of studies attempting to utilise these technologies for precision agriculture on smallholder farms, despite the vast potential of UAVs for such applications. Furthermore, the generation of meaningful outputs from UAV-acquired data can prove to be challenging, as processing is computationally intensive and it may require expensive specialised software and user expertise, which are not always readily available.

Considering the recent advancements in geospatial cloud computing platforms and machine learning, many of the aforementioned obstacles can now be overcome. Through this project, we aimed to evaluate and demonstrate the use of multispectral UAV imagery, in conjunction with the abovementioned technological advancements, which can be leveraged to potentially improve the productivity of smallholder farms by mapping their cultivated areas, quantifying their crop water use and assessing their crop health.

7.2 Revisiting the objectives of the study and summary of the key findings

The overall aim of this project was to demonstrate how UAV-acquired data could be used in conjunction with geospatial cloud computing technologies and advanced data analytics to provide agricultural practitioners, managers and decision-makers with the required information, so that they can assist smallholder farmers to improve their agricultural productivity, while sustainably and optimally using their available resources.

While the evaluation of UAVs for PA has been well-documented, there have only been a select few studies that have focused specifically on smallholder farm applications. Therefore, there is a limited understanding of how these technologies can be best applied to facilitate PA practices within the unique circumstances that smallholder farmers face. In order to address this knowledge gap, we conducted a scoping review and bibliometric analysis of the studies that focus on the actual application of UAVs to guide PA practices within smallholder farms (Chapter 2). The results of these investigations revealed that UAVs have largely been used for monitoring crop growth and development, for guiding fertiliser management and for mapping crops, but they also have the potential to facilitate other PA practices. The methods and technologies that were used generally involved the derivation of vegetation indices (such as NDVI, EVI, SAVI, etc.) by using multi-spectral UAV-acquired data. These indices were then often used in conjunction with the data collected in-situ to develop models using advanced data analytics to predict crop growth dynamics, as well as to map the location, density and distribution of crops. Despite the immense potential that UAVs have for monitoring crops on smallholder farms to facilitate PA practices, their application has generally lagged behind their potential, due to factors such as affordability, restrictive policies and legislation, the lack of technical capacity and insufficient in-situ data for model development and testing.

However, many of these barriers can be overcome in the future, given the continuous advancements in these technologies, a reduction in the ownership and operational costs, as well as the changing policies and legislation. Therefore, there remains cautious optimism regarding their potential to radically transform agricultural management and the operations within SSA smallholder agricultural systems.

While the potential of these technologies to monitor crop growth and development cannot be understated, it is important to identify and evaluate approaches that consider the unique characteristics that are typically present in SSA smallholder systems, so that these approaches can be widely adopted and not only to serve a select few. To this end, this project developed advanced, reproducible and adaptable semi-automated image analysis techniques that require minimal in-situ data and that leverage the computing power of GEE, as well as advanced data analytics that can be used to (i) map the location and distribution of crops, and (ii) monitor crop growth dynamics (i.e. vegetation health, water use and crop water stress).

An essential component of adopting any PA practice is to first map the location and distribution of the croplands, so that management interventions can be implemented at the right place and time. Chapter 4 provided a comprehensive overview and assessment of how UAV-acquired data, GEE and advanced data analytics can be used to map croplands at a very high spatial resolution. The results of these investigations demonstrated that smallholder croplands could be very accurately mapped at a very high spatial resolution by using multi-spectral UAV imagery. Furthermore, it was found that marginal sacrifices in spatial resolution can be made to expedite the processing and reduce the costs, without sacrificing accuracy. While a limitation of the investigations was a lack of in-situ data for model training and development, it was shown that the techniques that were implemented can provide accurate results without the need for additional in-situ measurements.

Several approaches have been documented in the literature to estimate crop water use and crop water stress by using remote sensing technologies. However, these have primarily been based on the use of satellite-earth observation data, with a lack of consensus regarding the best UAV-based approach to adopt for such purposes. Subsequently, many of these approaches must be adapted to accommodate UAV-acquired data.

Furthermore, the development of new and innovative approaches may be necessary for these techniques to be applied within the resource-constrained context of SSA smallholder farming systems, i.e. for them to be applicable in a relatively resource-strained environment. Chapters 5 and 6 provided an overview and comprehensive assessment of such approaches. Crop evapotranspiration within the study site was estimated by using a vegetation index-based approach. UAV-derived vegetation indices were used in conjunction with meteorological data (which can be acquired from various sources in-situ, both remote-sensing or modelled) to estimate crop water use, which was then evaluated against in-situ measurements that were acquired from an eddy covariance flux tower (Chapter 5). Several VI-based methods were implemented and assessed, with each of these showing satisfactory performances, when compared against in-situ measurements. These techniques offer a relatively simple and efficient means of estimating crop water use within smallholder farms, as they require relatively easily-accessible and minimal data inputs. Nevertheless, further assessments of these approaches against in-situ measurements are advocated, prior to their operational implementation.

The estimation of crop water stress in Chapter 6 proved to be more challenging than the estimation of the crop water use, and it required the development of an innovative approach to fulfil this objective. In most instances, the sensors onboard UAVs that are used in PA applications lack sufficient spectral detail, in order to estimate crop water stress directly from the UAV-acquired data. Therefore, in order to estimate crop water stress using UAVs, higher spectral resolution sensors are required, which are extremely costly. Alternatively, long-term in-situ measurements of key plant phenological stress indicators are required to develop predictive models. Since each of these approaches is not well-suited for typically resource-constrained smallholder farming systems, an innovative approach was developed by using machine learning to leverage the synergies between freely-available satellite-earth observation and UAV-acquired data to predict crop water stress. The predictive model showed satisfactory levels of performance in detecting crop water stress, when compared to the key phenological growth indicators that were measured throughout the duration of the study period, as well as against a crop water stress indicator derived from in-situ measurements. Persistent water stress was identified throughout the study period, which potentially impacted the yields. Using the proposed crop water stress monitoring method, these impacts can potentially be mitigated and they can contribute to the improved agricultural productivity and profitability of these farmers.

7.3 Contributions of research to new knowledge

Overall, the research that was presented and described in this project makes several key contributions to new knowledge, particularly with regards to the adoption of fourth industrial revolution agricultural practices, for improving smallholder farm management and operations. The following contributions are particularly noteworthy:

- An up-to-date and concise bibliometric and systematic evaluation of literature pertaining to the actual application of UAVs for crop monitoring in smallholder farms, in order to facilitate PA, did not exist previously. Therefore Chapter 2 provides a much-needed resource for acquiring greater insights into the use of UAVs to facilitate PA practices on smallholder farms, prior to utilising these technologies within such settings.
- Despite their immense potential for accurately mapping crops on smallholder farms, the application of UAV and cloud computing technologies in such settings is limited. The semi-automated workflow developed in Chapter 3 demonstrates how UAV-acquired imagery can be used in concert with GEE to develop accurate and spatially-explicit cropland extent or LULC maps with which to guide management and decision making. Furthermore, the developed workflow can be easily shared, replicated and modified by other users who undertake similar tasks.
- While several studies have documented how UAV-acquired data can be used to estimate crop water use, there is no consensus regarding which approach is the best, or would be the most suitable, for application within resource-constrained smallholder farming systems. Chapter 4 addressed this knowledge gap by identifying and evaluating a relatively-simplistic UAV-based crop water use estimation method, which requires fairly minimal data. A rigorous comparison of the UAV-derived crop water-use estimates, validated against EC data, revealed unique insights into their relative accuracy and reliability. The findings of these investigations demonstrated the potential of these approaches to provide fairly accurate estimates of crop water use, which are essential for improving agricultural water resources management within smallholder farms.

- The in-situ measurements collected in this study, as well as the spectral resolution properties of the multi-spectral UAV imagery, prevented the detection of water stress, using some of the most common remote sensing-based indicators, such as the CWSI and NDWI. To address this limitation, a novel ML-based framework was developed and tested that integrated UAV-acquired multispectral data with Sentinel-2 satellite imagery for predicting NDWI. The results of this investigation highlighted the potential that this approach has for detecting crop water stress. Furthermore, the technique utilises freely-available satellite imagery and is particularly well-suited for application within the resource-constrained context of smallholder farming systems.

7.4 Challenges experienced during the duration of this study

Due to capacity constraints, such as, inter alia, finances, human resources and duration of the study, various limitations were experienced throughout the investigation period. These are summarised as follows:

- The methodology that was implemented to identify suitable literature for the scoping review may have contributed to the exclusion of relevant literature. Subsequently, the overall breadth of the review may potentially be lacking, with some degree of bias being introduced in the key findings and insights.
- For PA practices to be guided and informed with any degree of confidence through the application of UAVs, geospatial cloud computing and machine learning, the data produced from the application of these approaches is usually compared against in-situ observations, to test their veracity. As a result, the investigations were limited to periods with sufficient observational data, and the findings of this study are therefore most applicable to these periods.
- Comparisons between the UAV-derived and modelled estimates against the observed data allow for the quantification of errors and uncertainties associated with the modelled estimates.

However, uncertainties associated with the observed data, for example, the energy balance closure error, may lead to a false perception of how well, or how poorly, the UAV- and machine learning-based approaches performed.

- The limited training data used in the study for model development may introduce inaccuracies and bias within the models.
- While UAVs, geospatial cloud computing and machine learning have created new and exciting opportunities for smallholder farmers to adopt and benefit from the fourth industrial revolution agricultural practices, the associated costs, the required technical expertise and the prohibitive legislation are still major obstacles to be overcome, prior to the widespread adoption of these approaches to guide and inform their operations.
- Bridging the digital literacy and communication barrier is essential to ensure the success of adopting UAV-based PA practices. While this limitation did not directly impact the findings of the study, it needs to be acknowledged and addressed when operationalising UAV-based PA practices.

7.5 Future research opportunities

This section presents suggestions for future research that can build on the findings of this study, in order to advance the knowledge in the field:

- In order to acquire additional insights and understanding around the potential of UAVs to facilitate PA practices in a smallholder farm setting, as well as the farmer's perceptions and willingness to adopt these technologies, a more inclusive literature review or knowledge review should be undertaken.
- The extension of the monitoring period, as well as increasing the frequency and the range of variables that are monitored, would allow for the development of new and improved models, and it would allow for a more robust and objective evaluation of their model performance.
- Investigating the potential of cost-effective alternatives, such as low-cost RGB sensors, in order to deliver a suite of information to guide and inform PA, would make these technologies more accessible to smallholder farmers.

- Advanced ML techniques, including deep learning, may better capture the complex, non-linear relationships and would be better-suited for the development of predictive models that are used to guide and inform management decisions. Similarly, the adoption of object-based image analysis procedures for the mapping of croplands may provide more accurate results.
- UAVs, geospatial cloud computing and machine learning, have the potential to provide useful data and information for a range of PA practices, beyond those investigated in this study. These include integrated weed management, pest and disease detection and fertiliser application.
- The development of user-friendly tools to process, analyse and visualise the UAV-acquired and -derived data can aid both expert and non-expert users in interpreting and communicating information, thereby enhancing their application and translating theory into practice. Furthermore, these tools can be used to facilitate collaborative training and knowledge transfer initiatives, which will serve to ensure sustainable adoption and longevity.

7.6 Concluding remarks

From both an African and South African perspective, smallholder farms are major contributors to agricultural production, and they are crucial for sustaining and improving the socio-economic well-being of many of the region's inhabitants. However, given the general lack of resources, these farms are typically characterised by sub-optimal productivity which, in turn, affects their competitiveness and profitability. The majority of the region's inhabitants already experience food insecurity, and this situation is likely to be compounded in the future. Subsequently, the adoption of sustainable agricultural practices takes on added significance, as the optimal use of limited resources will be required to enhance productivity and to improve the yields, in order to meet the projected demand for food.

The adoption of PA practices that are facilitated by the use of UAV technologies has the potential to radically transform the African agricultural sector, particularly in the case of the smallholder farmer. The findings presented in this study have demonstrated the considerable potential that UAV technologies have for quantifying the spatiotemporal crop growth dynamics within smallholder farms, whilst also highlighting their broader application in other aspects of PA.

However, before these technologies are readily adopted to guide and inform agricultural management and decision-making within smallholder farming systems, further research is still required, in order to develop confidence in the application of these UAV-based methods, as well as to refine these methods, so that they are well-suited for application within the resource-constrained smallholder farmer context. The key to the success of these research efforts to operationalise the application of UAV technologies within smallholder farms is to bridge the digital divide and to improve digital literacy. This will necessitate effective capacity-building initiatives and knowledge transfer between researchers, agricultural managers and practitioners, as well as the farmers themselves. Furthermore, such initiatives can assist in gender and youth mainstreaming, as women play a major role in the agricultural sector, while the youth may now be attracted to the agricultural sector, as the modern nature of these practices appeals to their interest. Overall, it is envisaged that the findings of this project will serve as a catalyst to stimulate further interest in the use of UAVs, geospatial cloud computing and machine-learning as tools, not only to address agricultural challenges, but other environmental issues as well. Subsequently, this project has laid the foundation for enhancing South Africa's (SA's) capacity in the use of smart technologies, for guiding policy and informing decision making, whilst also facilitating SA to become a major role player in the digital water space.

CAPACITY AND COMPETENCY DEVELOPMENT

Water is at the epicentre of many of the challenges that are faced, both locally and internationally. Given that these issues are multifaceted, solutions for addressing them require both interdisciplinary and transdisciplinary approaches (Krueger et al., 2016). Therefore, it is important to train and develop people in this sector, so that they possess an in-depth understanding of their domain, while being able to identify and understand the rapport that coexists between the disciplines. This is likely to foster innovative and sustainable solutions for addressing the many challenges that are faced within the water resources sector. Human capacity development has taken place through this project, in the form of (i) strengthening and enhancing the institutional capacity, (ii) capacity development for early career/establishing researchers, as well as postgraduates, and (iii) community engagement and knowledge transfer, to improve the agricultural output and food security of smallholders. The following capacity and competency development has taken place:

a. Postgraduates

Table a List of postgraduate students

Name	Gender	Race	Degree	Discipline	Notes
Ms Ameera Yacoob	Female	Indian	MSc	Hydrology	Registered: 2023 Graduated: 2025
Ms Evania Chetty	Female	Indian	MSc Agric	Food Security	Registered: 2023 Graduated: 2025
Ms Sanelisiwe Mchunu	Female	Black	BSc Hons	Hydrology	Registered: 2024 Graduated: 2025

i. Miss Ameera Yacoob registered for an MSc in Hydrology in 2023 and was directly funded by this project. To date, Miss Yacoob has:

- Successfully completed her MSc studies and graduated *cum laude* in 2025.
- Presented her research at the:
  - 2nd South African Hydrological Society Conference (October 2024).
  - 7th Fountainhill Estate Research Symposium (October 2023).
  - Sustainability Research and Innovation Congress (SRI 2024), Africa Satellite Event (21-24 May 2024).
  - UKZN's Postgraduate Research & Innovation Symposium (November 2023; October 2024), where she won awards for her respective talks.

    - South African National Committee on Irrigation and Drainage (SANCID) Symposium (06-08 May 2025).
- Throughout her MSc journey, Ameera also developed capacity and competency in the following areas:
    - The installation of an eddy covariance flux tower and automatic weather station, undertaking routine measurements (bi-weekly) and maintaining and monitoring the system from June 2023 to May 2024, under the supervision of Prof. Alistair Clulow, Mr Vivek Naiken and Dr Shaeden Gokool.
    - Collecting in-situ data (leaf area index, chlorophyll content, canopy temperature and canopy height) to monitor and evaluate crop growth and development, from June 2023 to May 2024.
    - The pre-processing and processing of UAV-acquired imagery.
    - Programming in Google Earth Engine and R statistical software.
    - Developed supervisory experience and supported Dr Gokool in the supervision of Miss Sanelisiwe Mchunu (discussed below).

- Since completing her MSc, Ameera registered for a PhD in 2025 with her research still focusing on the use of UAV technologies for addressing environmental challenges and, as part of her studies, she has also recently acquired her UAV pilot's licence.
- Ameera has also been selected to participate in the upcoming 2025 DTU Next Generation Digital Action Tech Summit taking place in Copenhagen, Denmark, based on her MSc and proposed PhD research.

ii. Miss Evania Chetty registered for a MSc in Agriculture, which is funded by WRC Project No. C2023/2024-01248. While Miss Chetty was not directly funded by this project (C2021/2022-00800), she directly contributed to this project and received technical and supervisory support through this project, given the strong overlap with her MSc research and the objectives of this project. To date Miss Chetty has:

- Successfully completed her MSc studies and graduated in 2025.
- Presented her research at the:
    - 2nd South African Hydrological Society Conference (October 2024).
    - 7th Fountainhill Estate Research Symposium (October 2023).

- Sustainability Research and Innovation Congress (SRI 2024).
- UKZN's Postgraduate Research & Innovation Symposium (October 2024), where she also won an award for her talk.

- Throughout her MSc journey, Evania also developed capacity and competency in the following areas:
  - The installation of an eddy covariance flux tower and automatic weather station.
  - Collecting in-situ data (leaf area index, chlorophyll content, canopy temperature and canopy height) to monitor and evaluate crop growth and development, from June 2023 to May 2024, as well as the collection of in-situ training data to map the LULC distribution within the study area from June 2023 to May 2024.
  - Pre-processing and processing of UAV-acquired imagery.
  - Programming in Google Earth Engine and R statistical software.

iii. Miss Sanelisiwe registered for a BSc Honours in Hydrology. Her Honours research project focused on the use of assessing the potential of using satellite-earth observation data to estimate crop water use in smallholder farms. While she did not directly contribute to addressing the objectives of this project (C2021/2022-00800), she received technical and supervisory support through this project, given the strong overlap with her research and the objectives of this project. To date Miss Mchunu has:

- Successfully completed her BSc Honours studies and graduated in 2025.
- Throughout her BSc Honours journey, Sanelisiwe also developed capacity and competency in the following areas:
  - The pre-processing and processing of UAV-acquired imagery.
  - Programming in Google Earth Engine.
  - Data analysis.

b. Early career researchers

Early career researchers and first-time project leaders, Drs Shaeden Gokool and Maqsooda Mahomed have been receiving invaluable mentorship and guidance from senior Project Team members (Professors Alistair Clulow and Tafadzwanashe Mabhaudhi, Dr Mbulisi Sibanda and Mr Richard Kunz), which has immensely contributed to the progress made in this project.

Furthermore, through the research undertaken in this project and WRC Project No. C2023/2024-01248, Dr Mahomed and Dr Gokool applied for, and were successful in being awarded, an AfOX (Africa Oxford Initiative) catalyst grant. As part of the grant, Dr Mahomed visited the University of Oxford to undertake a period of study under the AfOx Scholarship alongside the REACH programme, University of Oxford (www.reachwater.org.uk). The REACH programme (2015-2025) is led by the University of Oxford, in partnership with other world class research institutions, and it is funded by the UK Foreign, Commonwealth & Development Office (FCDO). The visit proved quite productive and has laid the foundation for the development of a collaborative research project between the University of KwaZulu-Natal and the University of Oxford, which proposes to develop a UAV-based, open-access and online operational decision support tool for smallholder farmers to improve their agricultural operations. In addition to this, Dr Gokool and Dr Mahomed enrolled in a UAV pilot's course to enhance their skills and theoretical understanding of UAV-based operations further. They have completed all theoretical assessments and are only required to complete a practical assessment before acquiring their pilot's licences.

c. Institutional capacity

Through the research undertaken in this project, the Project Team has been exposed to a variety of different research methodologies and ways of thinking with regards to how to address the objectives of the study. This has further served to enhance the institutional capacity and to promote interdisciplinary and transdisciplinary principles into future research endeavours. Furthermore, the Project Team was able to acquire NDVI sensors (Apogee Instruments, Inc., Logan, UT, USA), which can be used in future projects, and it developed capacity through the training of staff and students in the installation, operation and maintenance of these sensors.

KNOWLEDGE DISSEMINATION

Dissemination of knowledge has occurred through a variety of avenues which are listed below.

a. Publications

i. GOKOOL S, MAHOMED M, KUNZ R, CLULOW A, SIBANDA M, NAIKEN V, CHETTY K AND MABHAUDHI T (2023) Crop monitoring in smallholder farms using unmanned aerial vehicles to facilitate precision agriculture practices: A scoping review and bibliometric analysis. *Sustainability* **15**(4). doi.org/10.3390/su15043557.

ii. GOKOOL S, MAHOMED M, BREWER K, NAIKEN V, CLULOW A, SIBANDA M AND MABHAUDHI T (2024) Crop mapping in smallholder farms using unmanned aerial vehicle imagery and geospatial cloud computing infrastructure. *Heliyon* **10**(5). doi.org/10.1016/j.heliyon.2024.e26913.

iii. YACOOB A, GOKOOL S, CLULOW A, MAHOMED M AND MABHAUDHI T (2024) leveraging unmanned aerial vehicle technologies to facilitate precision water management in smallholder farms: A scoping review and bibliometric analysis. *Drones* **8**(9). doi.org/10.3390/drones8090476.

iv. YACOOB, A, GOKOOL, S, CLULOW, A, MAHOMED, M, NAIKEN, V and MABHAUDHI, T (2026) A machine learning approach for quantifying crop water stress in smallholder farms using unmanned aerial vehicle multispectral imagery. Agricultural Water Management 324. doi.org/10.1016/j.agwat.2026.110142.

v. CHETTY, E, MAHOMED, M and GOKOOL, S (2026) A Comparative Analysis of Multi-Spectral and RGB-Acquired UAV Data for Cropland Mapping in Smallholder Farms. Drones 10 (1). doi.org/10.3390/drones10010072.

b. Presentations and symposiums

i. Dr Shaeden Gokool delivered an oral presentation on “Mapping land use land cover in smallholder agricultural systems using very high spatial resolution unmanned aerial vehicle imagery” at the inaugural South African Hydrological Society Symposium (October 2022).

ii. Dr Shaeden Gokool delivered an oral presentation on "The use of UAV-derived data to guide and inform precision agriculture practices in smallholder farms" at the 7th Fountainhill Estate Research Symposium (October 2023).

iii. Dr Shaeden Gokool and members of the Project Team hosted an exhibit at the Sustainability Research and Innovation Congress Africa (SRI 2024) Satellite Event (May 2024).

iv. Miss Ameera Yacoob delivered an oral presentation on "The estimation of evapotranspiration and depiction of crop health using UAV-derived data to guide and inform precision agriculture in smallholder farms" at the 7th Fountainhill Estate Research Symposium (October 2023).

v. Miss Ameera Yacoob delivered an oral presentation on "estimating evapotranspiration and crop water stress from UAV-derived data to facilitate precision water management" at UKZN's Postgraduate Research & Innovation Symposium (November 2023) and won an award for her presentation.

vi. Miss Evania Chetty delivered an oral presentation on "Exploring the use of RGB Unmanned Aerial Vehicles for crop monitoring and mapping within a smallholder farm setting: A case study in Swayimane" at the 7th Fountainhill Estate Research Symposium (October 2023).

vii. Miss Ameera Yacoob delivered an oral presentation on "Assessing unmanned aerial vehicle data for evapotranspiration estimation: A case study in Swayimane, KwaZulu-Natal, South Africa" at the 2nd South African Hydrological Society Symposium (October 2024).

viii. Miss Ameera Yacoob delivered an oral presentation on "Assessing unmanned aerial vehicle data for evapotranspiration estimation: A case study in Swayimane, KwaZulu-Natal, South Africa" at UKZN's Postgraduate Research & Innovation Symposium (November 2024) and won an award for her presentation.

ix. Miss Evania Chetty delivered an oral presentation on "Exploring the use of unmanned aerial vehicle RGB data for crop monitoring and mapping within a smallholder setting" at the 2nd South African Hydrological Society Symposium (October 2024).

x. Miss Evania Chetty delivered an oral presentation on "Exploring the use of unmanned aerial vehicle RGB data for crop monitoring and mapping within a smallholder setting" at UKZN's Postgraduate Research & Innovation Symposium (November 2024) and won an award for her presentation.

xi. Miss Ameera Yacoob delivered an oral presentation on “The use of UAVs to facilitate precision agricultural applications in smallholder farms” at the South African National Committee on Irrigation and Drainage (SANCID) Symposium (May 2025).

c. Popular articles

The research related to this project has featured in several of the Centre for Water Resources Research (CWRR) monthly newsletters, which are widely distributed to various individuals, institutions and organisations involved in the water resources and environmental sector. The newsletter can be accessed from:
https://cwrr.ukzn.ac.za/wpcontent/uploads/2023/10/CWRR_Newsletter_Issue_4_2023.pdf
https://cwrr.ukzn.ac.za/wpcontent/uploads/2024/09/CWRR_Newsletter_Issue_4_2024.pdf

d. Community engagement

Regular community engagement between Project Team members and the local community of Swayimane has been a strong feature of this project. The Project Team and smallholder farmers worked closely together to share knowledge and ensure that the project’s objectives also catered to their needs.

i. A stakeholder meeting organised by the Institute of Natural Resources (INR) took place on September 13, 2023, at the Mbava community hall in the Swayimane area. The event served as a forum for exchanging information, perspectives, first-hand accounts and novel methodologies on agricultural practices among small-scale farmers. The presence of INR members doing similar research in the area facilitated the engagement of CWRR MSc students with local communities about their conventional agricultural practices. The students collaborated to create a presentation that explained their respective objectives and anticipated methodology. The farmers showed a strong desire to acquire a knowledge about the use of drones in precision agriculture and the advantages of adopting this technology in augmenting crop yields, as well as mitigating concerns related to food security. The students regarded the experience as being both educational and productive. In addition, the project would like to organise a workshop to facilitate the transfer of knowledge from the students to farmers about the operational protocols of UAVs, since capacity development is a primary aim that is pursued by the project participants.

In addition, Dr Shaeden Gokool, Dr Maqsooda Mahomed and Miss Kershani Chetty delivered talks at three career day events to enlighten scholars about the potential career opportunities that can be pursued in this research space.

ii. A career day is a valuable opportunity to cultivate a learner's mindset and provide them with a chance to learn about careers that align with their interests and skills, so that they can start at an early age to narrow down what career to pursue in the future. During September and October 2023, members of the Project Team participated at career days organised by the Springhaven, Ridgeview and Allandale Primary Schools. Learners were given an overview of a variety of careers offered by UKZN and they were given further insight into the cutting-edge research that the members of the Project Team are currently involved in.

APPENDIX A

Table B1 Summary of published studies on the use of UAVs to facilitate precision agricultural applications in smallholder farms

Author	Broad themes	Main objective	UAV and sensor	Method	Key findings
Blaes et al. (2016)	• Monitoring crop development and estimating yield, Fertilizer management	• Assess crop growth response to soil fertility treatments.	• SenseFly eBee fitted with Canon S110NIR camera.	• Development of linear regression models based on the relationship between ground coverage, plant height and a vegetation index (VI). • Monitor changes in the VI in response to fertility.	• Due to the large variability in factors influencing crop growth at the study site, the response of VIs to fertility treatments could not be adequately quantified.
Du et al. (2017)	• Monitoring crop development and estimating yield	• Monitor wheat growth status.	• Small quadrotor (not specified) fitted with SONY ILCE-6000.	• Development of regression models based on the relationship between satellite-derived VIs and in-situ grain protein content. • Correlation analysis between satellite derived and UAV-derived VIs.	• The use of UAV-derived VIs can be a useful complement to satellite-based derived vegetation indices to monitor wheat growth status.
Wahab et al. (2018)	• Monitoring crop development and estimating yield	• Assess the vigour and yield of maize during various growth stages.	• Agribotix Enduro quadcopter fitted with two GoPro Hero 4 cameras.	• Development of linear regression models based on the relationship between UAV-derived VI, chlorophyll content measured using a soil plant analysis development (SPAD) meter and in-situ grain yield.	• The use of a UAV derived VI was able to adequately quantify maize growth and vigour, despite the complex heterogeneous nature of the smallholder farming systems.
Schut et al. (2018)	• Monitoring crop development and estimating yield, Fertilizer management	• Demonstrate the utility of using UAV imagery to assess the spatial variability of crop yield and its response to fertilizer treatments.	• SenseFly eBee™ UAV fitted with a Canon S110 NIR camera.	• Development of linear regression models based on the relationship between UAV-derived VI and measurements of ground coverage and light interception.	• UAV-derived VI was able to adequately detect differences in yield and responses to fertilizer treatments.

Table A1 continued

Hall et al. (2018)	• Image classification	• Delineation and classification of smallholder maize crops.	• UAV (not specified) fitted with two GoPro Hero Silver 12-megapixel cameras.	• Collection of training data from visual inspection of the high spatial resolution UAV imagery. • Object-based image classification performed using the support vector machine (SVM) classification algorithm.	• Maize crops were successfully delineated and classified with the classification exercising achieving an overall accuracy of ~ 94.00 %.
Wang et al. (2018)	• Image classification	• Characterizing lodged and non-lodged wheat within a smallholder farm.	• DJI Phantom Vision 2 Plus fitted with DJI FC200 camera.	• Unsupervised classification. • Use of colour and textural features to distinguish lodged from non-lodged wheat.	• Lodged and non-lodged wheat was successfully identified with the classification exercise achieving an overall accuracy of ~ 90.00 %. • The method employed herein does not require training data which is typically required in most image classification exercises.
Yonah et al. (2018)	• Monitoring crop development and estimating yield	• Evaluate the utility of UAVs to guide farm management practices.	• SenseFly eBee™ UAV fitted with Canon®S110 and MultiSPEC4C cameras.	• In-situ measurement of aboveground biomass, grain yield and leaf area index (LAI). • Derivation of various VIs	• UAV-derived information can aid in food security monitoring efforts in smallholder farms due to their ability to provide spatially explicit information on crop development under various management and environmental conditions.
Chen et al. (2019)	• Monitoring crop development	• Evaluate the potential of using UAV imagery to estimate nitrogen nutrition index (NNI)	• SenseFly eBee SQ UAV fitted with a Parrot Sequoia+ camera.	• In-situ samples of aboveground biomass were collected and plant nitrogen uptake was also determined. • In-situ samples were divided into training and validation subsets. • Regression models were developed using the in-situ training data and various VIs.	• UAVs possess immense potential to estimate NNI and guide fertilizer management applications in smallholder farms but further research is required to develop a practical operationalized approach.
Zhao et al. (2020)	• Image classification	• Development and evaluation of a unique approach for agricultural crop mapping to improve classification performance.	• Aibot X6 six-rotor UAV fitted with a Headwall Nano-Hyperspec sensor.	• Identification of bands contaminated with noise and then determining the most influential bands to the classification. • Determine the spectrally sensitive crop information. • Employ the conditional random field framework to perform a spatial-spectral classification	• Improved classification performance when compared against more frequently utilized classification algorithms.

Table A1 continued

Guo et al. (2020)	•	Mapping soil organic carbon (SOC)	•	Identify suitable variables which can be acquired from multi-spectral imagery to map SOC.	•	UAV (not specififed) fitted with a MicaSense RedEdgeTM 3 multispectral camera.	• Collection of soil samples and divide these into training and validation subsets. • Development of linear regression and machine learning models based on the relationship between spectral bands, VIs and SOC measurements.	•	The use of time-series multi-spectral imagery and machine learning based approaches can prove to be extremely useful for digital soil mapping applications
Chew et al. (2020)	•	Image classification	•	Develop a classification algorithm to identify select crop types and other land use land cover (LULC) classes.	•	SenseFly eBee Plus fitted with a SenseFly S.O.D.A camera.	• Collection of training and validation data from visual inspection of the UAV image. • The classification model was developed by applying a deep neural network with transfer learning.	•	Certain crops within the smallholder farms were classified with a high accuracy, however, crops used for intercropping were less accurately predicted.
Breunig et al. (2020)	•	Monitoring crop development and yield estimation, Delineating management zones	•	Evaluation of the influence of image spatial resolution on the accuracy of above ground biomass estimation and management zone delineation	•	DJI Matrice 100 fitted with a Parrot Sequoia camera.	• Development of linear regression models based on the relationship between above ground biomass measured in-situ and UAV-derived VI.	•	The optimal spatial resolution of the management zone map will largely depend on the farmer's precision agricultural requirements. • For e.g., a very-high spatial resolution UAV-based management zone map would be ideal to improve the efficiency of fertilizer or herbicide application. Whereas a medium-coarse spatial resolution satellite-based map can be useful to make quick decisions regarding large-scale interventions.
Cucho-Pardin et al. (2020)	•	Image classification	•	Development and application of open-source remote sensing tools to support agricultural decision making	•	Mikrokopter Okto-XL fitted with a Tetracam agricultural digital camera and IMAGRI-CIP camera.	• Supervised classification using the maximum likelihood classifier.	•	An overall classification accuracy of ~ 82.00 % was achieved. • The development of open-source tools assists in making UAV-based remote sensing analysis more accessible to those wanting to employ these technologies to guide farmers on their operations.

Table A1 continued

Peter et al. (2020)	• Monitoring crop development and estimating yield	• Evaluate the optimal spatial resolution to quantify maize crop growth dynamics.	• SenseFly eBee fitted with a Parrot Sequioa camera.	• Development of linear regression models based on the relationship between chlorophyll content measured using SPAD metres, yield and VIs.	• UAV imagery with a spatial resolution closer to the maize plant size (14-27 cm) was the optimum resolution rather than imagery with a finer or coarser spatial resolution. • Considering a broad range of vegetation indices may prove to be more beneficial than using a single one to monitor crop health and productivity.
Gracia-Romero et al. (2020)	• Monitoring crop development and estimating yield, Fertilizer management	• Assessing the influence of various nitrogen fertilization treatments on crop growth dynamics.	• Mikrokopter Oktokopter XL 4S fitted with a Lumix GX7 camera.	• Assess the correlation between RGB derived VIs and in-situ measurements of chlrophyll content using SPAD metres and Dualex Scientific sensor, as well as the leaf pigment readings with yield.	• VIs derived from the UAV imagery were found to be the best and most suitable to capture key information across the entire maize plot area.
Adewopo et al. (2020)	• Monitoring crop development and estimating yield	• Evaluating the potential of utilizing UAV-derived vegetation indices to predict maize grain yields.	• SenseFly eBee UAV fitted with a multispectral 4C camera.	• Development of linear regression models based on the relationship between in-situ measurements of yield and normalized difference vegetation index (NDVI), canopy cover and plant height. • Development of linear regression models based on the relationship between in-situ measurements of yield and UAV-derived NDVI.	• Yield variability could not be accurately predicted from UAV-derived vegetation indices with the accuracy of predictions being lower than reported in other studies.
Argento et al. (2021)	• Monitoring crop development and estimating yield, Fertilizer management	• Evaluate the potential of UAV-derived data to guide variable rate Fertilizer management.	• DJI quadcopter P4P fitted with a Parrot Sequioa camera.	• Development of linear regression models based on the relationship between UAV-derived VIs and plant traits measured in-situ.	• UAV-derived data was able to guide management decisions and contributed to an improved efficiency of fertilizer application by ~ 10.00 %.

Table A1 continued

Ndlovu et al. (2021)	• Monitoring crop development	• Evaluate the potential of utilizing multi-spectral UAV imagery and machine learning techniques to estimate maize leaf water content indicators.	• DJI Matrice 300 series fitted with a MicaSense Altum camera.	• In-situ measurements of leaf area and fresh weight were taken and used as inputs to determine maize leaf water indicators. • These measurements were then divided into training and validation subsets. • Machine learning models were then developed and validated using these in-situ indicators and UAV-derived VIs.	• Near infrared and red-edge derived VIs were best suited to capture maize leaf water content characteristics. • Multi-spectral UAV-derived data was able to accurately account for the spatial variability of maize water content variations.
Brewer et al. (2022a)	• Monitoring crop development	• Evaluate the potential of using multi-spectral-thermal UAV imagery and machine learning to estimate maize chlorophyll content.	• DJI Matrice 300 series fitted with a MicaSense Altum camera.	• In-situ measurements of chlorophyll content were taken using SPAD metres. • These measurements were then divided into training and validation subsets. • A random forest machine learning model was then developed and validated using these in-situ indicators and UAV-derived VIs.	• Multi-spectral-thermal UAV-derived data was able to accurately account for the spatial variability of maize chlorophyll content variations.
Brewer et al. (2022b)	• Monitoring crop development	• Evaluate the potential of using multispectral-thermal UAV imagery and machine learning to estimate maize foliar temperature and stomatal conductance.	• DJI Matrice 300 series fitted with a MicaSense Altum camera.	• In-situ measurements of maize foliar temperature and stomatal conductance were taken using a digital laser infrared GM320 handheld thermometer and SC-1 leaf porometer, respectively. • Measurements for each of the variables were then divided into their respective training and validation subsets. • A random forest machine learning model was then developed and validated using these in-situ indicators and UAV-derived VIs.	• Multi-spectral-thermal UAV-derived data was able to accurately estimate proxies of water stress throughout the entire growing period. • The accuracy of maize foliar temperature estimates was generally higher than stomatal conductance estimates.

Table A1 continued

Jiang et al. (2022)	• Monitoring crop development, Fertilizer management	• Evaluate the utility of using UAV-derived data to estimate NNI	• senseFly eBee UAV fitted with a Parrot Sequoia camera	• In-situ measurements of agronomic variables, agrometeorological and field management data. • Machine learning based approaches were used to characterize the relationships between the UAV-derived data, agronomic variables and management data	• The adoption of machine learning based approaches allows for the efficient handling and optimal utilization of multiple data sources to produce accurate estimates of NNI which can be used to diagnose nitrogen status across smallholder farms.
Kleinschroth et al. (2022)	• Landscape planning	• Evaluate the utility of UAV-derived imagery to facilitate collaborative land management.	• quadcopter-type Mavic Pro and senseFly eBee UAV fitted with a SODA camera.	• UAV imagery captured at 3 different viewing angles. • Focus group discussions among various stakeholders to classify the landscape based on the UAV-imagery. • Interpretability of the UAV imagery was then assessed.	• Oblique images were easiest to interpret among the various focus groups, particularly the smallholder farmers. • This is an important finding as it can assist researchers and practitioners to better utilize indigenous knowledge within their operations.

APPENDIX B

a. Sugarcane phenotyping

The sugarcane ratoon crop completed a growth cycle of 547 days (18 months) with successive harvests from November 30, 2022, to May 30, 2024. The crop progressed through distinct developmental phases: germination (G), tillering (T), stalk elongation (SE), and maturation (M) (Figure C1). Data collection commenced ≈ 7.5 months into the growth cycle (July 18, 2023), revealing that the crop had already entered the SE phase. Subsequently, literature was consulted to identify typical timelines and characteristics of the G, T, SE and M phases (Table C1). The initial stages of M were assessed by correlating observational data with existing research despite the absence of specific cultivar details. Notably, the data collection period (July 18, 2023 to March 15, 2024) encompassed only the SE and early M phases before the scheduled harvest in May 2024.

a.i Germination

During the ratoon stool activation phase, initiated post-harvest, dormant buds sprout into primary canes, which is crucial for the subsequent growth cycle (Stoller, 2024). Adequate soil moisture is vital; water stress can delay or inhibit sprouting, resulting in fewer, weaker shoots (Toppa et al., 2011). Factors such as stool health, environmental conditions, and post-harvest practices play a critical role (Stoller, 2024). Concurrently, fibrous roots at the stool base facilitate anchorage and nutrient uptake; however, water stress detrimentally affects root proliferation and function (Moore and Berding, 2013). Simultaneously, new leaves develop, enhancing photosynthesis through stored nutrients, though reduced by water stress (Moore and Berding, 2013). Additionally, secondary shoots, or tillers, emerge from lateral buds on the primary canes, increasing stand density and yield potential (Meyer et al., 2011; Xu et al., 2021).

a.ii Tillering

Tillering in sugarcane involves sequential gemma budding on the primary stalk, forming secondary and tertiary stalks essential for the crown formation and final stalk population (Stoller, 2024). Each tiller develops fibrous roots, with crown roots occupying the top 30 cm of soil within 90-120 days (Stoller, 2024). Peak tillering relies on competition for light, water, and nutrients, achieving optimal yields with 10-13 tillers per metre for complete ground cover (Stoller, 2024).

Water stress hinders growth, reduces tillering potential, and lowers yield by limiting leaf area and photosynthetic efficiency, affecting the crop's overall vigour and productivity (Inman-Bamber, 2004). Post-tillering, stalks increase in height and accumulate sucrose at the base internodes as older leaves desiccate and senesce (Meyer et al., 2011).

a.iii Stalk elongation

During the SE phase in sugarcane, the root system undergoes dynamic lateral and deep growth (Smith et al., 2005; Pierre et al., 2019), forming cord roots extending over 1.5 m, primarily in the upper 0.35–0.4 m of soil (Stoller, 2024). Although the crop is inherently drought-tolerant, -ater stress restricts SE by limiting root development (Inman-Bamber and Smith, 2005) and nutrient uptake (Misra et al., 2020) essential for height and sucrose accumulation (Meyer et al., 2011). Optimal light, moisture, and temperature levels promote vertical growth, potentially adding an internode weekly (Stoller, 2024). Conversely, water stress negatively impacts flowering by reducing panicle quantity and reproductive success (Mehdi et al., 2024).

a.iv Maturation

During the M phase of sugarcane, vigorous post-tillering growth facilitates the relocation of surplus photosynthates to the base internodes for storage (Stoller, 2024). By late summer to early autumn, a 2.5-metre-tall cane exhibits yellowing leaves in the middle third, indicating sucrose accumulation (Stoller, 2024). As late autumn and early winter approach, M intensifies while growth decreases, marking the completion of M (Stoller, 2024). This period sees increased sucrose transfer from leaves to mature internodes (Glassop et al., 2007). Water stress compromises sugar production by hindering sett germination and impairing flowering. This leads to reduced panicle formation and fertility, thereby significantly impacting M.

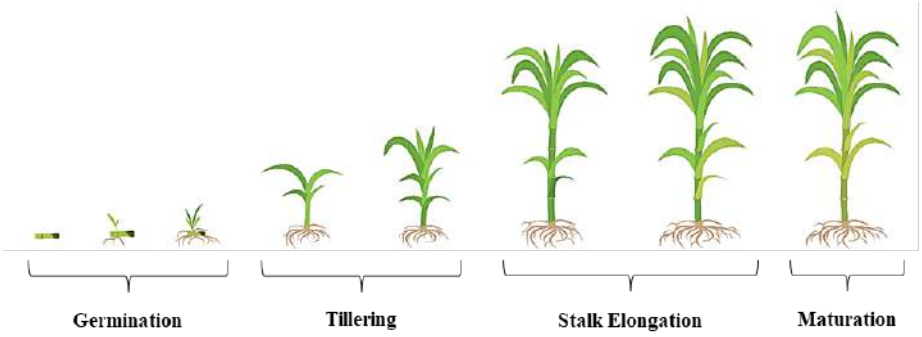

Figure B1 The growth phases of a sugarcane ratoon crop

Table B1 Growth stages and descriptions of sugarcane

Days after emergence	Growth stage	Description	Picture
0-30	Germination	Regrowth initiates from the residual stubble after the previous crop's harvest (Sakaigaichi et al., 2013). The swelling of buds on the stubble leads to the emergence of new shoots (Edgerton, 1934).	
31-120	Tillering	Tillering, a critical yield-determining phase (Riaz et al., 2023), involves the rapid development of multiple shoots from the stubble base, establishing the plant population (Matsuoka, 2012).	
121-390	Stalk Elongation	During the SE phase, sugarcane exhibits rapid stem growth, significant leaf area expansion (Somard et al., 2021), and peak photosynthetic activity, resulting in maximal biomass accumulation (Lofton et al., 2012).	
391-547	Maturation	Growth decelerates as the stalks mature, increasing sugar content due to sucrose accumulation (Lofton et al., 2012). Leaf senescence commences, indicating the plant's preparation for harvest (Martins et al., 2016).	

APPENDIX C

a. Assessment of in-situ data quality

The average air temperature within the sugarcane field ranged from 7.3 to 27.9 °C (Figure D1). Mean wind velocity was recorded at 2.0 m s^{-1} (Figure D1), while the saturated vapour pressure was measured at 2.19 kPa (Figure D2). Relative humidity (RH) exhibited notable seasonal variation. Higher RH values were observed during summer months, ranging from 69-99%, whereas winter RH values ranged from 38-96% (Figure D2). Measurements of daily mean Rn and G yielded values of 6.75 MJ m^{-2} and 0.35 MJ m^{-2}, respectively (Figure D3). Cumulative precipitation over the 10-month measurement period totalled 1228 mm, with seasonal variability. Summer months recorded higher precipitation, peaking at 331 mm in December, compared to a maximum monthly accumulation of 11 mm in July during winter (Figure D3).

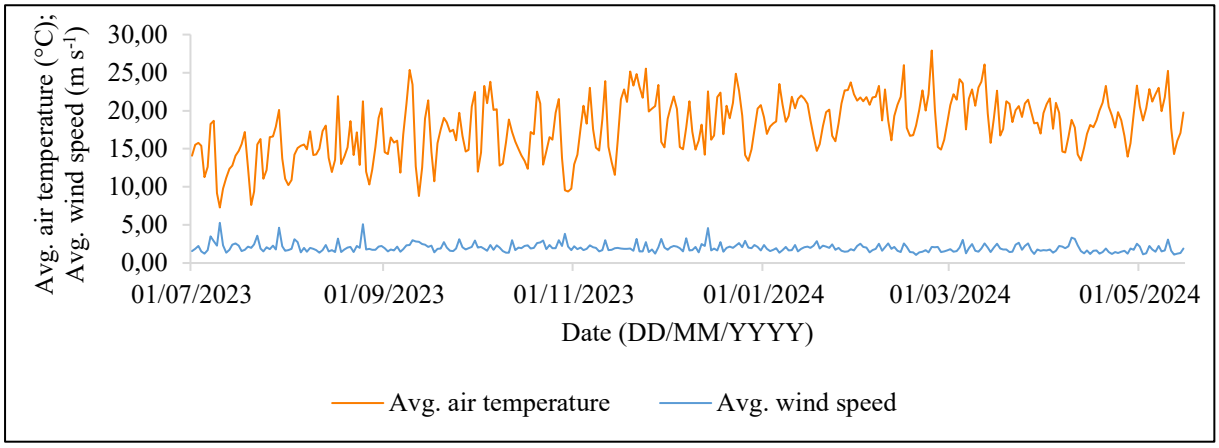

Figure C1 Average daily air temperature (°C) and wind speed (m s^{-1}) measured from July 2023, to May 2024

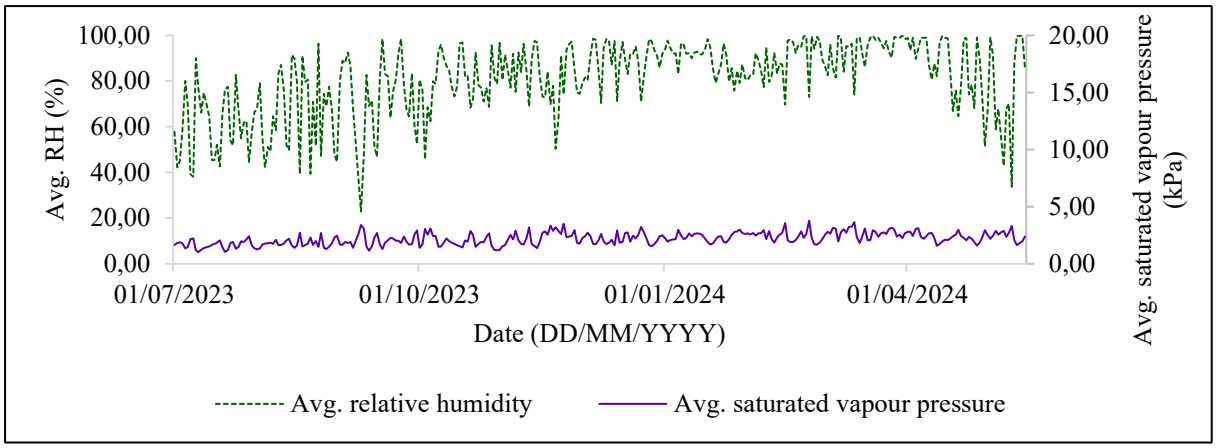

Figure C2 Daily averages of RH (%) and saturated vapour pressure (kPa) from July 2023 May 15 2024

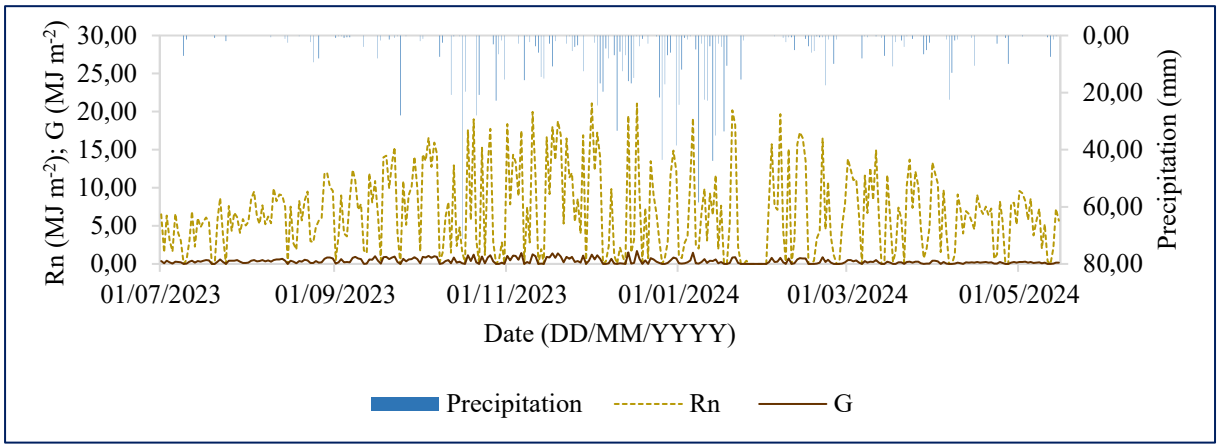

Figure C3 Daily mean values of Rn (MJ m^{-2}), G (MJ m^{-2}), and precipitation (mm) from July 2023, to May 2024

The series analysis reveals a pronounced seasonal trend in ETo and ET-EC (Figure D4). ETo consistently surpasses ET-EC across the observation period, with both metrics exhibiting evident seasonal variations. Daily values reached their lowest in June, peak in December, and gradually decrease through May. This cyclical pattern is consistent with expected seasonal climate changes, where warmer temperatures, increased rainfall, and higher solar radiation during summer promote elevated ET rates, while cooler and drier winter conditions suppress them. The persistent difference between ETo and ET-EC, with ETo consistently higher, corresponds to a Kc ranging from 0.39-0.52 over the monitoring period (Figure D5). This Kc variation indicates changes in crop water requirements and physiological responses to environmental conditions across the SE and M growth stages.

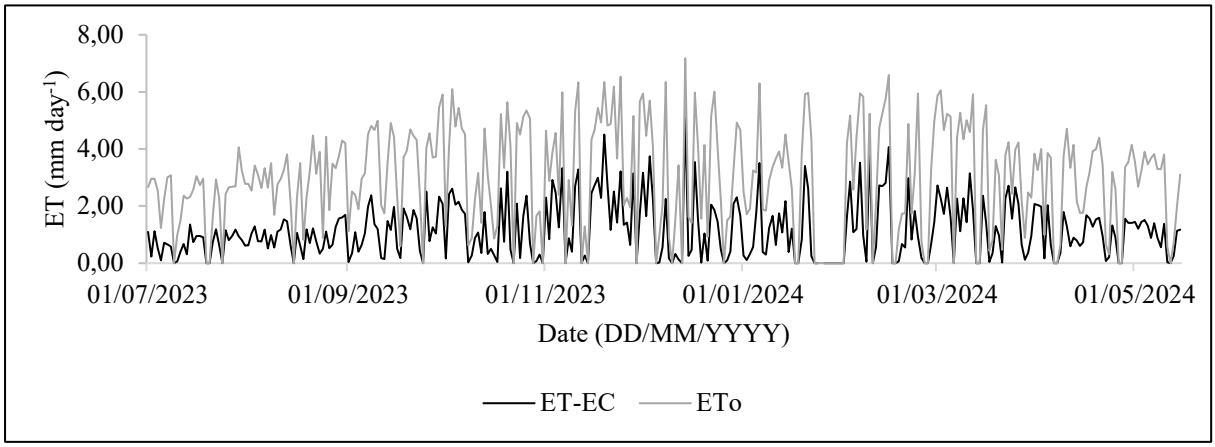

Figure C4 Daily ET-EC (mm day^{-1}) with ETo (mm day^{-1}) during the sugarcane growing season

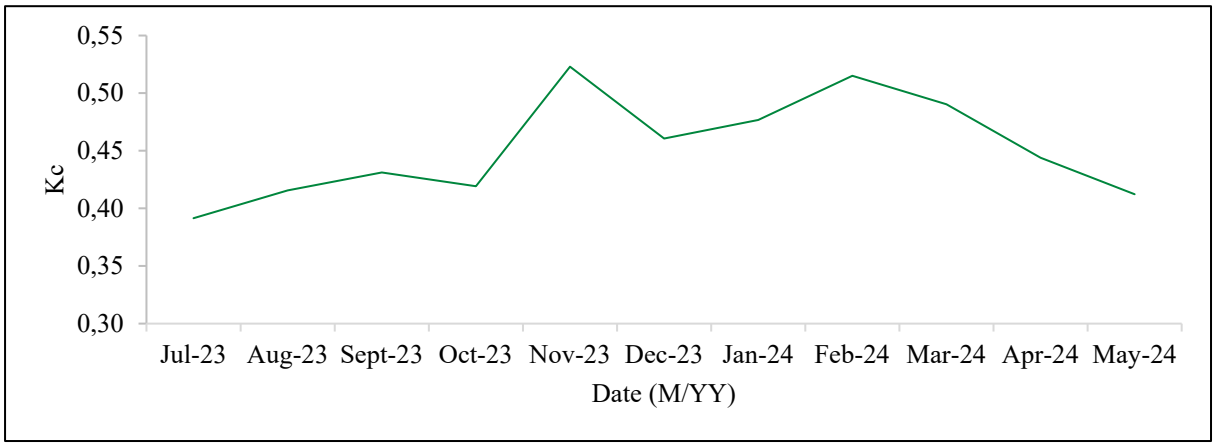

Figure C5 Monthly distribution of observed mean Kc values from July 2023 to May 2024

APPENDIX D

a. Eddy covariance system calibration and energy balance measurements

In the context of the pre-instrumentation setup calibration procedures, the CO_2/H_2O Open-Path Gas Analyzer (EC150, Campbell Scientific, Logan, UT, USA) was positioned in a controlled laboratory environment adjacent to the LI-610 device (LI-610, Licor Inc., Lincoln, NE, USA). Subsequently, the apparatus was linked to a power source, and all tubing connections were secured. The calibration of the gas analyzer was verified against standard gas samples, and the resulting baseline measurements were recorded. Following this, the dew point setting on the LI-610 was established, allowing for system stabilization (Figure E1a). Subsequent steps involved connecting the LI-610 output with the gas analyzer, introducing zero air, and adjusting the analyzer to nullify CO_2 and H_2O readings. In the calibration's span aspect, gases with predefined CO_2 and H_2O concentrations were introduced, necessitating corresponding adjustments to the analyzer. Validation of calibration was conducted across various concentration levels. Lastly, the gas analyzer was restored to its customary operational configuration.

Subsequently, the gas analyzer and the LI-670 Flow Control Unit (LI-670, Licor Inc., Lincoln, NE, USA) were linked to a power source and subjected to warming-up (Figure E1b). Tubing and connections were secured to ensure operational integrity. The initial calibration status of the gas analyzer was validated using established standard gas samples, and baseline measurements were documented. The output of the LI-670 was then connected with the gas analyzer, followed by the introduction of zero air to facilitate the adjustment of the analyzer settings to nullify CO_2 and H_2O readings. Calibration gases with predetermined CO_2 and H_2O concentrations were subsequently employed for span calibration, with due consideration given to aligning the flow rate on the LI-670 with the gas analyzer's requisites. A stabilisation period was allowed before adjustments to the analyzer settings were made. Calibration procedures were iterated across various concentration levels to ensure linearity and precision. Ultimately, the gas analyzer was restored to its customary operational configuration.

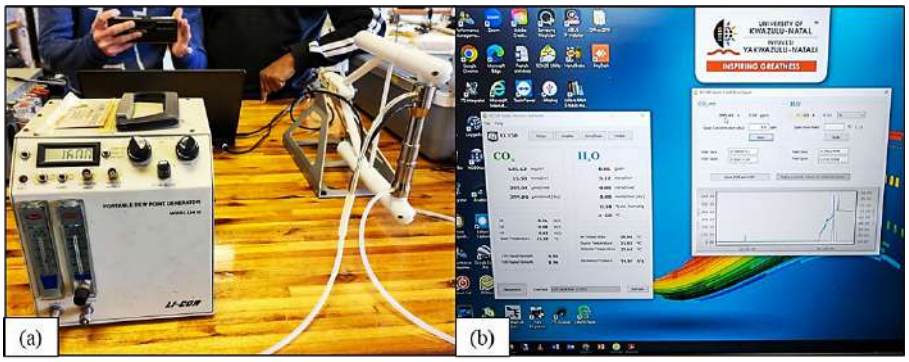

Figure D1 **Calibration setup for the CO_2/H_2O Open-Path Gas Analyzer (EC150) using (a) the LI-610 Dew Point Generator and (b) the LI-670 Flow Control Unit, with data acquisition and analysis conducted via the EC100 Series Monitor Software**

Figure D2 provides an illustration of the condition of the sonic anemometer during which time there was a loss of data for a two week period due to avian interference.

Figure D2 **Soil accumulation on the co-located 3-D sonic anemometer and CO_2/H_2O Open-Path Gas Analyser, attributed to avian interference, resulting in data loss from January 23, 2024, to February 2, 2024**

Table D1 EC instrumentation details (adapted from manufacturer descriptions)

Instrument	Description	Image	Supplier/Source
Rain Gauge: TE525MM-L, Texas Electronics, Dallas, TX, USA.	The TE525 device channels precipitation into a receptacle system, which undergoes tipping once it reaches its predetermined calibration level. The bucket's tipping mechanism is activated by a magnet affixed to it, which triggers a switch. The pulse-counting circuitry in the datalogger is responsible for tallying the switch's instantaneous closing.		(Campbell Scientific, 2024)
4-Component Net Radiometer: CNR4-L, Kipp & Zonen, Delft, The Netherlands.	The CNR4 is a net radiometer of research quality designed to quantify the energy equilibrium between incoming and outgoing radiation. The apparatus combines a pyranometer and a pyrgeometer, which measure short-wave and long-wave infrared radiation, respectively.		(Campbell Scientific, 2024)
3-D Sonic Anemometer: CSAT3A, Campbell Scientific, Logan, UT, USA.	The CSAT3A is a sonic anemometer capable of measuring three orthogonal wind components and the speed of sound. The capacity to assess the turbulent variations of horizontal and vertical wind inside EC systems enables the subsequent computation of momentum flux and friction velocity.		(Campbell Scientific, 2024)

Table D1 continued

Instrument	Description	Image	Supplier/Source
CO_2/H_2O Open-Path Gas Analyzer: EC150, Campbell Scientific, Logan, UT, USA.	As a stand-alone analyzer, the device measures absolute carbon dioxide and water vapour concentrations, air temperature, and barometric pressure.		(Campbell Scientific, 2024)
Soil heat flux plates: HFP01-L, Campbell Scientific, Logan, UT, USA.	The HFP01 employs a thermopile to quantify temperature differentials throughout its surface under the assumptions of stable heat flux, constant thermal conductivity of the body, and minimal impact of the sensor on the thermal flow pattern. Moreover, the signal of the HFP01 exhibits a direct relationship with the magnitude of the heat flow in the immediate vicinity.		(Campbell Scientific, 2024)
Soil Temperature Averaging Probes: TCAV-L, Campbell Scientific, Logan, UT, USA.	The TCAV-L measures the mean temperature of the uppermost 6-8 cm layer of soil, which is crucial for assessing energy balance in flux systems. The TCAV employs type E thermocouples, consisting of a chrome wire and a constantan wire connected at a measuring junction. Additionally, the temperature can be determined by measuring the disparities in potential generated at the junction.		(Campbell Scientific, 2024)

Table D1 continued

Instrument	Description	Image	Supplier/Source
Water Content Reflectometers: CS616, Campbell Scientific, Logan, UT, USA.	The CS616-LC can quantify the volumetric water content from 0% to saturation. This technique employs time-domain measuring techniques without necessitating the use of a reflectometer. The insertion of probe rods may be conducted either from the surface or by burying the probe at any orientation relative to the surface.		(Campbell Scientific, 2024)
Infrared radiometer (IRR): SI-111, Apogee Instruments, Logan, UT, USA.	The SI-111 is a very accurate infrared radiometer used for non-contact measurements of an object's surface temperature. The measurement encompasses the subject's surface and the sensor body's temperatures. The datalogger utilizes the readings to accurately determine the body's temperature.		(Campbell Scientific, 2024)
Type E Fine-Wire Thermocouples: EXTT-E-24, Omega Inc., Stamford, CT, USA.	The FW3 is a Type E thermocouple with a diameter of 0.003 inches. It accurately measures atmospheric temperature gradients or fluctuations with research-grade precision. The FW3's compact size negates the requirement for a solar radiation shield. It comprises a connector that attaches the thermocouple to a datalogger via the FWC-L cable.		(Campbell Scientific, 2024)

Table D1 continued

Instrument	Description	Image	Supplier/Source
Temperature/RH Probe: HC2S3, Rotronic AG, Bassersdorf, Switzerland.	The HC2S3 is a temperature and humidity probe that exhibits high precision and is well-suited for extended periods of use in unattended scenarios. The probe uses a sophisticated capacitive sensor to measure relative humidity. The probe is equipped with a filter that safeguards the sensor from the intrusion of dust and particles, enhancing its performance and dependability.		(Campbell Scientific, 2024)
CR3000 Datalogger: Campbell Scientific, Logan, UT, USA.	The CR3000 can effectively manage extended eddy-covariance and complete energy-balance systems. The datalogger offers three alternative power-supply choices: alkaline, rechargeable, or no battery. The micrologger's ability to function on a battery recharged using a solar panel for lengthy periods eliminates the need for AC power, owing to its low power consumption. The device halts operation when the main power supply falls below 9.6 V, mitigating the potential for imprecise readings.		(Campbell Scientific, 2024)
CR1000 Datalogger: Campbell Scientific, Logan, UT, USA.	Robust and suitable for complex configurations, the CR1000 operates with an external keyboard/display and power supply. It supports extended use with a rechargeable battery powered by a solar panel, eliminating reliance on AC power. The system automatically shuts down when power drops below 9.6 V to prevent inaccurate readings.		(Campbell Scientific, 2024)

Estimates of energy balance components for sugarcane under rainfed conditions demonstrate variability influenced by several factors, including local climatic conditions, soil type, crop developmental stage, and agronomic practices. Specifically, Rn shows a significant range affected by solar irradiance, cloud cover, and surface reflectance properties, with typical values between 10-20 MJ m^{-2} day^{-1} and potentially exceeding these limits. Soil heat flux, which denotes the exchange of thermal energy between the soil and its environment, is influenced by soil moisture content, soil type, and vegetative cover, with expected values ranging from 0.5-2 MJ m^{-2} day^{-1} (Figure E3). Latent heat flux, representing the energy expended during ET, typically ranges from 5 to 15 MJ m^{-2} day^{-1}. In contrast, H, which characterizes heat transfer through conduction and convection, varies from 1 to 5 MJ m^{-2} day^{-1}. As illustrated in Figure E3, the observed fluxes generally align with established acceptable ranges; however, a slight deviation was noted for H, particularly during the summer.

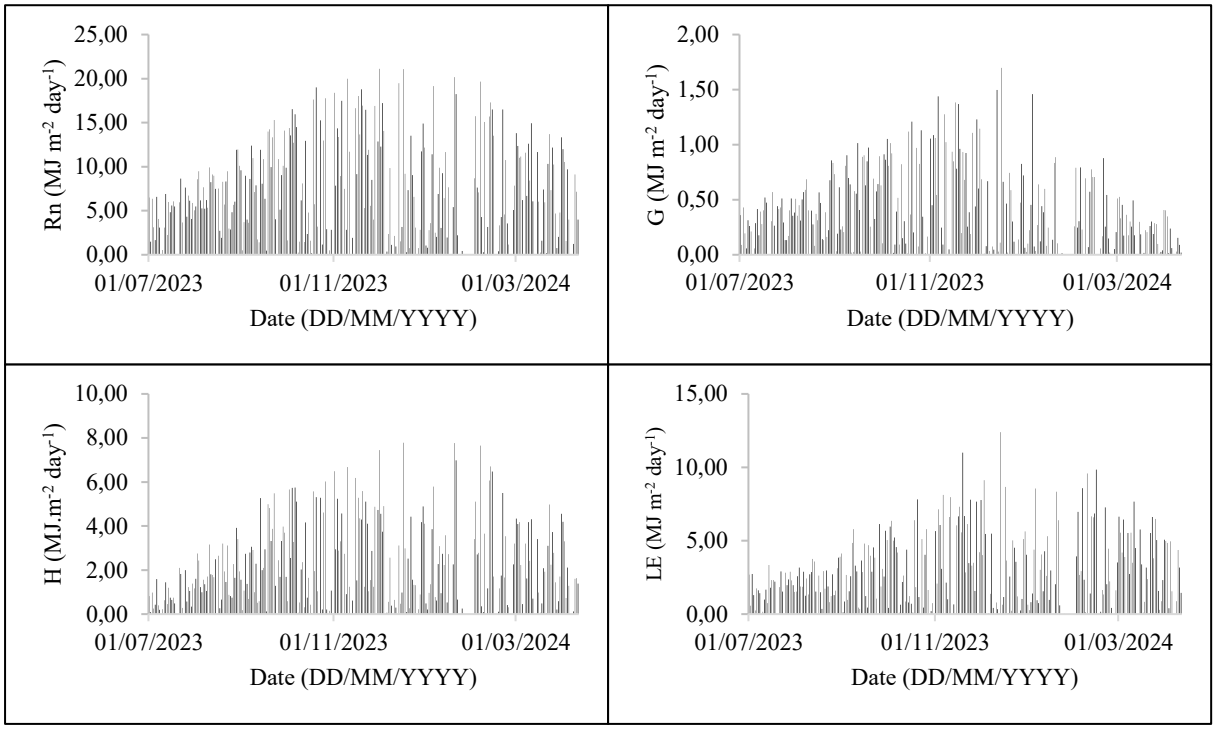

Figure D3 Top left) Rn, (Top right) G, (Bottom left) H, and (Bottom right) LE, all in MJ m^{-2} day^{-1}, showing typical ranges and the temporal dynamics for each energy flux over the stalk elongation and early maturation phases of the sugarcane phenological cycle

APPENDIX E

Table E1 Details of in-situ measurement devices (adapted from manufacturer descriptions) used to monitor plant growth and development

Device	Description	Image	Supplier/Source
SPAD502 chlorophyll meter: Minolta Corporation, Ltd., Osaka, Japan.	The SPAD502 chlorophyll meter quantifies the relative chlorophyll concentration by measuring leaf absorbance in the red and near-infrared spectral bands. The device calculates a SPAD value directly correlated to the CC in the leaf.		(Konica Minolta, 2024)
LAI2200 Plant Canopy Analyser: Li-Cor, Inc., Lincoln, NE, USA.	The LAI2200 Plant Canopy Analyzer calculates LAI and other canopy structural parameters using radiation measurements obtained through a "fisheye" optical sensor. The device employs measurements taken above and below the canopy at various zenith angles to assess light interception, with LAI derived through a radiative transfer model.		(LI-COR, 2024)
Testo Thermal Imager 882: Testo SE & Co. KGaA, Lenzkirch, Germany.	The Testo 882 Thermal Imager is a robust and user-friendly thermal imaging camera designed for high-accurate non-contact measurement and display of surface temperature distribution.		(Testo, 2024)

APPENDIX F

Table F1 Additional flight specifications for DJI M300 non-RTK version with MicaSense Altum camera at 100 m altitude

Specification	Specification detail
Max takeoff weight	9 kg
Max flight time	55 minutes (no payload)
Operating temperature	-20 °C to 50 °C
Max wind resistance	15 m s^{-1}
Max descent speed	7 m s^{-1}
Max ascent speed	6 m s^{-1}
Max transmission distance	15 km (FCC); 8 km (CE)
Positioning accuracy	Horizontal: ±1.5 m, vertical: ±0.5 m
Obstacle sensing range	0.5 m to 40 m (front, rear, left, right, up, down)
Global navigation satellite system (GNSS)	GPS+GLONASS+BeiDou+Galileo
Battery type	TB60 intelligent flight battery
Battery capacity	5935 mAh
Payload capacity	Up to 2.7 kg
Max hovering time	45 minutes
Controller	DJI Smart Controller Enterprise
Operating frequency	2.400-2.4835 GHz; 5.725-5.850 GHz
Transmission system	OcuSync Enterprise

APPENDIX G

a. Development of a web-based application to view and access the UAV-derived outputs

Google Earth Engine (GEE) is a freely available, cloud computing platform which enables access to high-performance computing power for planetary-scale geospatial analysis (Gorelick et al., 2017). GEE provides users with easy access to a multi-petabyte curated catalogue of earth observation data sets, built-in algorithms for manipulating and analyzing data, as well as a programming interface to create, customize and automatically run algorithms (Padarian et al., 2015; Gorelick et al., 2017; Sidhu et al., 2018). Additionally, users are able to ingest and process their own data using all of the aforementioned features available within the platform (Gorelick et al., 2017). A particularly noteworthy feature of this platform is that it permits the development of dynamic web-based apps which are also freely available and can be used to process and rapidly communicate results in an aesthetically appealing and comprehendible manner to a wide range of users (Tamiminia et al., 2020). In light of this, in this study we have proposed the development of a data processing and viewing app which processes all the UAV imagery that has been captured throughout the course of the study and produces various outputs which can be visualized or downloaded to guide and inform decision making. The app (Figure H1) can be accessed from the link below. The app has been designed to simplify the process of deriving crop related information so that users of all experience levels can benefit from the processing power of Google Earth Engine to process UAV imagery

https://shaedengokool.users.earthengine.app/view/swayimane-smallholder-farm-crop-monitoring-app-beta-version

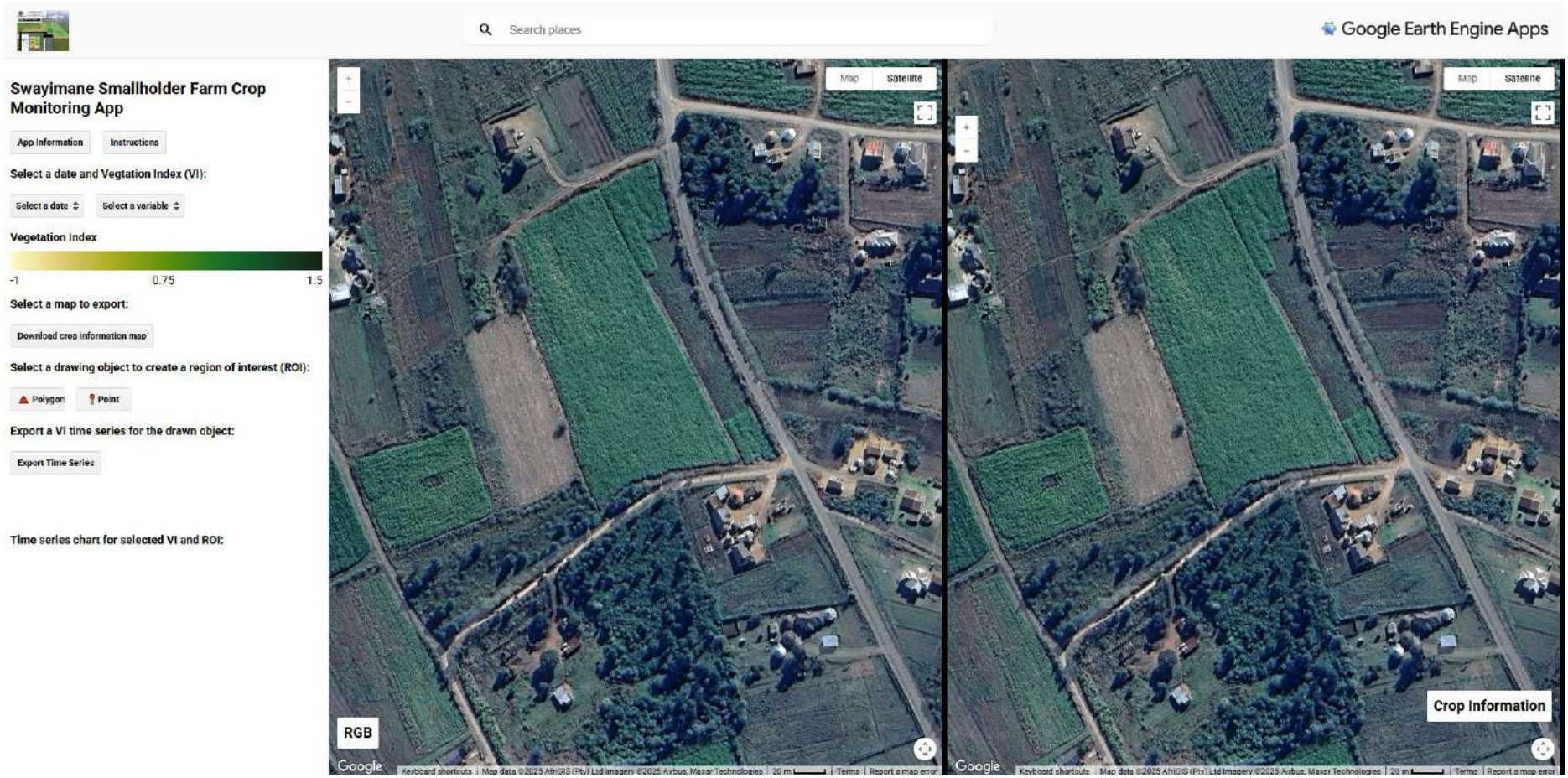

Figure G1 The Swayimane smallholder farm crop monitoring app interface

b. Instructions on how to use the app

- Step 1: Select a date and a crop related variable to display from the "select a date" and "select a variable" dropdowns, respectively. This will display an RGB image and crop related variable for the corresponding date.
- Step 2: The selected crop variable for the corresponding dates can then be downloaded as a GeoTiff file by clicking on the “Download crop information map” button. After a few seconds a panel will then be added to the second map panel with a clickable link to download the data. Once you have clicked the link you can then close the panel. If you would like to download a crop variable map for a different date, change your selection using the "select a date" and "select a variable" dropdowns and then repeat the process.
- Step 3: Select a drawing object to create a region of interest (ROI) for which to query data for. This will then allow you to draw a polygon or a point in the second map panel labelled "Crop information". You can use the RGB image displayed in the first Map panel labelled "RGB" to guide your selection of where you would like to draw your ROI. Please note that you will only be able to draw one object at a time. Once the ROI has been drawn a time series chart depicting the selected crop related variable will also simultaneously be added to the information panel display.
- Step 4: Once the ROI has been created, the user can export a time series of all crop related information for the entire image collection by clicking on the "Export time series" button. After a few seconds a panel will then be added below the Export time series button with a clickable link to download the data (Figure H2). If you would like to generate a time series for another ROI, close the download panel and then draw a new ROI on the VI map and repeat the process as previously.

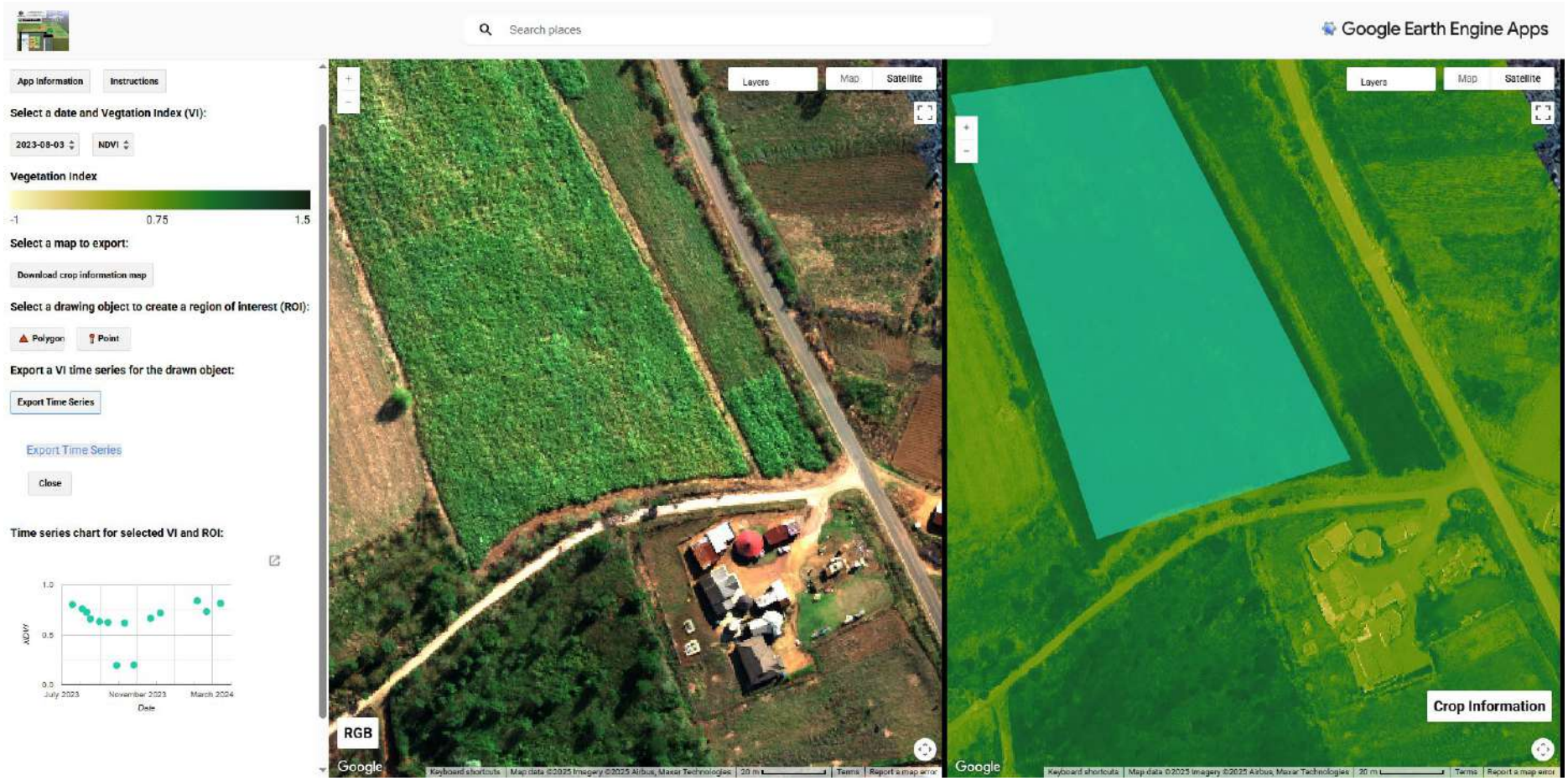

Figure G2 An example of the Swayimane smallholder farm crop monitoring app in use

APPENDIX H

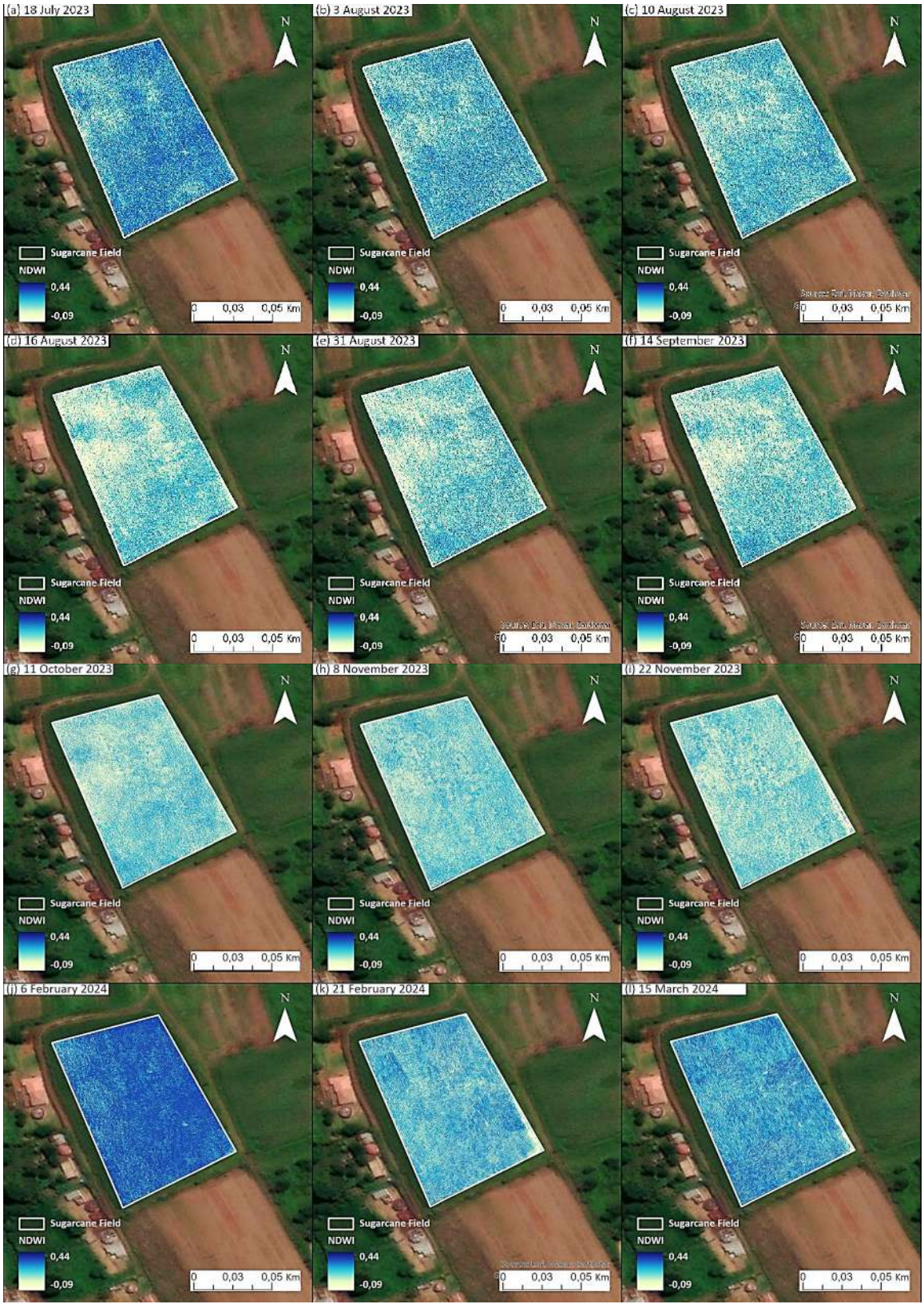

Figure H1 Spatio-temporal NDWI maps derived from ensemble model two

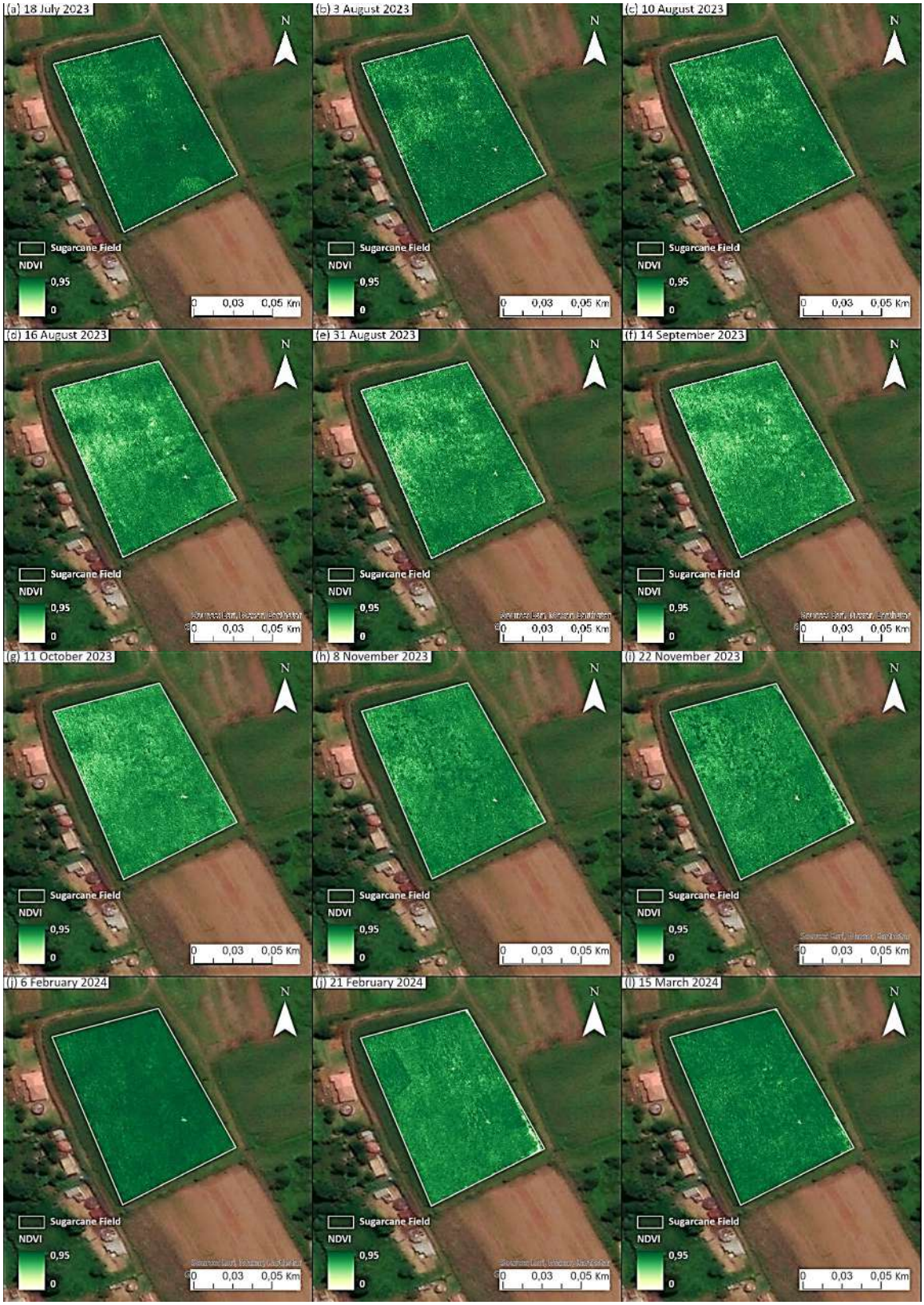

Figure H2 NDVI maps from twelve UAV flights over the study area

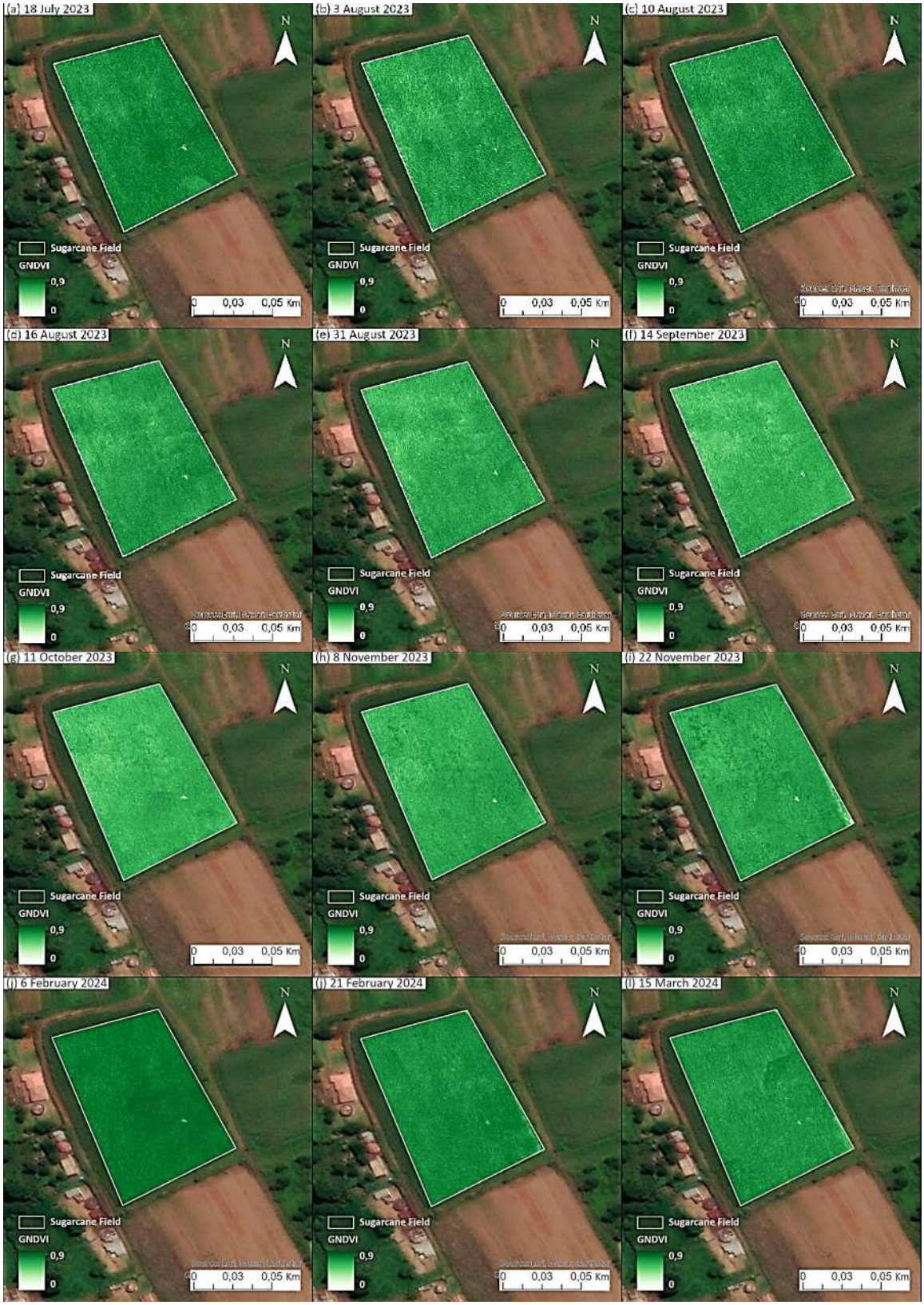

Figure H3 **GNDVI variations captured in UAV flights showcasing temporal trends in vegetation health**

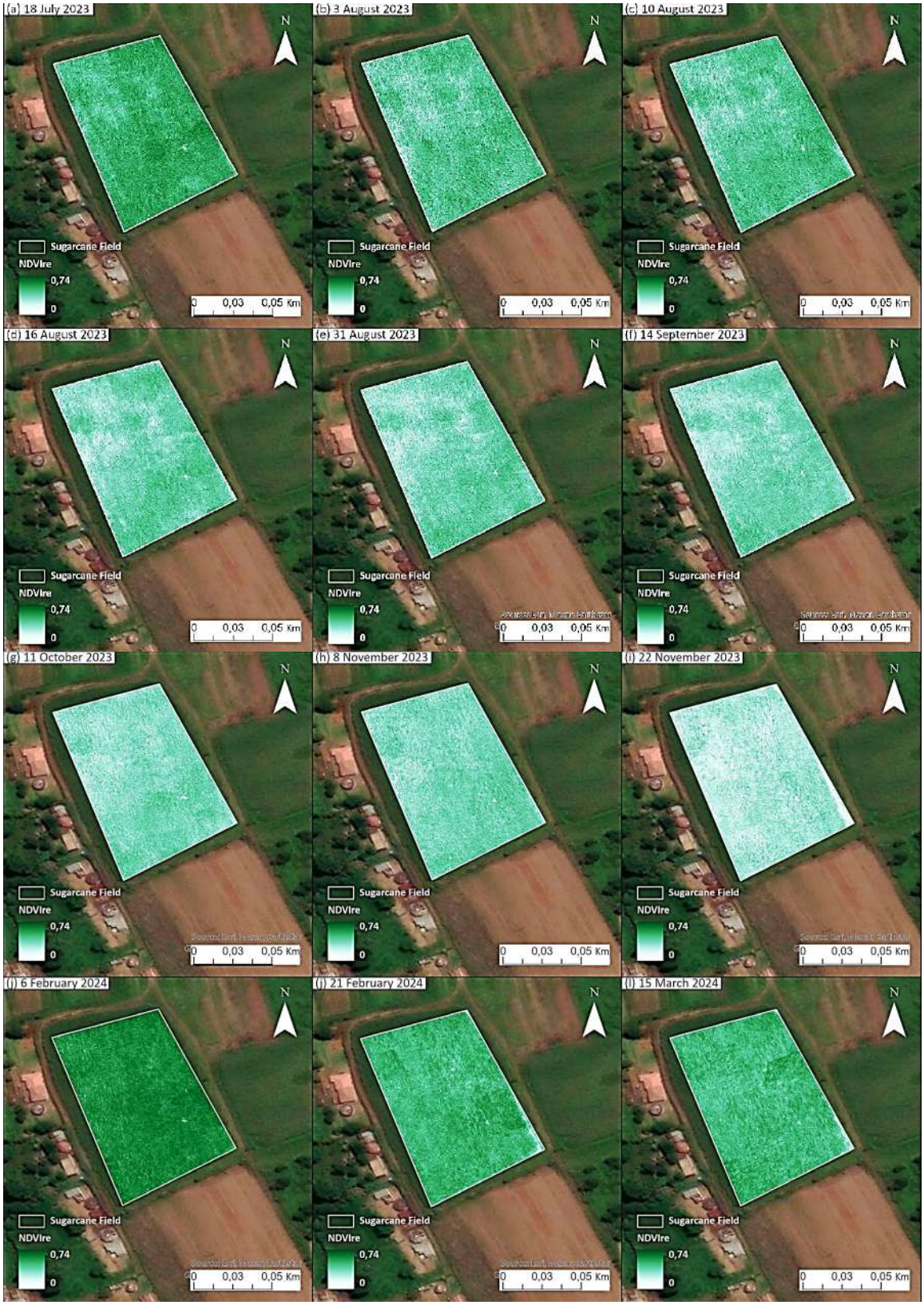

Figure H4 Comparative analysis of NDVIre maps from twelve UAV flights for vegetation monitoring

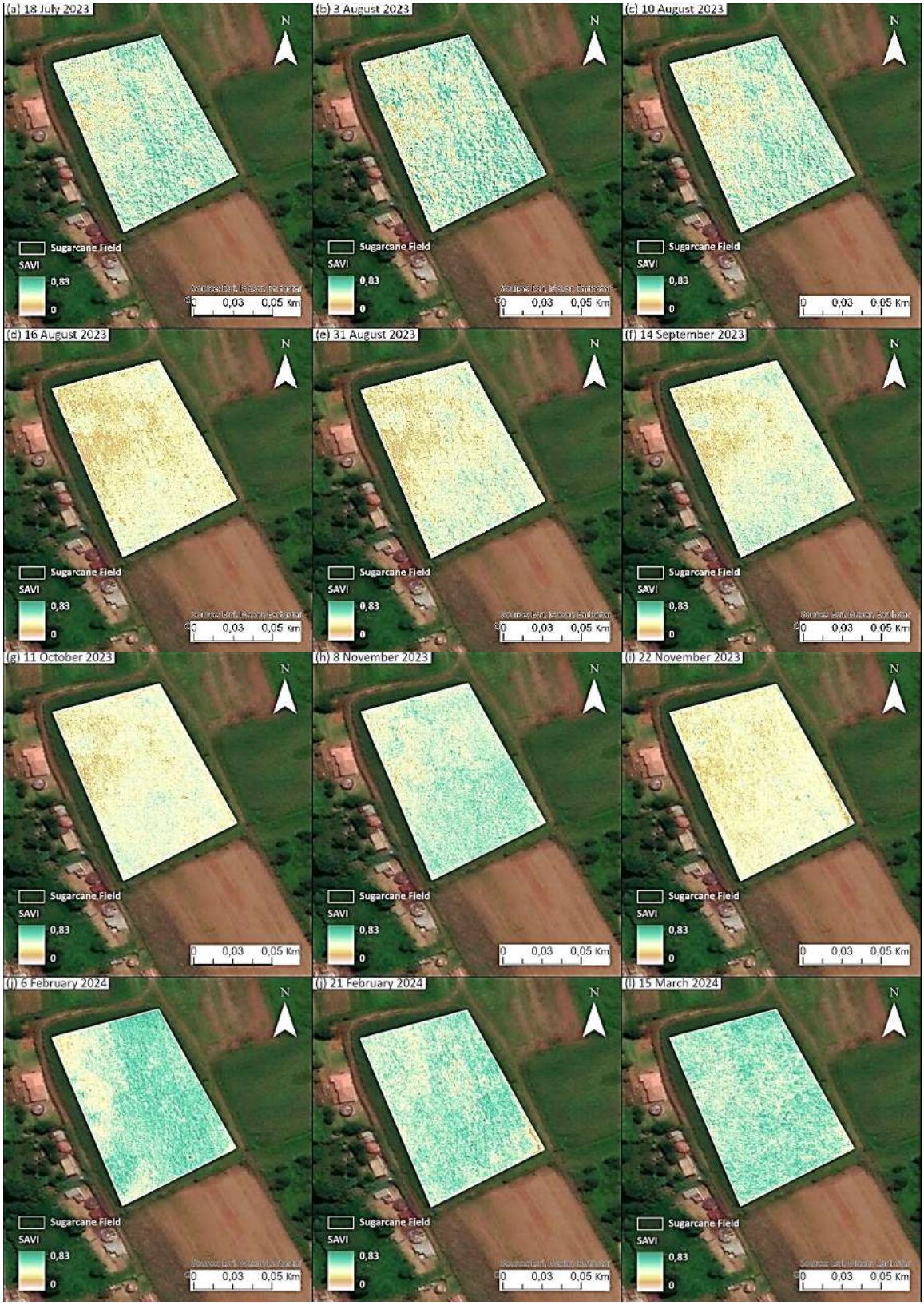

Figure H5 Temporal changes in SAVI values mapped across different UAV survey dates for trend analysis

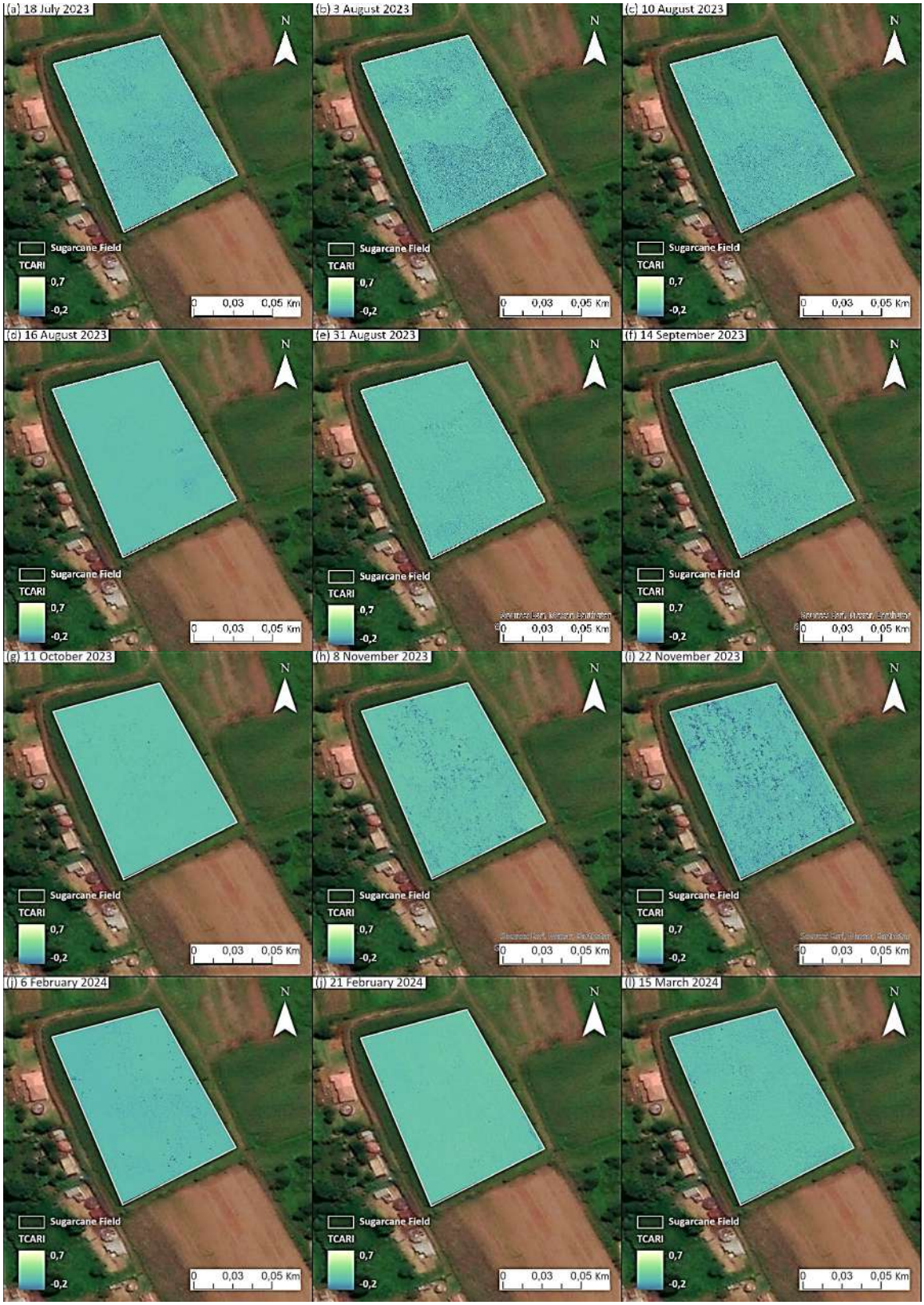

Figure H6 TCARI index mapping revealing CC variations across different UAV flights

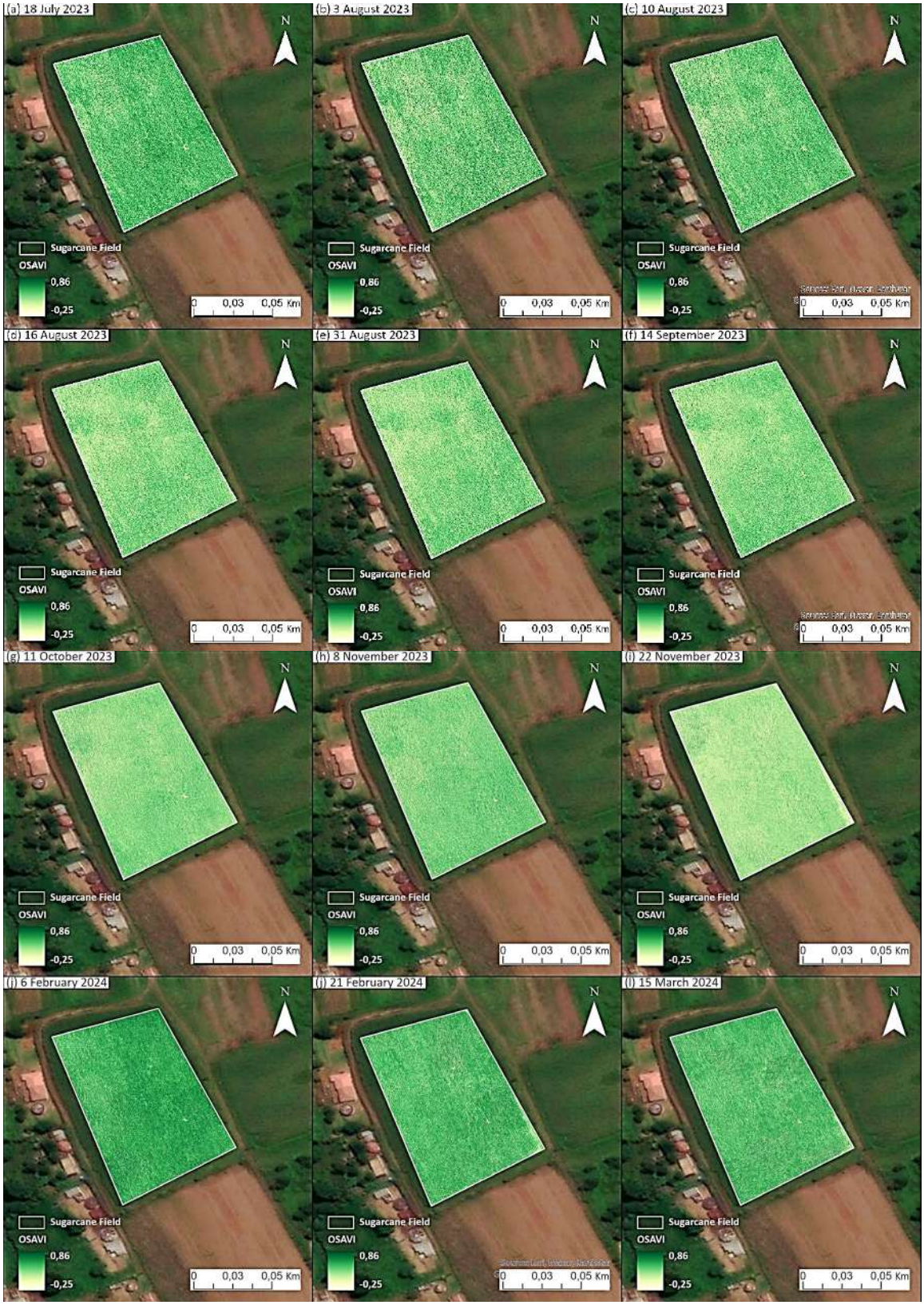

Figure H7 OSAVI index representations from multiple UAV flights indicating vegetation vigour dynamics

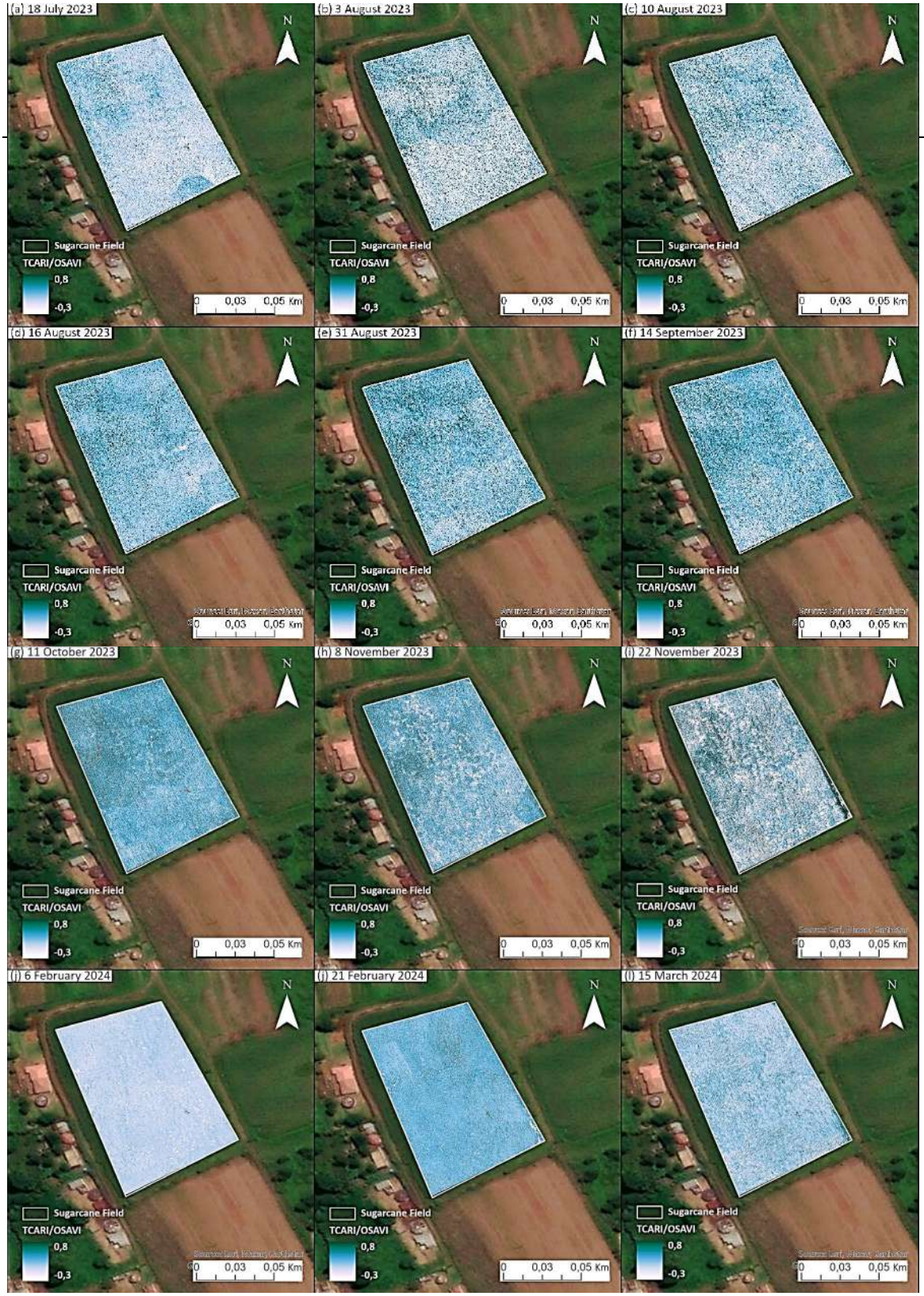

Figure H8 Spatial visualisation of TCARI/OSAVI ratios for assessing plant physiological status